Cotutelle Doctoral Program

Doctoral Dissertation on

Solution of Coupled Thermoelasticity Problem In Rotating Disks

by

Ayoob Entezari

Supervisors:

Prof. M. A. Kouchakzadeh[1] and Prof. Erasmo Carrera[2]

Advisor:

Dr. Matteo Filippi[2]

[1]Sharif University of Technology
Department of Aerospace Engineering, Tehran, Iran

[2]MUL2 research group,
Polytechnic University of Turin, Italy

[2]Polytechnic University of Turin,
Department of Mechanical and Aerospace Engineering, Italy

26 September, 2017

Outlines

1. Introduction to rotating disks
2. Fundamentals of Linear Thermoelasticity
3. Literature review & present work
4. Analytical approach
5. Numerical approach
6. Conclusion

Outlines

1. **Introduction to rotating disks**
2. Fundamentals of Linear Thermoelasticity
3. Literature review & present work
4. Analytical approach
5. Numerical approach
6. Conclusion

Introduction to rotating disks

Applications

- ✓ Aerospace (aero-engines, turbo-pumps, turbo-chargers, etc.)
- ✓ Mechanical (spindles, flywheel, brake disks, etc.)
- ✓ Naval
- ✓ Power plant (steam and gas turbines, turbo-generators,)
- ✓ Chemical plant
- ✓ Electronics (electrical machines)

Introduction to rotating disks

Configurations

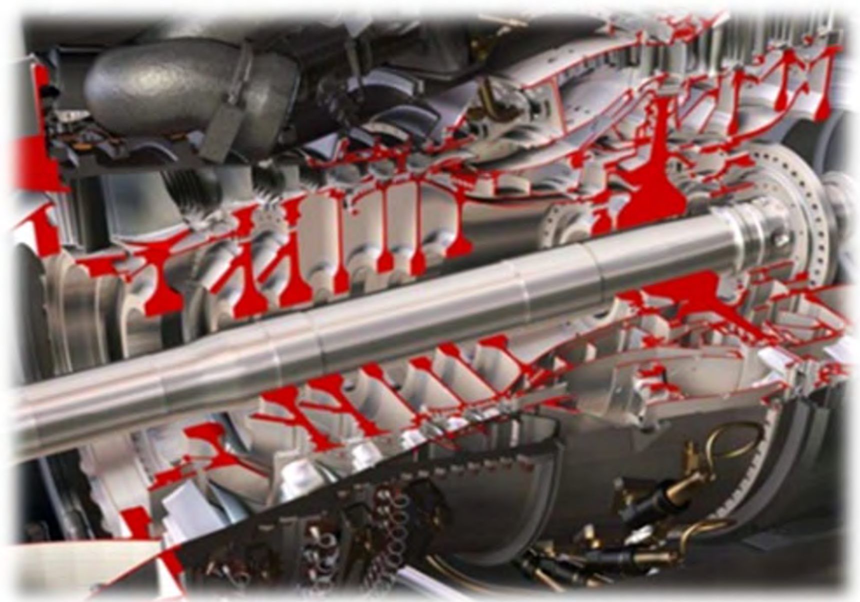

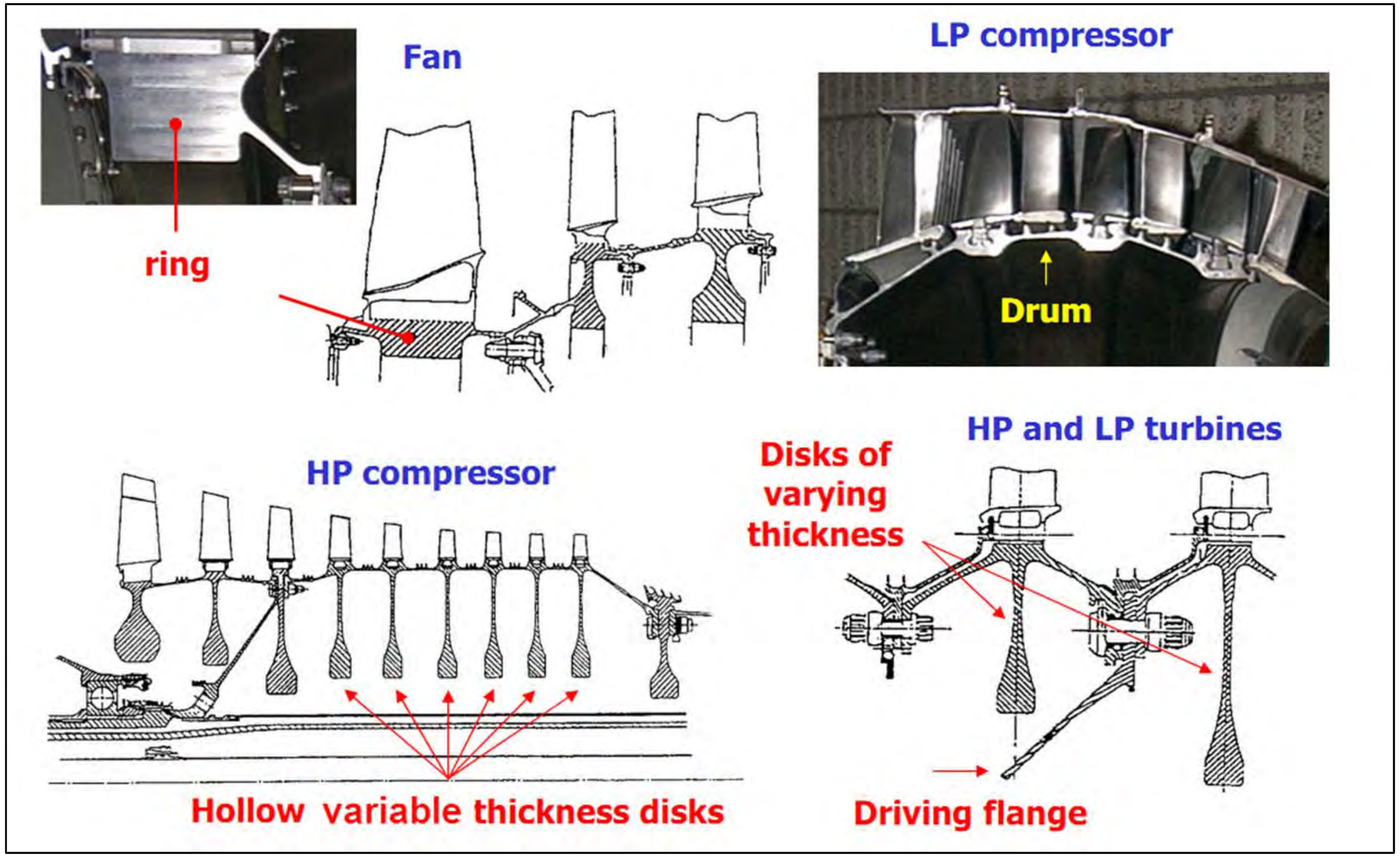

Introduction to rotating disks

Operating conditions

- ❑ **Main Loads**
  - ✓ Centrifugal forces
  - ✓ Thermal loads.

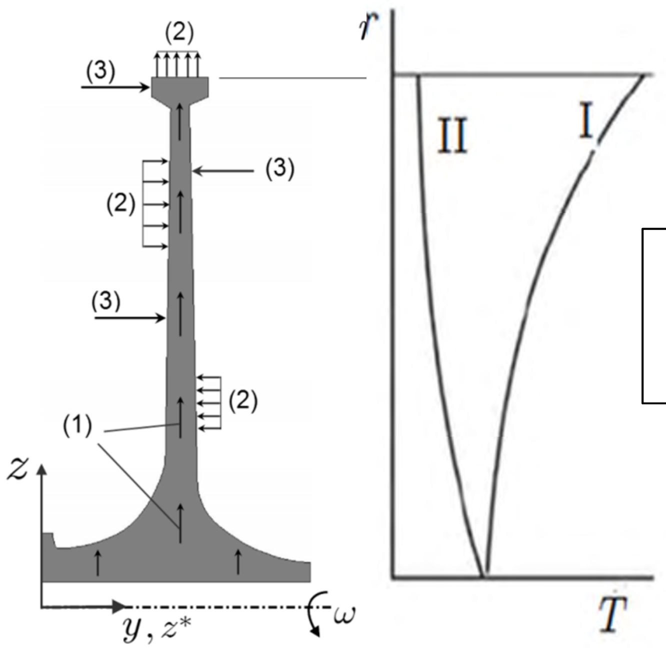

start and stop cycles
I) start up,
II) shut down

- ❑ **Transient thermal load**
  - ✓ In some of applications, the disks may be exposed to sudden temperature changes in short periods of time (for Ex. start and stop cycles)
  - ✓ These sudden changes in temperature can cause time dependent thermal stresses.
  - ✓ Thermal stresses due to large temperature gradients are higher than the steady-state stresses.
  - ✓ In such conditions, the disk should be designed with consideration of transient effects.

Introduction to rotating disks

Disk materials

- ✓ Metals: steels, super alloys
- ✓ Ceramic matrix composites (CMC)
- ✓ Functionally graded materials (FGMs)

---

ceramic-metal FGM

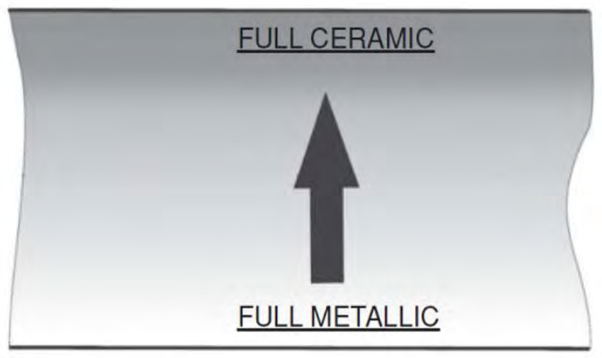

ceramic-metal FGM

Effective properties of FGMs

$$\boxed{P_{eff} = V_m P_m + V_c P_c = V_m (P_m - P_c) + P_c}$$

P_m and P_c : properties of metal and ceramic
V_m and V_c : volume fractions of metal and ceramic
$V_m = f(x, y, z)$

FGM disk

power gradation law for metal volume fraction along the radius

$$V_m = \left(\frac{b-r}{b-a}\right)^n$$

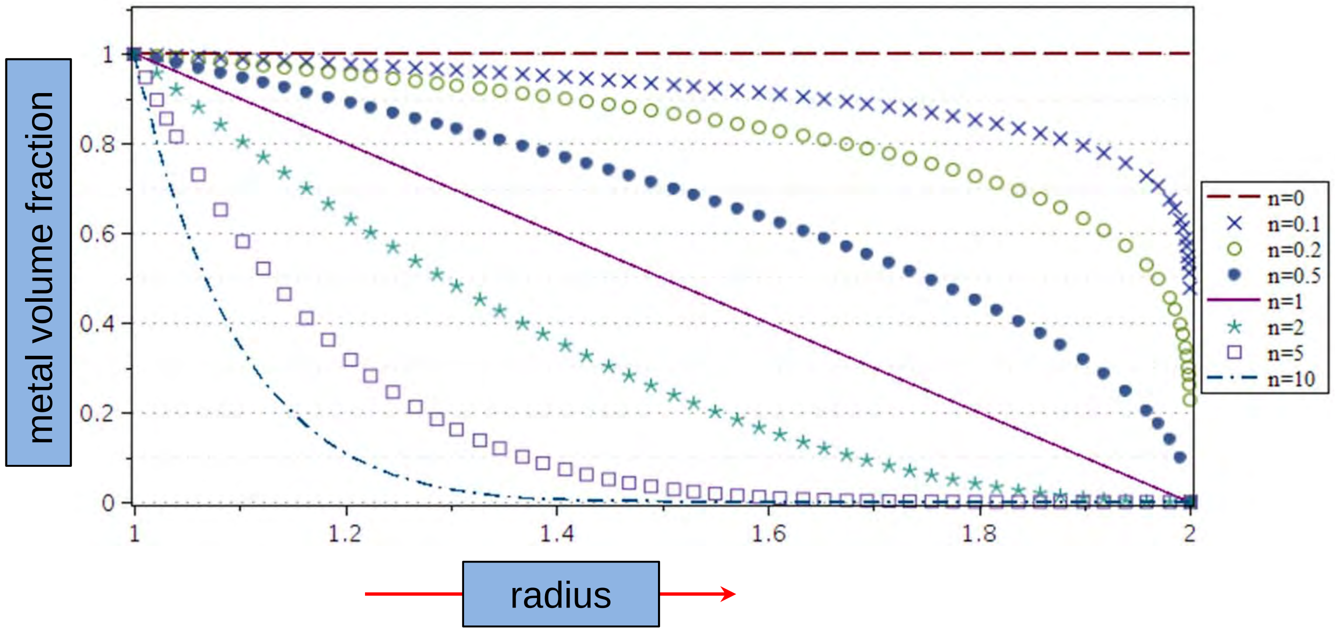

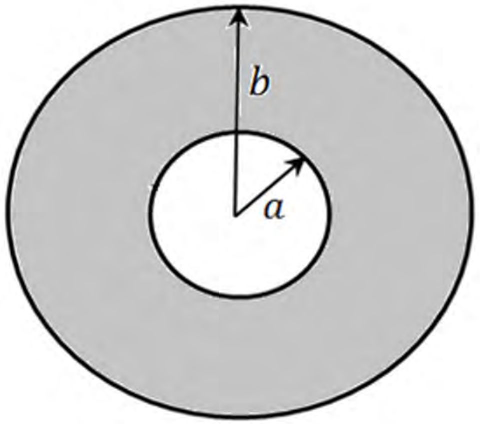

Effective properties of FGMs

$$P_{eff} = V_m P_m + V_c P_c = V_m (P_m - P_c) + P_c$$

Outlines

1. Introduction to rotating disk
2. **Fundamentals of Linear Thermoelasticity**
3. Literature review & present work
4. Analytical approach
5. Numerical approach
6. Conclusion

Classification of thermoelastic problems

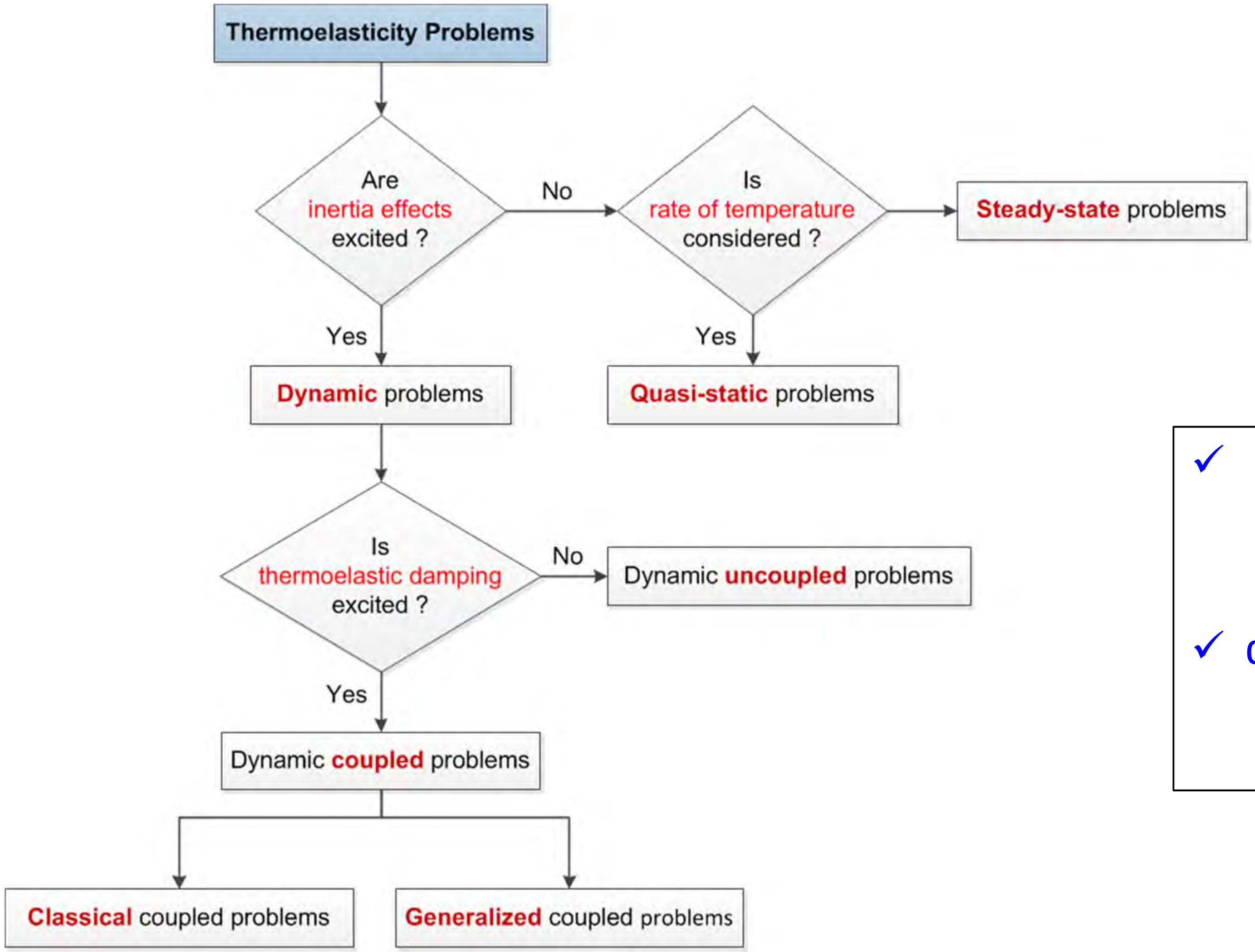

- ✓ Inertia effects
  - static problems
  - dynamic problems
- ✓ displacement and temperature fields interaction
  - uncoupled problems
  - coupled problems

Fundamentals of Linear Thermoelasticity

Classification of thermoelastic problems

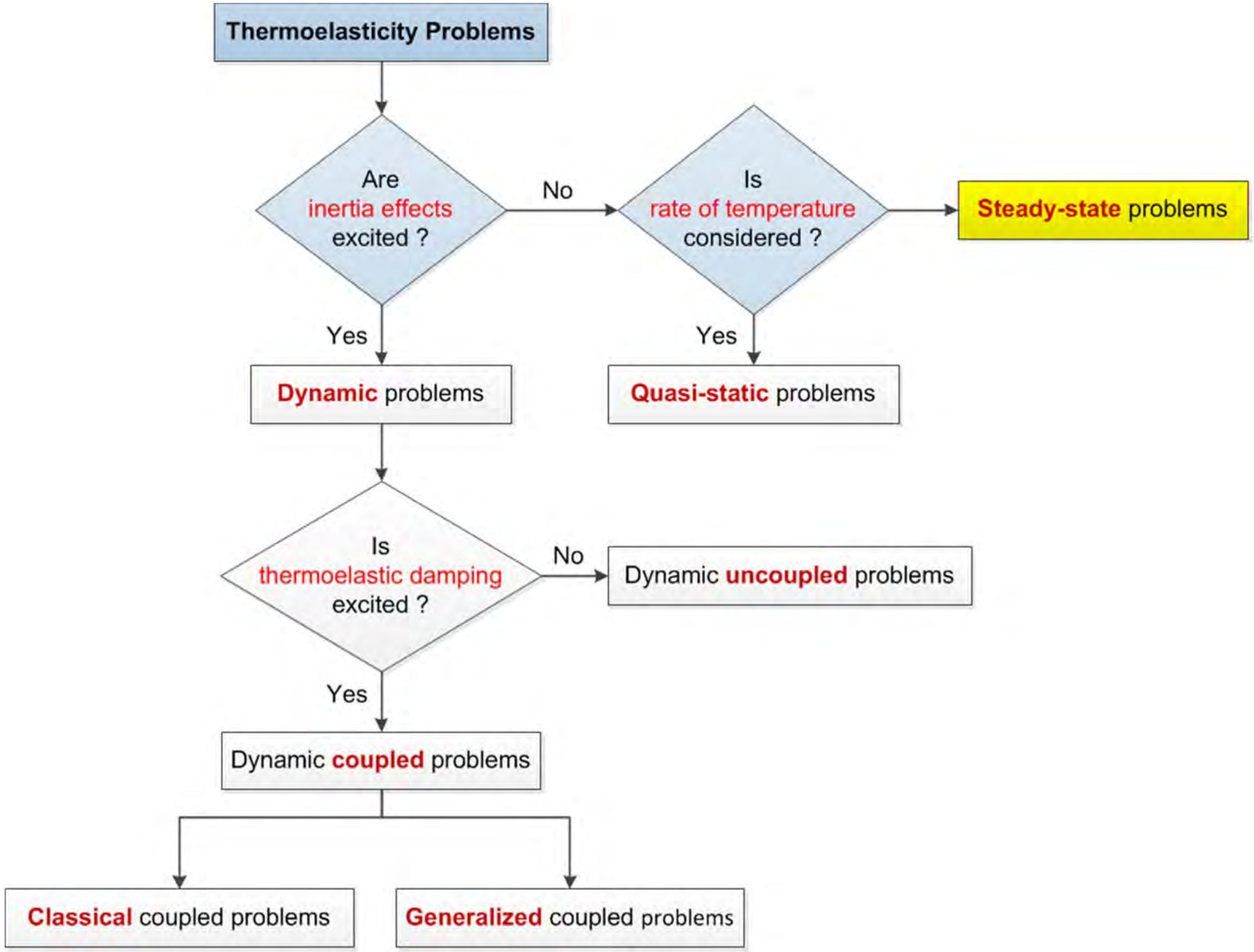

static steady-state problems

equation of motion

$$(C_{ijkl}u_{k,l})_{,j} - (\beta_{ij}T)_{,j} + X_i = 0$$

energy equation

$$(\kappa_{ij}T_{,j})_{,i} = R$$

- $T \longrightarrow$ temperature change
- $u_i \longrightarrow$ displacements
- $C_{ijkl} \longrightarrow$ elastic coefficients
- $X_i \longrightarrow$ body forces
- $\beta_{ij} \longrightarrow$ thermoelastic moduli
- $\kappa_{ij} \longrightarrow$ thermal conductivity
- $R \longrightarrow$ internal heat source

Fundamentals of Linear Thermoelasticity

Classification of thermoelastic problems

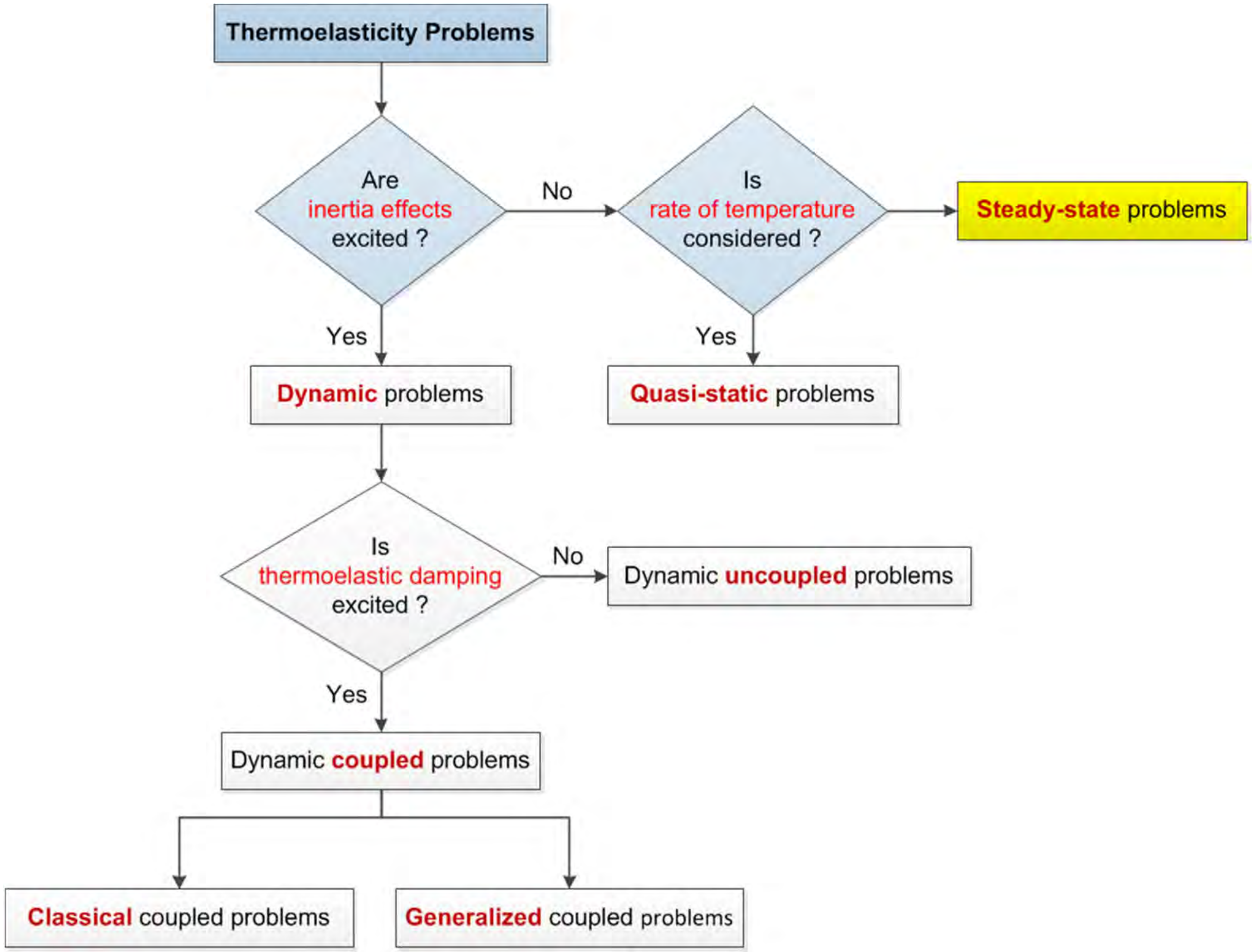

static steady-state problems

Under axisymmetric & plane stress assumptions

equation of motion

$$\frac{d}{dr}(rh\sigma_r) - h\sigma_\theta + \rho\omega^2 hr^2 = 0$$

energy equation

$$T(r) = T_a + \frac{(T_b - T_a)}{\ln(r_a/r_b)} \ln(r/r_b)$$

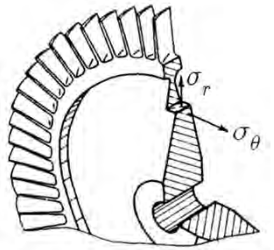

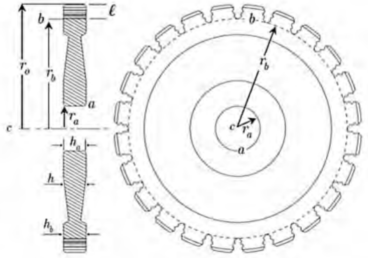

Classification of thermoelastic problems

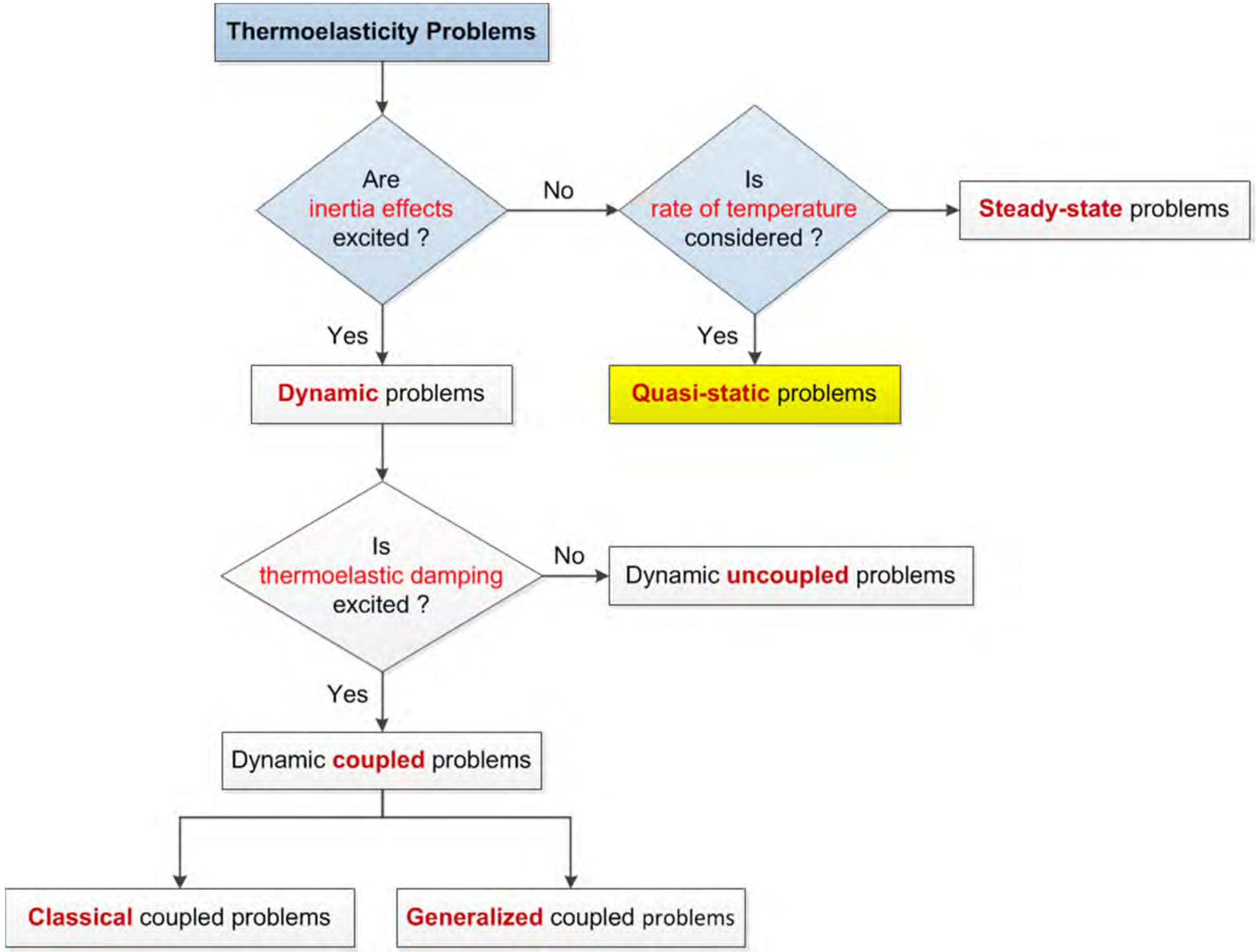

Quasi-static problems

equation of motion

$$(C_{ijkl}u_{k,l})_{,j} - (\beta_{ij}T)_{,j} + X_i = 0$$

energy equation

$$\rho c\dot{T} - \left(\kappa_{ij}T_{,j}\right)_{,i} = R$$

- $\rho \rightarrow$ density
- $c \rightarrow$ specific heat

Classification of thermoelastic problems

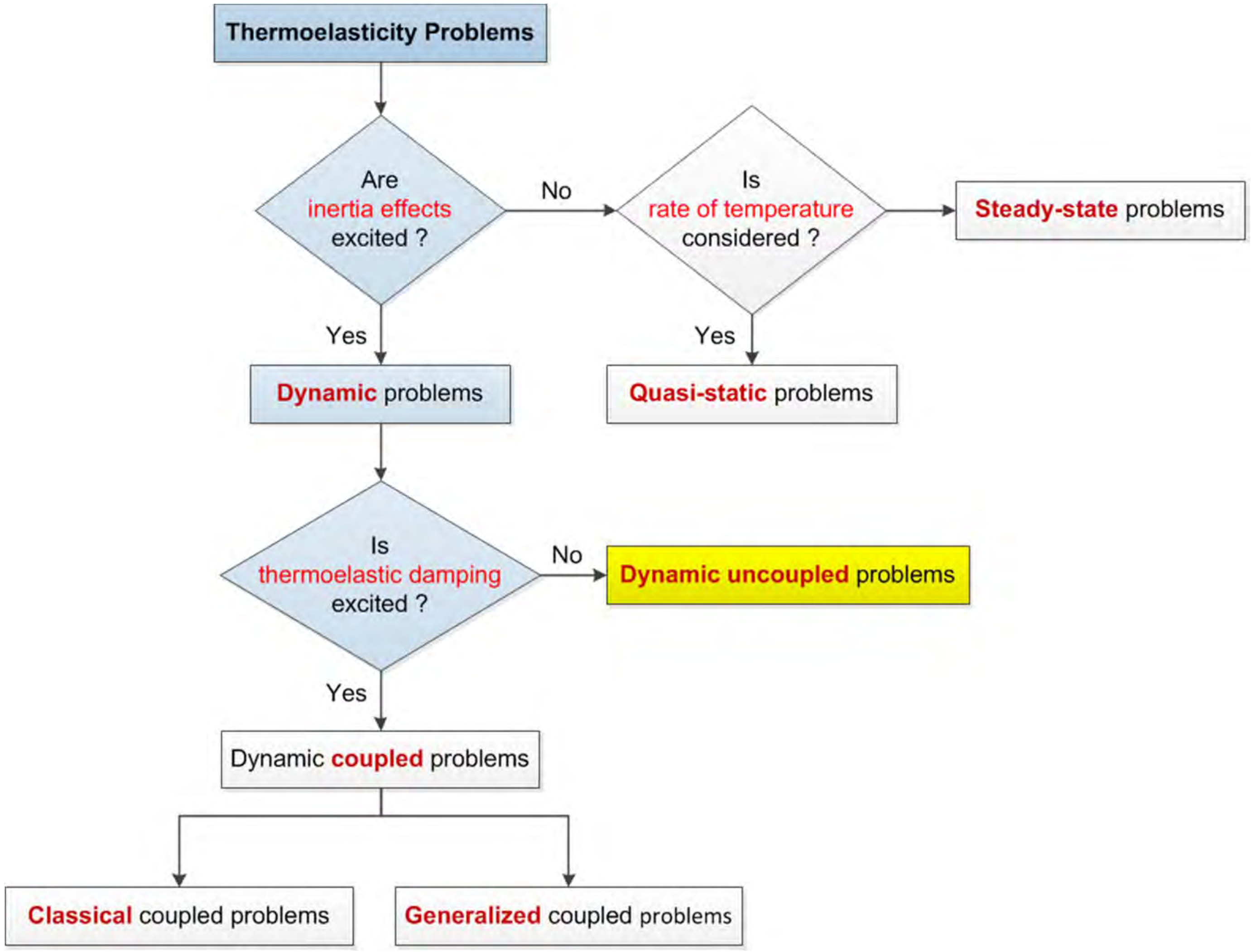

Dynamic uncoupled problems

equation of motion

$$(C_{ijkl}u_{k,l})_{,j} - (\beta_{ij}T)_{,j} + X_i = \rho\ddot{u}_i$$

energy equation

$$\rho c\dot{T} - \left(\kappa_{ij}T_{,j}\right)_{,i} = R$$

Fundamentals of Linear Thermoelasticity

Classification of thermoelastic problems

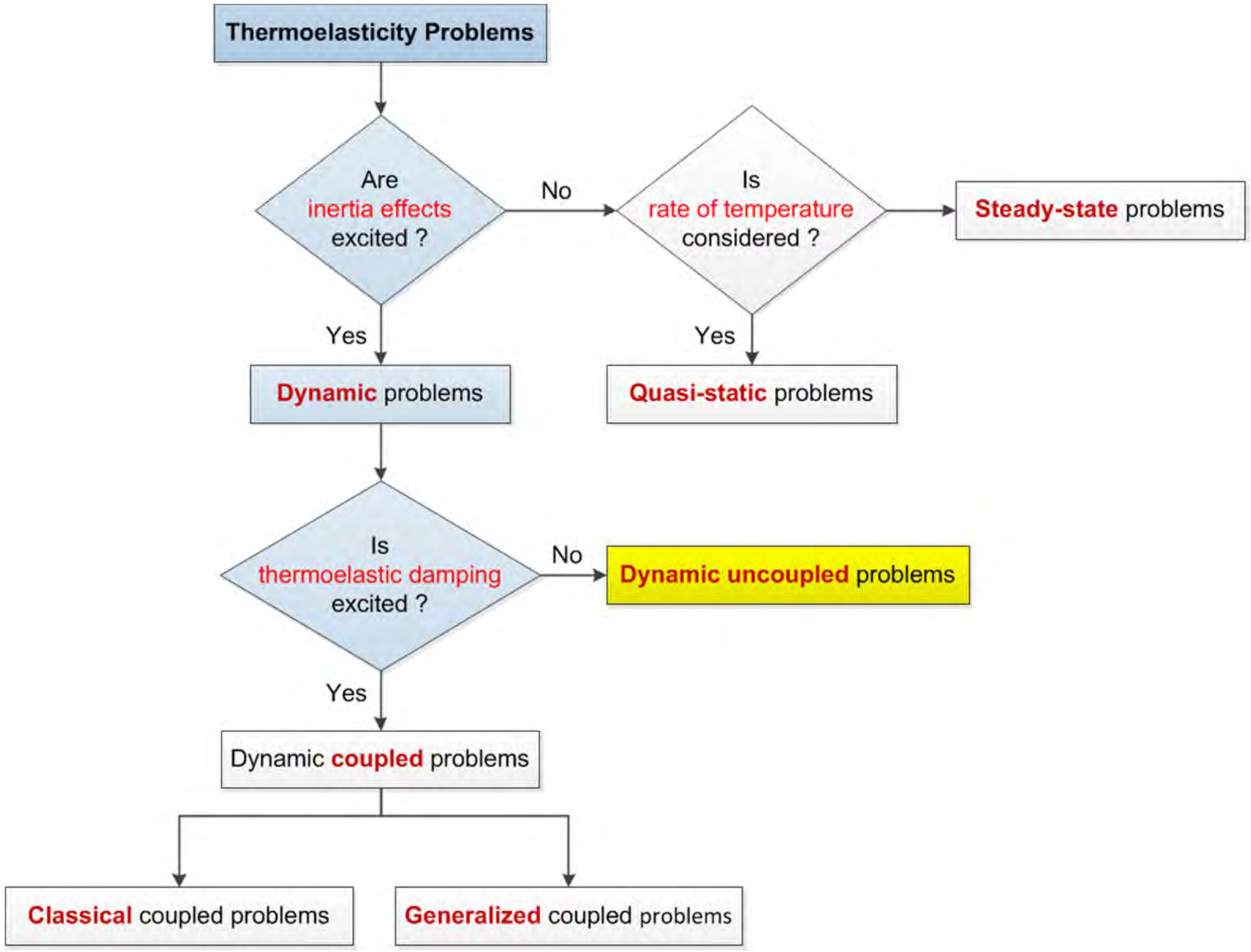

Dynamic uncoupled problems

Considering mechanical damping

equation of motion

$$(C_{ijkl}u_{k,l})_{,j} - (\beta_{ij}T)_{,j} + X_i = \rho\ddot{u}_i + \zeta\dot{u}_i$$

energy equation

$$\rho c\dot{T} - \left(\kappa_{ij}T_{,j}\right)_{,i} = R$$

- $\zeta \rightarrow$ mechanical damping coefficient of material

Classification of thermoelastic problems

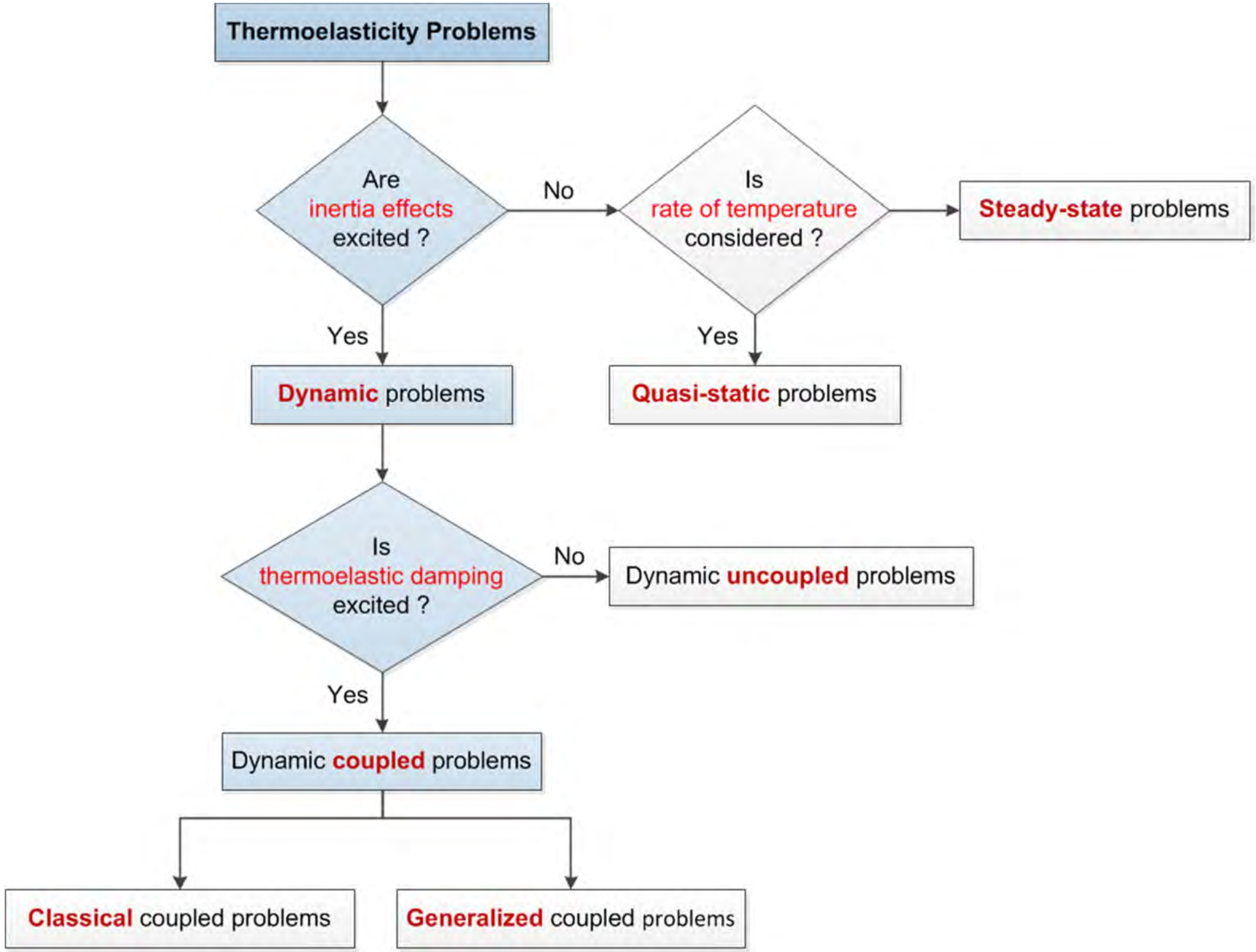

Coupled thermoelasticity

- ✓ the time rate of strain is taken into account in the energy equation
- ✓ elasticity and energy equations are coupled.
- ✓ these coupled equations must be solved simultaneously.

equation of motion

energy equation

Mechanical and thermal BCs and ICs

$$T(x_i,t), u_i(x_i,t)$$

Classification of thermoelastic problems

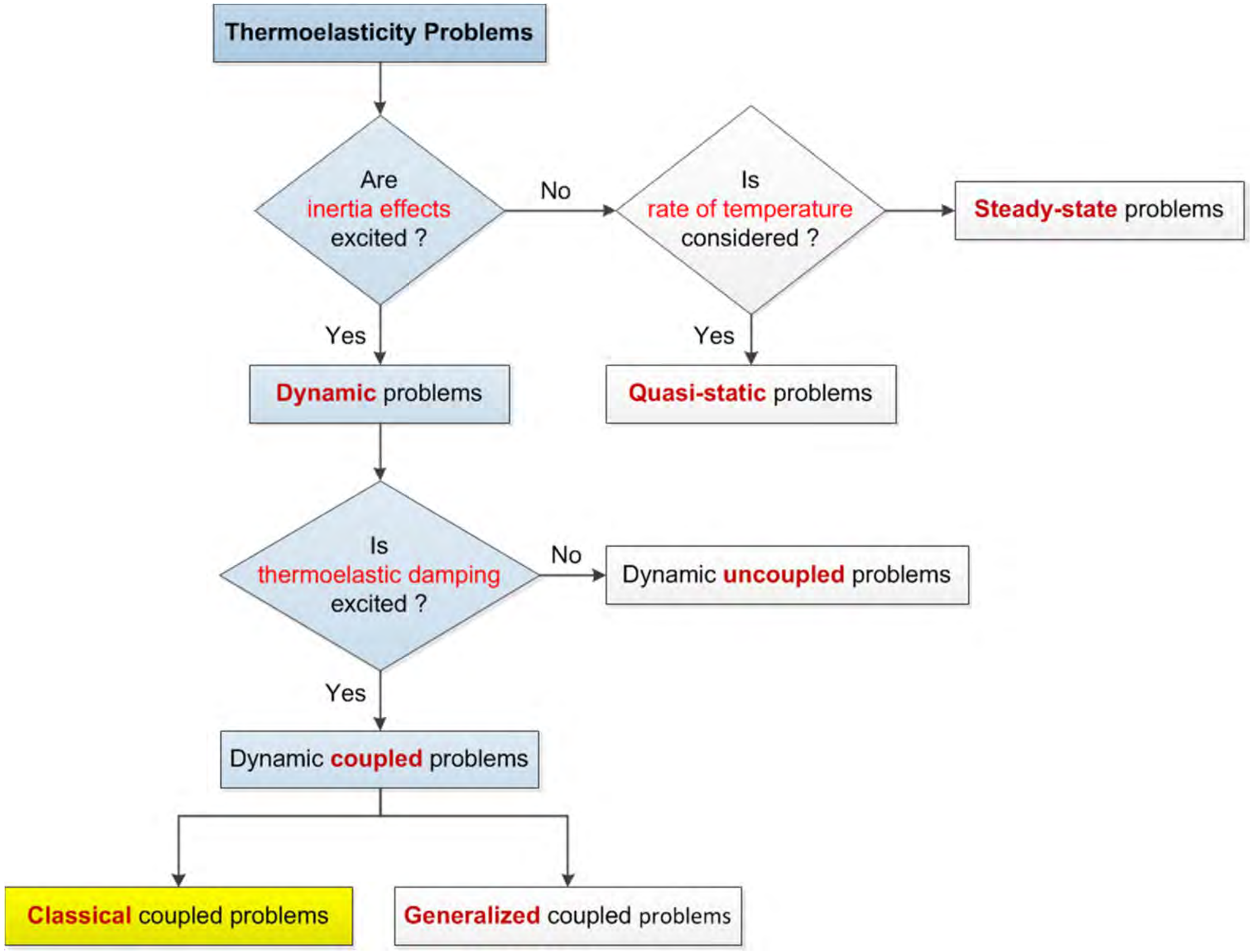

Classical coupled problems

equation of motion

$$(C_{ijkl}u_{k,l})_{,j} - (\beta_{ij}T)_{,j} + X_i = \rho\ddot{u}_i$$

energy equation

$$\rho c\dot{T} - \left(\kappa_{ij}T_{,j}\right)_{,i} + T_0\beta_{ij}\dot{u}_{i,j} = R$$

- $T_0 \rightarrow$ reference temperature

Fundamentals of Linear Thermoelasticity

Classification of thermoelastic problems

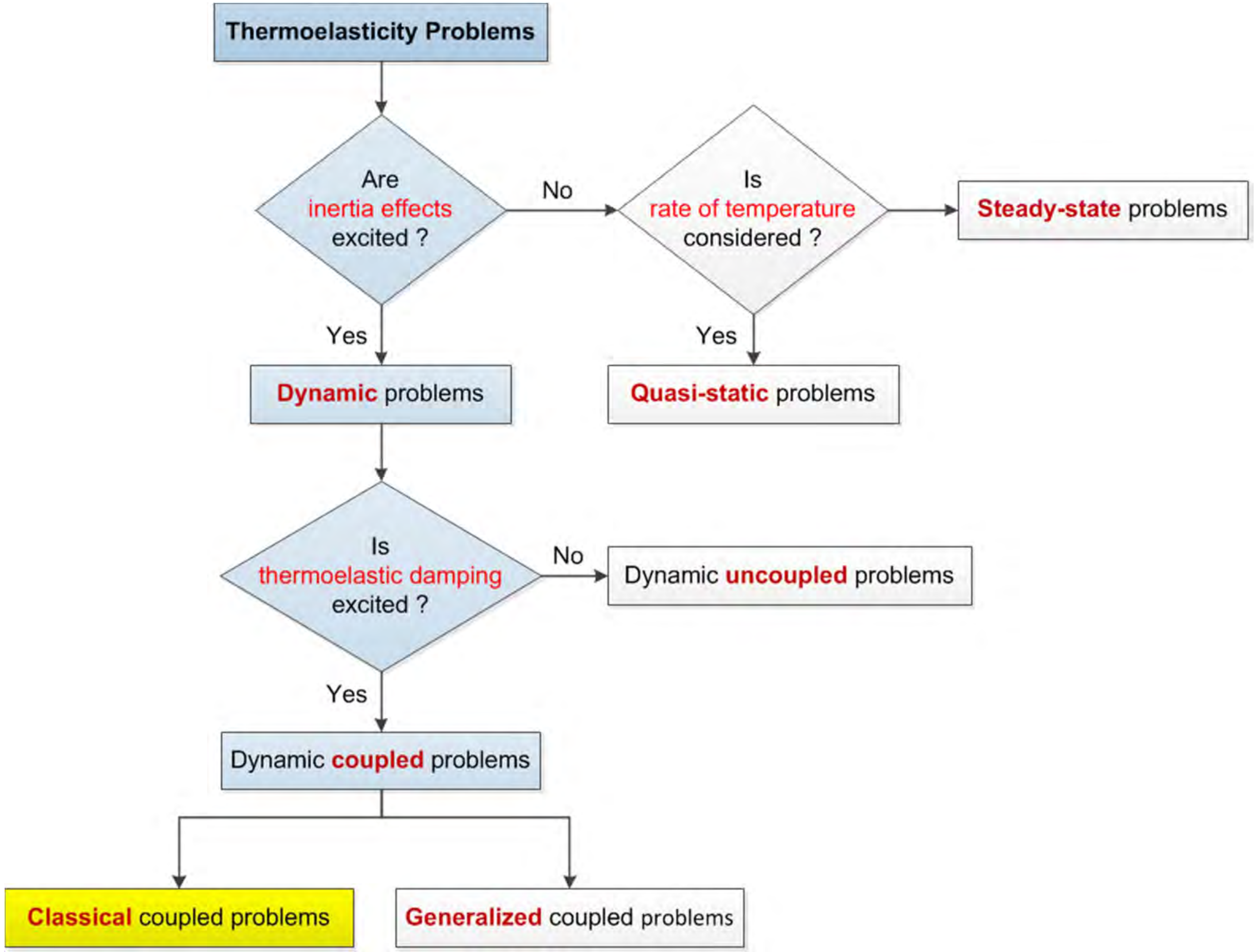

Classical coupled problems

equation of motion

$$\left(C_{ijkl}u_{k,l}\right)_{,j} - \left(\beta_{ij}T\right)_{,j} + X_i = \rho\ddot{u}_i$$

energy equation

$$\rho c\dot{T} - \left(\kappa_{ij}T_{,j}\right)_{,i} + T_0\beta_{ij}\dot{u}_{i,j} = R$$

- ✓ $T_0 \rightarrow$ reference temperature

infinite propagation speed for the thermal disturbances !!!

Classification of thermoelastic problems

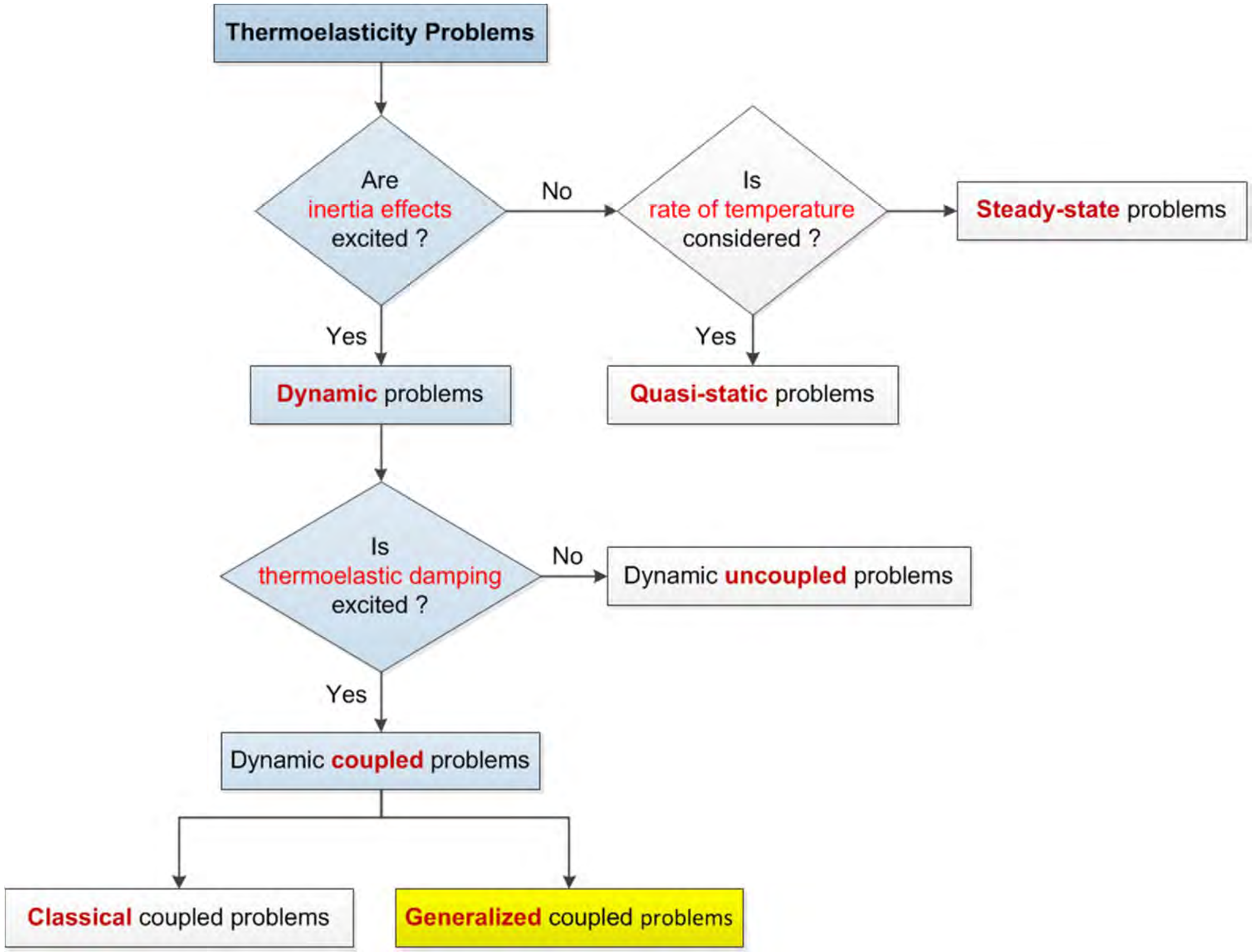

- in the **classical thermoelasticity**
  - ✓ heat conduction equation is of a parabolic type.
  - ✓ Predicting infinite speed for heat propagation
  - ✓ The prediction is not physically acceptable.
  - ✓ thermal wave disturbances are not detectable.
- **generalized theories** of thermoelasticity
  - ✓ non-classical **theories** with the finite speed of the thermal wave.

Fundamentals of Linear Thermoelasticity

Classification of thermoelastic problems

Generalized Theories of coupled Thermoelasticity

Lord-Shulman (LS) model

$$(C_{ijkl}u_{k,l})_{,j} - (\beta_{ij}T)_{,j} + X_i = \rho\ddot{u}_i$$

$$\rho c t_0 \ddot{T} + \rho c \dot{T} - (\kappa_{ij}T_{,j})_{,i} + t_0 T_0 \beta_{ij}\ddot{u}_{i,j} + T_0\beta_{ij}\dot{u}_{i,j} = R + t_0\dot{R}$$

- $t_0 \rightarrow$ LS relaxation time

Green-Lindsay (GL) model

$$(C_{ijkl}u_{k,l})_{,j} - (\beta_{ij}T)_{,j} - (t_1\beta_{ij}\dot{T})_{,j} + X_i = \rho\ddot{u}_i$$

$$\rho c t_2 \ddot{T} + \rho c \dot{T} - 2\tilde{c}_i \dot{T}_{,i} - (\kappa_{ij}T_{,j})_{,i} + T_0\beta_{ij}\dot{u}_{i,j} = R$$

- $t_1, t_2 \rightarrow$ GL relaxation times
- $\tilde{c}_i \rightarrow$ GL material constants

Green-Naghdi (GN) model

without energy dissipation

$$(C_{ijkl}u_{k,l})_{,j} - (\beta_{ij}T)_{,j} + X_i = \rho\ddot{u}_i$$

$$\rho c \ddot{T} - \left(\kappa_{ij}{}^{*}T_{,j}\right)_{,i} + T_0\beta_{ij}\ddot{u}_{i,j} = R$$

- $\kappa_{ij}{}^{*} \rightarrow$ GN material constants

Outlines

1. Introduction to rotating disk
2. Fundamentals of Linear Thermoelasticity
3. **Literature review & present work**
4. Analytical approach
5. Numerical approach
6. Conclusion

Conclusion of the literature review

- Coupled thermoelasticity problems are still topics of active research.
- Analytical solution of the these problems are mathematically difficult.
- Number of papers on analytical solutions is limited.
- Numerical methods are often used to solve these problems.
- Numerical solutions of these problems have been presented in many articles.
- Finite element method is still applied as a powerful numerical tool in such problems.
- The major presented solutions are related to the basic problems (infinite medium, half-space, layer and axisymmetric problems).
- Analytical and numerical solution of rotating disk problems has never before been presented.

Present work

- **Main purpose**
  - ➢ Study of coupled thermoelastic behavior in disks subjected to thermal shock loads
    - ✓ based on the generalized and classic theories
    - ✓ Disks with constant and variable thickness
    - ✓ Made of FGM
- **Implementation**
  - ➢ Analytical approach
  - ➢ Numerical approach

Outlines

1. Introduction to rotating disk
2. Fundamentals of Linear Thermoelasticity
3. Literature review & present work
4. **Analytical approach**
   - **Solution method**
   - Numerical evaluation
5. Numerical approach
6. Conclusion

Analytical approach - Solution method

Governing equations

Consider
- An annular rotating disk with constant thickness,
- made of isotropic & homogeneous material,
- Under axisymmetric thermal and mechanical shock loads.

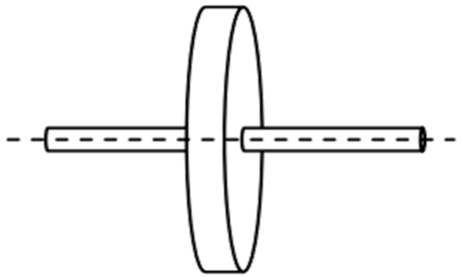

Based on LS generalized coupled theory

Eq. of motion $(C_{ijkl}u_{k,l})_{,j} - (\beta_{ij}T)_{,j} + X_i = \rho\ddot{u}_i$ $\Rightarrow$

$$\left\{\kappa\left[\frac{\partial^2}{\partial r^2}+\frac{1}{r}\frac{\partial}{\partial r}\right]-\rho c\frac{\partial}{\partial t}\left(1+t_0\frac{\partial}{\partial t}\right)\right\}T$$
$$-\tilde{\beta}T_0\left\{t_0\left[\frac{\partial^3}{\partial r\partial t^2}+\frac{1}{r}\frac{\partial^2}{\partial t^2}\right]+\frac{\partial^2}{\partial r\partial t}+\frac{1}{r}\frac{\partial}{\partial t}\right\}u=0 \qquad \text{I}$$

energy Eq. $\rho c t_0\ddot{T}+\rho c\dot{T}-(\kappa_{ij}T_{,j})_{,i} + t_0T_0\beta_{ij}\ddot{u}_{i,j}+T_0\beta_{ij}\dot{u}_{i,j}=R+t_0\dot{R}$ $\Rightarrow$

$$\left\{(\tilde{\lambda}+2\mu)\left[\frac{\partial^2}{\partial r^2}+\frac{1}{r}\frac{\partial}{\partial r}-\frac{1}{r^2}\right]-\rho\frac{\partial^2}{\partial t^2}\right\}u-\tilde{\beta}\frac{\partial T}{\partial r}=-\rho r\omega^2 \qquad \text{II}$$

$$\tilde{\lambda}=\frac{2\mu}{\lambda+2\mu}\lambda \qquad \tilde{\beta}=\frac{2\mu}{\lambda+2\mu}(3\lambda+2\mu)\alpha$$

- λ & μ $\rightarrow$ Lame constants
- α $\rightarrow$ coefficient of linear thermal expansion

Analytical approach - Solution method

Governing equations

Coupled System Of Equations

$$
\begin{cases}
\text{I} \quad \left\{\kappa\left[\frac{\partial^2}{\partial r^2}+\frac{1}{r}\frac{\partial}{\partial r}\right]-\rho c\frac{\partial}{\partial t}\left(1+t_0\frac{\partial}{\partial t}\right)\right\}T-\tilde{\beta}T_0\left\{t_0\left[\frac{\partial^3}{\partial r\partial t^2}+\frac{1}{r}\frac{\partial^2}{\partial t^2}\right]+\frac{\partial^2}{\partial r\partial t}+\frac{1}{r}\frac{\partial}{\partial t}\right\}u=0 \\
\text{II} \quad \left\{(\tilde{\lambda}+2\mu)\left[\frac{\partial^2}{\partial r^2}+\frac{1}{r}\frac{\partial}{\partial r}-\frac{1}{r^2}\right]-\rho\frac{\partial^2}{\partial t^2}\right\}u-\tilde{\beta}\frac{\partial T}{\partial r}=-\rho r\omega^2
\end{cases}
$$

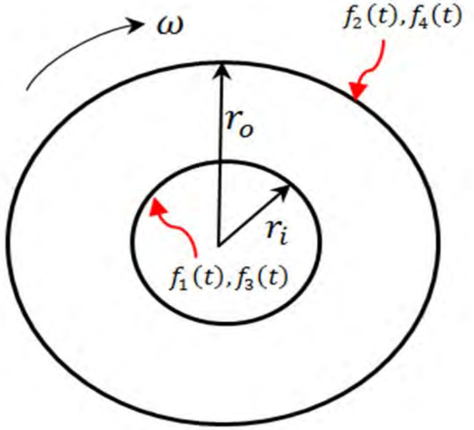

thermal BCs. & ICs

$$k_{11}\frac{\partial T}{\partial r}\Big|_{r=r_i}+k_{12}T(r_i,t)=f_1(t)$$
$$k_{21}\frac{\partial T}{\partial r}\Big|_{r=r_o}+k_{22}T(r_o,t)=f_2(t)$$

$$T(r,0)=g_1(r),$$
$$\dot{T}(r,0)=g_2(r)$$

Mechanical BCs. & ICs

$$k_{31}\frac{\partial u}{\partial r}\Big|_{r=r_i}+k_{32}u(r_i,t)=f_3(t)$$
$$k_{41}\frac{\partial u}{\partial r}\Big|_{r=r_o}+k_{42}u(r_o,t)=f_4(t)$$

$$u(r,0)=g_3(r),$$
$$\dot{u}(r,0)=g_4(r)$$

r_i	Inner radius of the disk
r_o	Outer radius of the disk
$f_1(t)$ -$f_4(t)$	time dependent known functions
k_{ij}	constant parameters
$g_1(r)-g_4(r)$	known functions of r

Analytical approach - Solution method

Governing equations in Non-dimensional form

Non-dimensional parameters

$$\hat{r} = \frac{r}{l}, \qquad \hat{t} = \frac{tV_e}{l}, \qquad \hat{t}_0 = \frac{t_0 V_e}{l}$$

$$\hat{\sigma}_{rr} = \frac{\sigma_{rr}}{\tilde{\beta} T_0}, \qquad \hat{\sigma}_{\theta\theta} = \frac{\sigma_{\theta\theta}}{\tilde{\beta} T_0}, \qquad \hat{T} = \frac{T}{T_0}$$

$$\hat{u} = \frac{(\tilde{\lambda} + 2\mu)u}{l\tilde{\beta} T_0}, \qquad \hat{\omega} = \sqrt{\frac{\rho l^2}{\tilde{\beta} T_0}}\,\omega$$

propagation speed of elastic longitudinal wave

$$V_e = \sqrt{(\tilde{\lambda} + 2\mu)/\rho}$$

unit length

$$l = k/\rho\, c V_e$$

Analytical approach - Solution method

Governing equations in Non-dimensional form

Coupled System Of Equations

$$\begin{cases} \text{I} \quad \left\{\frac{\partial^2}{\partial \hat{r}^2}+\frac{1}{\hat{r}}\frac{\partial}{\partial \hat{r}}-\frac{1}{\hat{r}^2}-\frac{\partial^2}{\partial \hat{t}^2}\right\}\hat{u}-\frac{\partial \hat{T}}{\partial \hat{r}}=-\hat{r}\hat{\omega}^2 \\ \text{II} \quad \left\{\frac{\partial^2}{\partial \hat{r}^2}+\frac{1}{\hat{r}}\frac{\partial}{\partial \hat{r}}-\frac{\partial}{\partial \hat{t}}\left(1+\hat{t}_0\frac{\partial}{\partial \hat{t}}\right)\right\}\hat{T}-\boxed{C\left\{\hat{t}_0\left[\frac{\partial^3}{\partial \hat{r}\partial \hat{t}^2}+\frac{1}{\hat{r}}\frac{\partial^2}{\partial \hat{t}^2}\right]+\frac{\partial^2}{\partial \hat{r}\partial \hat{t}}+\frac{1}{\hat{r}}\frac{\partial}{\partial \hat{t}}\right\}\hat{u}}=0 \end{cases}$$

where

$$C=\frac{T_0\tilde{\beta}^2}{\rho c(\tilde{\lambda}+2\mu)}$$

Thermoelastic damping or coupling parameter

- Non-dimensional propagation speed of thermal wave $\rightarrow \hat{V}_T=\sqrt{1/\hat{t}_0}$
- Non-dimensional propagation speed of elastic longitudinal wave $\rightarrow \hat{V}_e=1$

Analytical approach - Solution method

Solution of non-dimensional equations

Coupled System Of Equations

$$\begin{cases} \left\{\dfrac{\partial^2}{\partial \hat{r}^2}+\dfrac{1}{\hat{r}}\dfrac{\partial}{\partial \hat{r}}-\dfrac{1}{\hat{r}^2}-\dfrac{\partial^2}{\partial \hat{t}^2}\right\}\hat{u}-\dfrac{\partial \hat{T}}{\partial \hat{r}}=-\hat{r}\widehat{\omega}^2 & \text{I} \\ \left\{\dfrac{\partial^2}{\partial \hat{r}^2}+\dfrac{1}{\hat{r}}\dfrac{\partial}{\partial \hat{r}}-\dfrac{\partial}{\partial \hat{t}}\left(1+\hat{t}_0\dfrac{\partial}{\partial \hat{t}}\right)\right\}\hat{T}-C\left\{\hat{t}_0\left[\dfrac{\partial^3}{\partial \hat{r}\partial \hat{t}^2}+\dfrac{1}{\hat{r}}\dfrac{\partial^2}{\partial \hat{t}^2}\right]+\dfrac{\partial^2}{\partial \hat{r}\partial \hat{t}}+\dfrac{1}{\hat{r}}\dfrac{\partial}{\partial \hat{t}}\right\}\hat{u}=0 & \text{II} \end{cases}$$

Thermal and mechanical BCs. & ICs

$$\hat{k}_{11}\frac{\partial \hat{T}}{\partial \hat{r}}\Big|_{\hat{r}=a}+\hat{k}_{12}\hat{T}(a,t)=\hat{f}_1(\hat{t}) \qquad \hat{k}_{21}\frac{\partial \hat{T}}{\partial \hat{r}}\Big|_{\hat{r}=b}+\hat{k}_{22}\hat{T}(b,t)=\hat{f}_2(\hat{t})$$

$$\hat{k}_{31}\frac{\partial \hat{u}}{\partial \hat{r}}\Big|_{\hat{r}=a}+\hat{k}_{32}\hat{u}(a,t)=\hat{f}_3(\hat{t}) \qquad \hat{k}_{41}\frac{\partial \hat{u}}{\partial \hat{r}}\Big|_{\hat{r}=b}+\hat{k}_{42}\hat{u}(b,t)=\hat{f}_4(\hat{t})$$

$$\hat{T}(\hat{r},0)=\hat{g}_1(\hat{r}), \quad \dot{\hat{T}}(\hat{r},0)=\hat{g}_2(\hat{r})$$

$$\hat{u}(\hat{r},0)=\hat{g}_3(\hat{r}), \quad \dot{\hat{u}}(\hat{r},0)=\hat{g}_4(\hat{r})$$

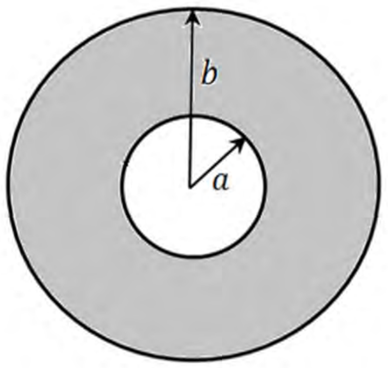

Analytical approach - Solution method

Solution of non-dimensional equations

$$\left\{\frac{\partial^2}{\partial \hat{r}^2}+\frac{1}{\hat{r}}\frac{\partial}{\partial \hat{r}}-\frac{\partial}{\partial \hat{t}}\left(1+\hat{t}_0\frac{\partial}{\partial \hat{t}}\right)\right\}\hat{T}-C\left\{\hat{t}_0\left[\frac{\partial^3}{\partial \hat{r}\partial \hat{t}^2}+\frac{1}{\hat{r}}\frac{\partial^2}{\partial \hat{t}^2}\right]+\frac{\partial^2}{\partial \hat{r}\partial \hat{t}}+\frac{1}{\hat{r}}\frac{\partial}{\partial \hat{t}}\right\}\hat{u}=0$$

energy Eq.

decomposition

$$\frac{\partial^2 T_1}{\partial r^2}+\frac{1}{r}\frac{\partial T_1}{\partial r}-\dot{T}_1-t_0\ddot{T}_1=0$$

$$k_{11}\frac{\partial T_1}{\partial r}|_{r=a}+k_{12}T_1(a,t)=f_1(t)$$

$$k_{21}\frac{\partial T_1}{\partial r}|_{r=b}+k_{22}T_1(b,t)=f_2(t)$$

$$T_1(r,0)=0 \quad , \quad \dot{T}_1(r,0)=0$$

$$\frac{\partial^2 T_2}{\partial r^2}+\frac{1}{r}\frac{\partial T_2}{\partial r}-\dot{T}_2-t_0\ddot{T}_2=C\left\{t_0\left(\ddot{u}_{,r}+\frac{\ddot{u}}{r}\right)+\dot{u}_{,r}+\frac{\dot{u}}{r}\right\}$$

$$k_{11}\frac{\partial T_2}{\partial r}|_{r=a}+k_{12}T_2(a,t)=0$$

$$k_{21}\frac{\partial T_2}{\partial r}|_{r=b}+k_{22}T_2(b,t)=0$$

$$T_2(r,0)=g_1(r) \quad , \quad \dot{T}_2(r,0)=g_2(r)$$

principle of superposition

$$T(r,t)=T_1(r,t)+T_2(r,t)$$

Analytical approach - Solution method

Solution of non-dimensional equations

$$\left\{\frac{\partial^2}{\partial \hat{r}^2}+\frac{1}{\hat{r}}\frac{\partial}{\partial \hat{r}}-\frac{1}{\hat{r}^2}-\frac{\partial^2}{\partial \hat{t}^2}\right\}\hat{u}-\frac{\partial \hat{T}}{\partial \hat{r}}=-\hat{r}\hat{\omega}^2$$

Eq. of motion

decomposition

$$\frac{\partial^2 u_1}{\partial r^2}+\frac{1}{r}\frac{\partial u_1}{\partial r}-\frac{u_1}{r^2}-\ddot{u}_1=0$$

$$k_{31}\frac{\partial u_1}{\partial r}|_{r=a}+k_{32}u_1(a,t)=f_3(t)$$

$$k_{41}\frac{\partial u_1}{\partial r}|_{r=b}+k_{42}u_1(b,t)=f_4(t)$$

$$u_1(r,0)=0 \quad , \quad \dot{u}_1(r,0)=0$$

$$\frac{\partial^2 u_2}{\partial r^2}+\frac{1}{r}\frac{\partial u_2}{\partial r}-\frac{u_2}{r^2}-\ddot{u}_2=T_{,r}-r\omega^2$$

$$k_{31}\frac{\partial u_2}{\partial r}|_{r=a}+k_{32}u_2(a,t)=0$$

$$k_{41}\frac{\partial u_2}{\partial \hat{r}}|_{r=b}+k_{42}u_2(b,t)=0$$

$$u_2(r,0)=g_3(r) \quad , \quad \dot{u}_2(r,0)=g_4(r)$$

principle of superposition

$$u(r,t)=u_1(r,t)+u_2(r,t)$$

Analytical approach - Solution method

Solution of non-dimensional equations

$$\left\{\frac{\partial^2}{\partial \hat{r}^2}+\frac{1}{\hat{r}}\frac{\partial}{\partial \hat{r}}-\frac{1}{\hat{r}^2}-\frac{\partial^2}{\partial \hat{t}^2}\right\}\hat{u}-\frac{\partial \hat{T}}{\partial \hat{r}}=-\hat{r}\hat{\omega}^2$$

Eq. of motion

decomposition

$$\frac{\partial^2 u_1}{\partial r^2}+\frac{1}{r}\frac{\partial u_1}{\partial r}-\frac{u_1}{r^2}-\ddot{u}_1=0$$

$$k_{31}\frac{\partial u_1}{\partial r}|_{r=a}+k_{32}u_1(a,t)=f_3(t)$$

$$k_{41}\frac{\partial u_1}{\partial r}|_{r=b}+k_{42}u_1(b,t)=f_4(t)$$

$$u_1(r,0)=0 \quad , \quad \dot{u}_1(r,0)=0$$

$$\frac{\partial^2 u_2}{\partial r^2}+\frac{1}{r}\frac{\partial u_2}{\partial r}-\frac{u_2}{r^2}-\ddot{u}_2=T_{,r}-r\omega^2$$

$$k_{31}\frac{\partial u_2}{\partial r}|_{r=a}+k_{32}u_2(a,t)=0$$

$$k_{41}\frac{\partial u_2}{\partial \hat{r}}|_{r=b}+k_{42}u_2(b,t)=0$$

$$u_2(r,0)=g_3(r) \quad , \quad \dot{u}_2(r,0)=g_4(r)$$

Bessel equation and can be separately solved using finite Hankel transform

Analytical approach - Solution method

Solution of non-dimensional equations

Finite Hankel transform

$$\mathcal{H}[T_1(r,t)] = \bar{T}_1(t,\xi_m) = \int_a^b rT_1(r,t)\,K_0(r,\xi_m)dr$$

$$\mathcal{H}[u_1(r,t)] = \bar{u}_1(t,\eta_n) = \int_a^b ru_1(r,t)\,K_1(r,\eta_n)dr$$

kernel functions

$$K_0(r,\xi_m) = J_0(\xi_m r)\left(k_{21}\frac{\partial Y_0(\xi_m r)}{\partial r}|_{r=b} + k_{22}Y_0(\xi_m b\right)\right) - Y_0(\xi_m r)\left(k_{21}\frac{\partial J_0(\xi_m r)}{\partial r}|_{r=b} + k_{22}J_0(\xi_m b\right)\right)$$

$$K_1(r,\eta_n) = J_1(\eta_n r)\left(k_{41}\frac{\partial Y_1(\eta_n r)}{\partial r}|_{r=b} + k_{42}Y_1(\eta_n b\right)\right) - Y_1(\eta_n r)\left(k_{41}\frac{\partial J_1(\eta_n r)}{\partial r}|_{r=b} + k_{42}J_1(\eta_n b\right)\right)$$

ξ_m and η_n are positive roots of the following equations

$$\left(k_{11}\frac{\partial Y_0(\xi_m r)}{\partial r}|_{r=a} + k_{12}Y_0(\xi_m a\right)\right)\left(k_{21}\frac{\partial J_0(\xi_m r)}{\partial r}|_{r=b} + k_{22}J_0(\xi_m b\right)\right) - \left(k_{21}\frac{\partial Y_0(\xi_m r)}{\partial r}|_{r=b} + k_{22}Y_0(\xi_m b\right)\right)\left(k_{11}\frac{\partial J_0(\xi_m r)}{\partial r}|_{r=a} + k_{12}J_0(\xi_m a\right)\right) = 0$$

$$\left(k_{31}\frac{\partial Y_1(\eta_n r)}{\partial r}|_{r=a} + k_{32}Y_1(\eta_n a\right)\right)\left(k_{41}\frac{\partial J_1(\eta_n r)}{\partial r}|_{r=b} + k_{42}J_1(\eta_n b\right)\right) - \left(k_{41}\frac{\partial Y_1(\eta_n r)}{\partial r}|_{r=b} + k_{42}Y_1(\eta_n b\right)\right)\left(k_{31}\frac{\partial J_1(\eta_n r)}{\partial r}|_{r=a} + k_{32}J_1(\eta_n a\right)\right) = 0$$

Analytical approach - Solution method

Solution of non-dimensional equations

Uncoupled sub-IBVPs (Bessel equations)

$$\frac{\partial^2 u_1}{\partial r^2} + \frac{1}{r}\frac{\partial u_1}{\partial r} - \frac{u_1}{r^2} - \ddot{u}_1 = 0$$

$$k_{31}\left.\frac{\partial u_1}{\partial r}\right|_{r=a} + k_{32}u_1(a,t) = f_3(t)$$

$$k_{41}\left.\frac{\partial u_1}{\partial r}\right|_{r=b} + k_{42}u_1(b,t) = f_4(t)$$

$$u_1(r,0) = 0 \quad , \quad \dot{u}_1(r,0) = 0$$

$$\frac{\partial^2 T_1}{\partial r^2} + \frac{1}{r}\frac{\partial T_1}{\partial r} - \dot{T}_1 - t_0\ddot{T}_1 = 0$$

$$k_{11}\left.\frac{\partial T_1}{\partial r}\right|_{r=a} + k_{12}T_1(a,t) = f_1(t)$$

$$k_{21}\left.\frac{\partial T_1}{\partial r}\right|_{r=b} + k_{22}T_1(b,t) = f_2(t)$$

$$T_1(r,0) = 0 \quad , \quad \dot{T}_1(r,0) = 0$$

Taking the finite Hankel transform

$$\ddot{\overline{u}}_1 + \eta_n^2\overline{u}_1 = \frac{2}{\pi}\left(f_4(t) - \frac{d_4}{d_3}f_3(t)\right)$$

$$t_0\ddot{\overline{T}}_1 + \dot{\overline{T}}_1 + \xi_m^2\overline{T}_1 = \frac{2}{\pi}\left(f_2(t) - \frac{d_2}{d_1}f_1(t)\right)$$

Solving ODEs

$$\overline{u}_1(t, \eta_n)$$

$$\overline{T}_1(t, \xi_m)$$

Analytical approach - Solution method

Solution of non-dimensional equations

Uncoupled sub-IBVPs (Bessel equations)

$$\ddot{\bar{u}}_1 + \eta_n^2 \bar{u}_1 = \frac{2}{\pi}\left(f_4(t) - \frac{d_4}{d_3} f_3(t) \right) \qquad t_0 \ddot{\bar{T}}_1 + \dot{\bar{T}}_1 + \xi_m^2 \bar{T}_1 = \frac{2}{\pi}\left(f_2(t) - \frac{d_2}{d_1} f_1(t) \right)$$

Solving ODEs

$$\bar{u}_1(t, \eta_n) \qquad \bar{T}_1(t, \xi_m)$$

Inverse finite Hankel transforms

$$u_1(r,t) = \sum_{n=1}^{\infty} \tilde{b}_n \bar{u}_1(t,\eta_n) K_1(r,\eta_n) \qquad T_1(r,t) = \sum_{m=1}^{\infty} \tilde{a}_m \bar{T}_1(t,\xi_m) K_0(r,\xi_m)$$

$$\tilde{a}_m = \frac{1}{\|K_0(r,\xi_m)\|^2} \quad , \quad \tilde{b}_n = \frac{1}{\|K_1(r,\eta_n)\|^2}$$

Analytical approach - Solution method

Solution of non-dimensional equations

$$\left\{\frac{\partial^2}{\partial \hat{r}^2}+\frac{1}{\hat{r}}\frac{\partial}{\partial \hat{r}}-\frac{1}{\hat{r}^2}-\frac{\partial^2}{\partial \hat{t}^2}\right\}\hat{u}-\frac{\partial \hat{T}}{\partial \hat{r}}=-\hat{r}\hat{\omega}^2$$

Eq. of motion

decomposition

$$\frac{\partial^2 u_1}{\partial r^2}+\frac{1}{r}\frac{\partial u_1}{\partial r}-\frac{u_1}{r^2}-\ddot{u}_1=0$$

$$k_{31}\frac{\partial u_1}{\partial r}|_{r=a}+k_{32}u_1(a,t)=f_3(t)$$

$$k_{41}\frac{\partial u_1}{\partial r}|_{r=b}+k_{42}u_1(b,t)=f_4(t)$$

$$u_1(r,0)=0 \quad , \quad \dot{u}_1(r,0)=0$$

$$\frac{\partial^2 u_2}{\partial r^2}+\frac{1}{r}\frac{\partial u_2}{\partial r}-\frac{u_2}{r^2}-\ddot{u}_2=T_{,r}-r\omega^2$$

$$k_{31}\frac{\partial u_2}{\partial r}|_{r=a}+k_{32}u_2(a,t)=0$$

$$k_{41}\frac{\partial u_2}{\partial \hat{r}}|_{r=b}+k_{42}u_2(b,t)=0$$

$$u_2(r,0)=g_3(r) \quad , \quad \dot{u}_2(r,0)=g_4(r)$$

$$T_2(r,t)=\sum_{m=1}^{\infty}\sum_{n=1}^{\infty}Q_{mn}(t)K_0(r,\xi_m) \quad , \quad u_2(r,t)=\sum_{m=1}^{\infty}\sum_{n=1}^{\infty}S_{mn}(t)K_1(r,\eta_n)$$

Analytical approach - Solution method

Solution of non-dimensional equations

Coupled System Of Equations

$$\begin{cases} \text{I} \quad \left\{\frac{\partial^2}{\partial\hat{r}^2}+\frac{1}{\hat{r}}\frac{\partial}{\partial\hat{r}}-\frac{1}{\hat{r}^2}-\frac{\partial^2}{\partial\hat{t}^2}\right\}\hat{u}-\frac{\partial\hat{T}}{\partial\hat{r}}=-\hat{r}\hat{\omega}^2 \\ \text{II} \quad \left\{\frac{\partial^2}{\partial\hat{r}^2}+\frac{1}{\hat{r}}\frac{\partial}{\partial\hat{r}}-\frac{\partial}{\partial\hat{t}}\left(1+\hat{t}_0\frac{\partial}{\partial\hat{t}}\right)\right\}\hat{T}-C\left\{\hat{t}_0\left[\frac{\partial^3}{\partial\hat{r}\partial\hat{t}^2}+\frac{1}{\hat{r}}\frac{\partial^2}{\partial\hat{t}^2}\right]+\frac{\partial^2}{\partial\hat{r}\partial\hat{t}}+\frac{1}{\hat{r}}\frac{\partial}{\partial\hat{t}}\right\}\hat{u}=0 \end{cases}$$

$$T(r,t)=\sum_{m=1}^{\infty}\tilde{a}_m\bar{T}_1(t,\xi_m)K_0(r,\xi_m)+\sum_{m=1}^{\infty}\sum_{n=1}^{\infty}Q_{mn}(t)K_0(r,\xi_m)$$

$$u(r,t)=\sum_{n=1}^{\infty}\tilde{b}_n\bar{u}_1(t,\eta_n)K_1(r,\eta_n)+\sum_{m=1}^{\infty}\sum_{n=1}^{\infty}S_{mn}(t)K_1(r,\eta_n)$$

Outlines

1. Introduction to rotating disk
2. Fundamentals of Linear Thermoelasticity
3. Literature review & present work
4. **Analytical approach**
   - Solution method
   - **Numerical evaluation**
5. Numerical approach
6. Conclusion

Analytical approach - Numerical evaluation

Specifications of numerical example

geometry

$$a = 1$$
$$b = 2$$

material properties

$$\lambda = 40.4\ \mathrm{GPa}$$
$$\mu = 27\ \mathrm{GPa}$$
$$\alpha = 23 \times 10^{-6}\ \mathrm{K}^{-1}$$
$$\rho = 2707\ \mathrm{kg/m^3}$$
$$k = 204\ \mathrm{W/m \cdot K}$$
$$c = 903\ \mathrm{J/kg \cdot K}$$

Boundary conditions

at $\hat{r} = a \rightarrow \begin{cases} -\dfrac{\partial \hat{T}}{\partial \hat{r}} = \hat{q}_{in}(t) \\ \hat{u} = 0 \end{cases}$

at $\hat{r} = b \rightarrow \begin{cases} \hat{T} = 0 \\ \hat{\sigma}_{rr} = 0 \end{cases}$

$$\hat{q}_{in}(t) = \begin{cases} 0 & \hat{t} \leq 0 \\ 1 & \hat{t} > 0 \end{cases}$$

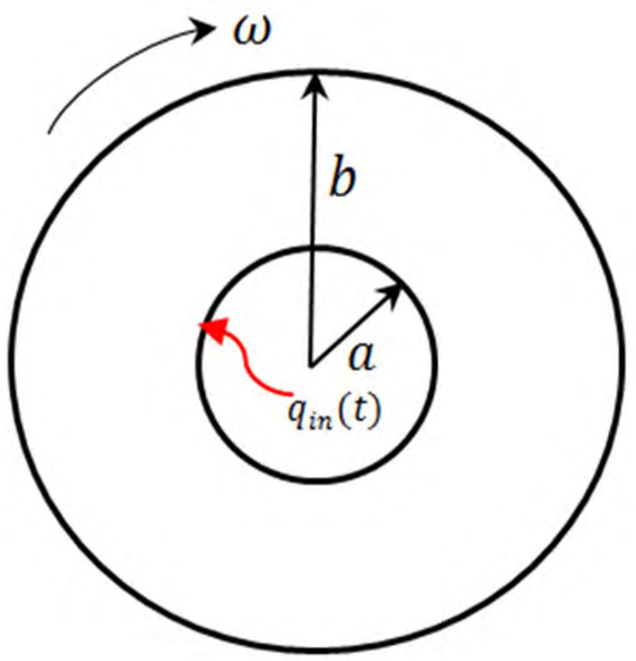

Analytical approach - Numerical evaluation

Validation

Based on classical theory of coupled thermoelasticity

Temperature

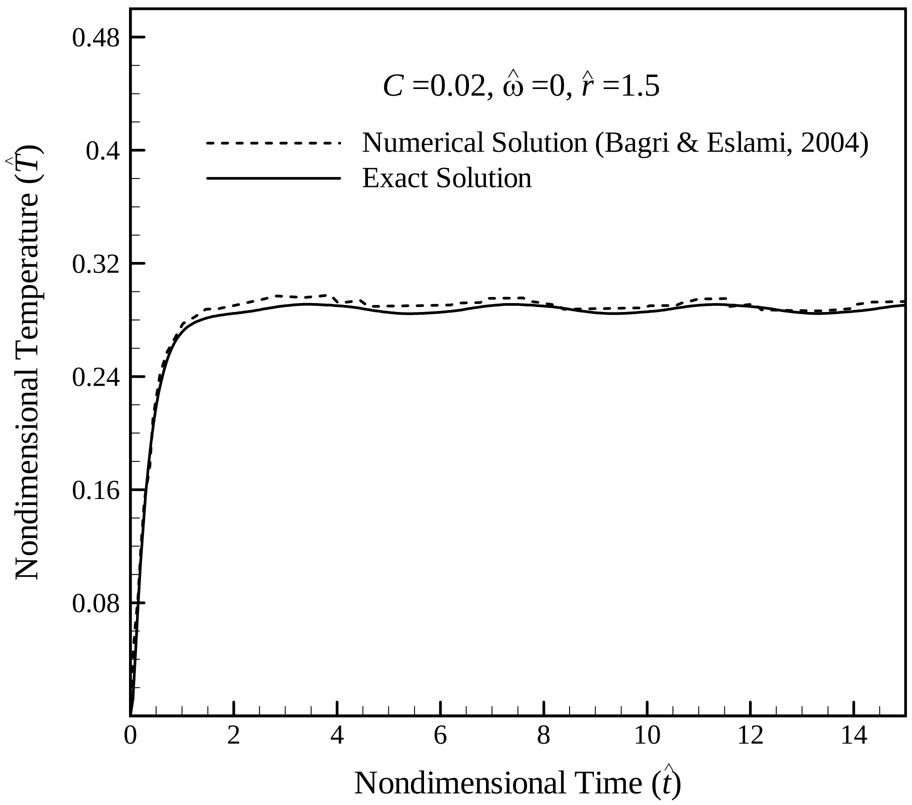

Radial displacement

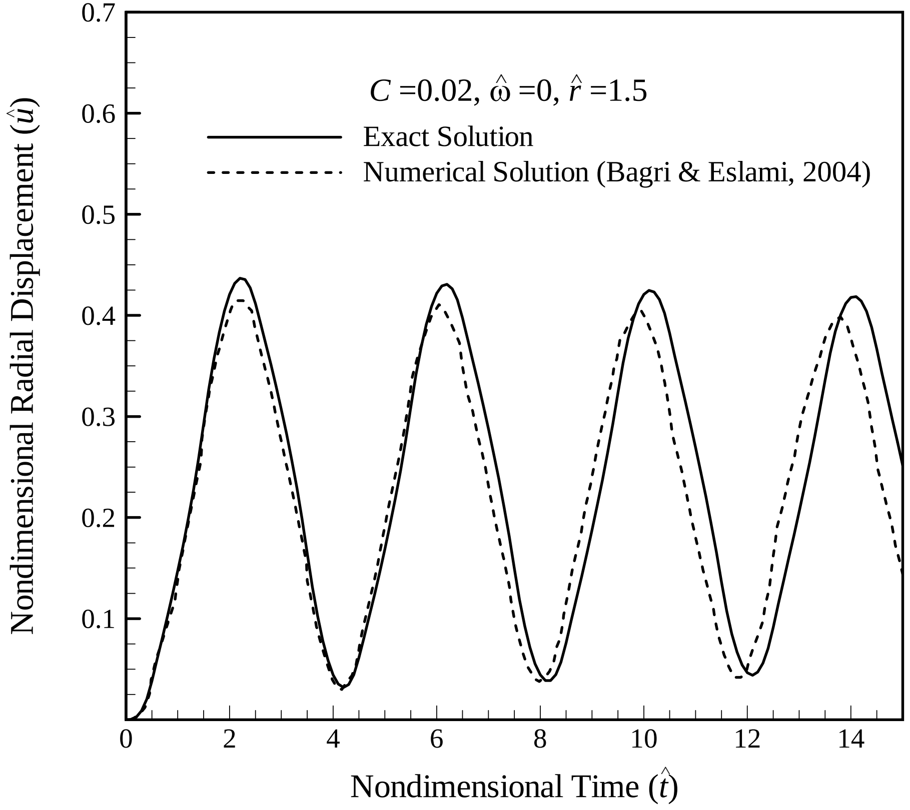

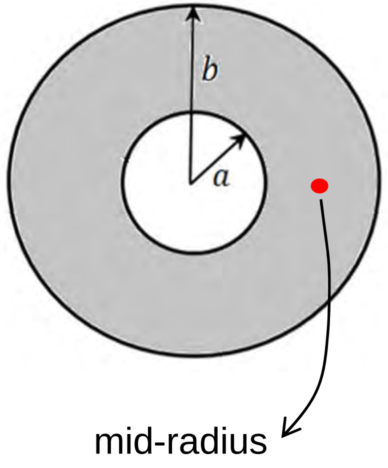

Time history of the non-dimensional solution at mid-radius

Analytical approach - Numerical evaluation

Validation

Based on LS generalized theory of coupled thermoelasticity

Temperature

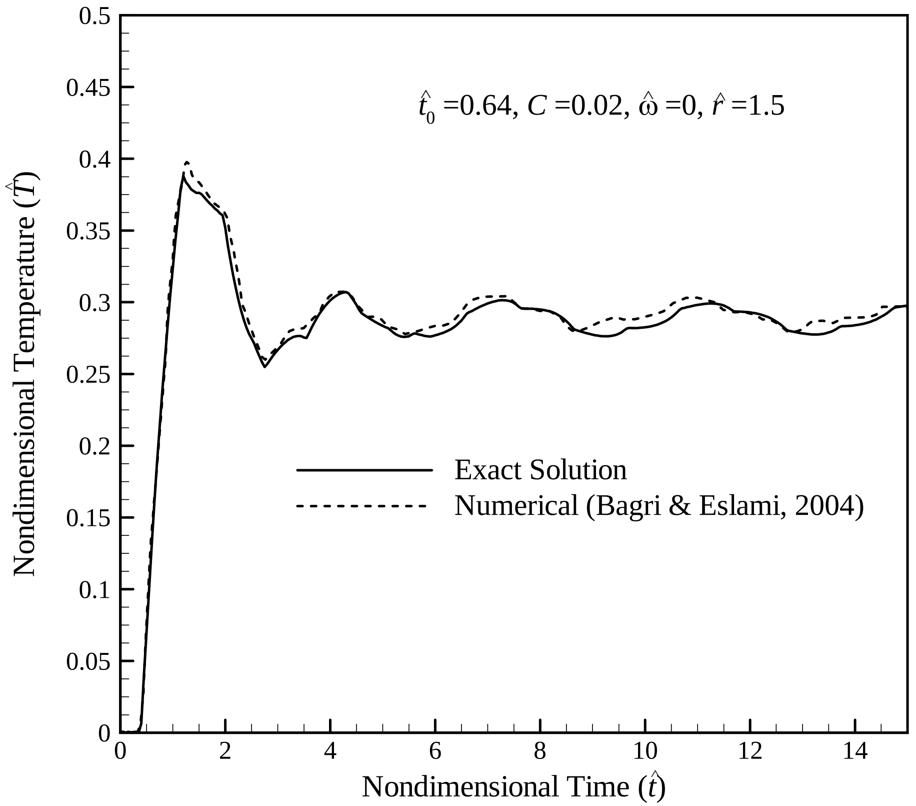

Radial displacement

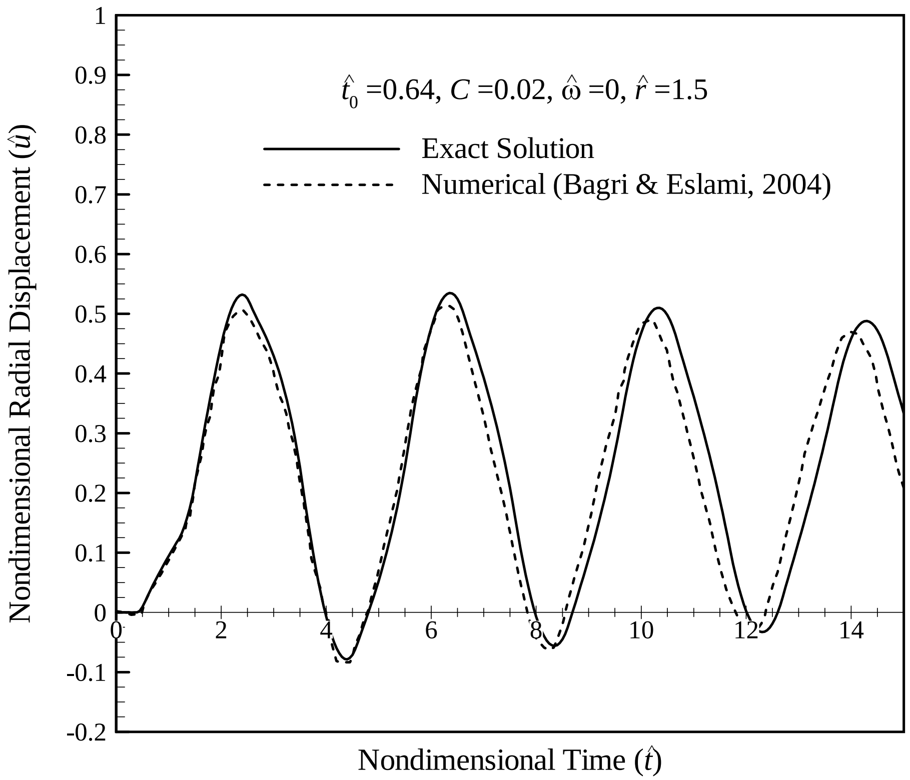

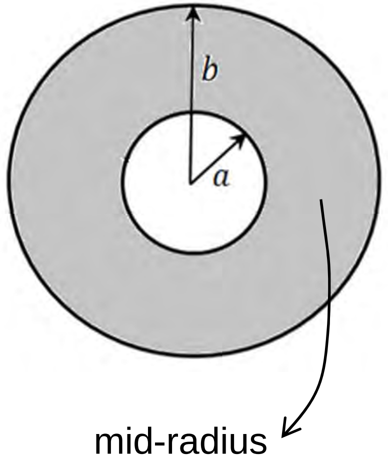

Time history of the non-dimensional solution at mid-radius

Analytical approach - Numerical evaluation

Results and discussion

Based on LS generalized theory of coupled thermoelasticity

temperature change

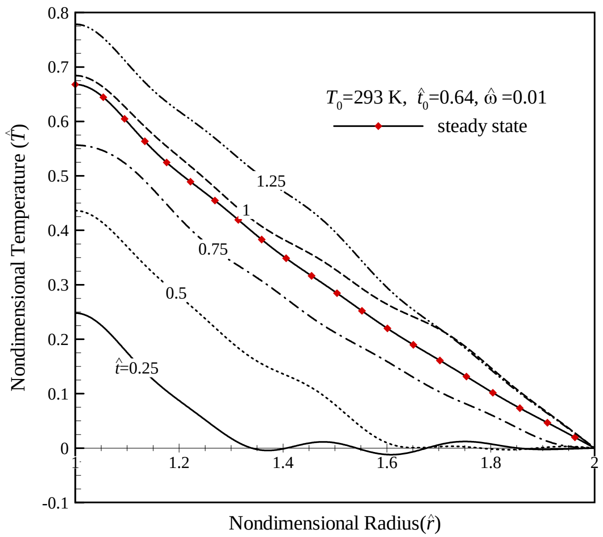

radius

radial displacement

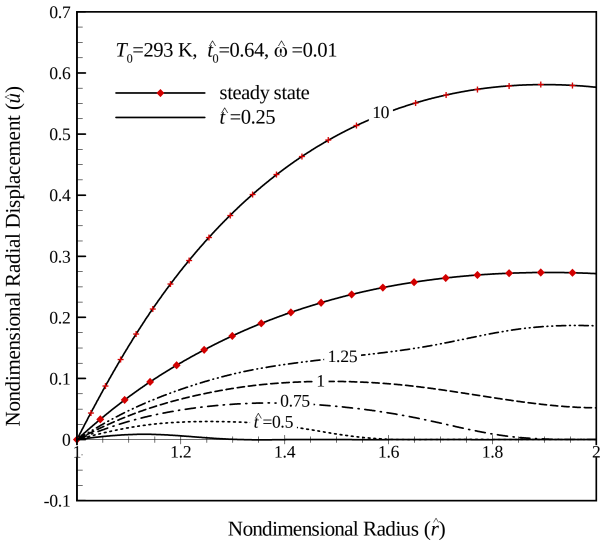

radius

radial stress

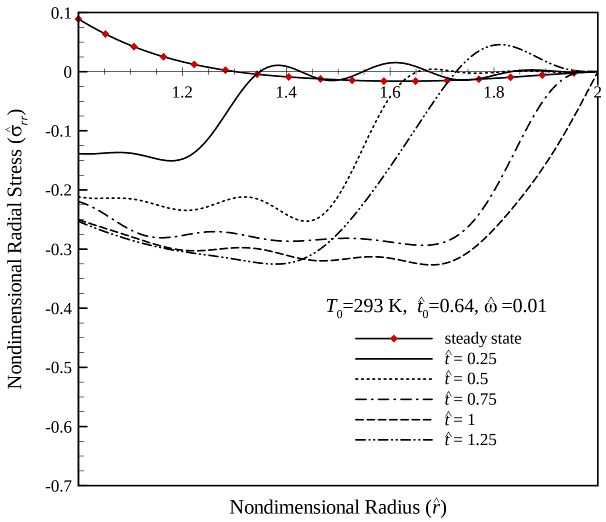

radius

circumferential stress

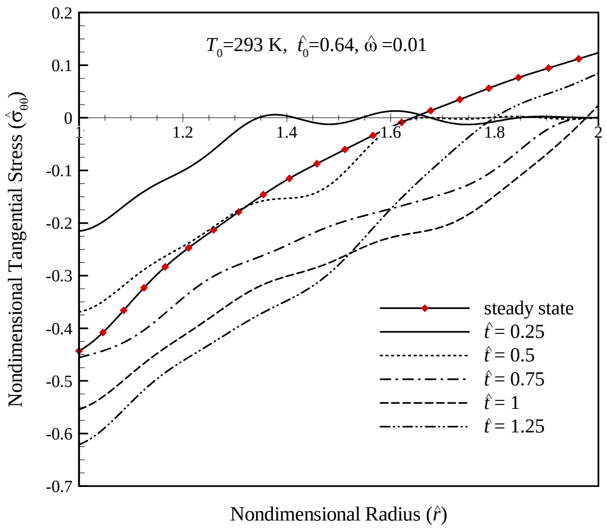

radius

Radial distribution for different values of the time.

Outlines

1. Introduction to rotating disk
2. Fundamentals of Linear Thermoelasticity
3. Literature review & present work
4. Analytical approach
5. **Numerical approach**
6. Conclusion

Outlines

1. Introduction to rotating disk
2. Fundamentals of Linear Thermoelasticity
3. Literature review & present work
4. Analytical approach
5. **Numerical approach**
   - **Motivation**
   - Development of method
   - Evaluations and results
6. Conclusion

Numerical approach

Motivations

- Analytical solutions are limited to those of a disk with simple geometry and boundary conditions.
- FE method is more widely used for this class of problems.
- 1D and 2D FE models are not able to provide all the desired information.
- 3D FE modeling techniques may be required for a detailed coupled thermoelastic analysis.
- 3D FE models still impose large computational costs, specially, in a time-consuming transient solution.
- There is a growing interest in the development of refined FE models with lower computational efforts.
- A refined FE approach was developed by Prof. Carrera *et al*.
- They formulated the FE methods on the basis of a class of theories of structures.

Numerical approach

Main characteristics of FE models refined by Carrera

- ✓ 3D capabilities
- ✓ lower computational costs
- ✓ ability to analyze multi-field problems and multi-layered structures

MUL2 research group,
Polytechnic University,
Turin, Italy
www.mul2.polito.it

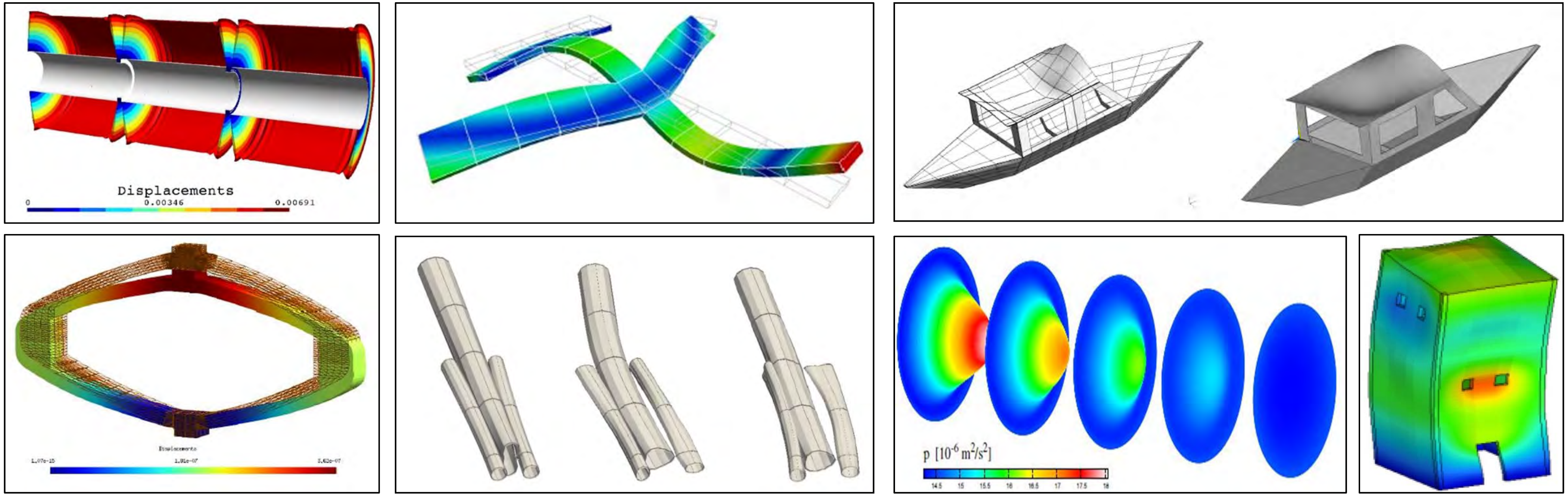

Outlines

1. Introduction to rotating disk
2. Fundamentals of Linear Thermoelasticity
3. Literature review & present work
4. Analytical approach
5. **Numerical approach**
   - Motivation
   - **Development of method**
   - Evaluations and results
6. Conclusion

Numerical approach - Development of method

Approaches to FE modeling

- Variational approach
- Weighted residual methods

- Weighted residual method based on Galerkin technique
  - ✓ Efficient, high rate of convergence
  - ✓ most common method to obtain a weak formulation of the problem

Numerical approach - Development of method

Governing equations

- ✓ For **anisotropic and nonhomogeneous** materials.
- ✓ Including **LS**, **GL** and **classical** theories of thermoelasticity.
- ✓ Considering **mechanical damping effect**.

Equation of motion
$\sigma_{ij,j} + X_i = \rho\ddot{u}_i + \zeta\dot{u}_i$

Hooke's law
$\sigma_{ij} = C_{ijpq}\varepsilon_{pq} - \beta_{ij}(T + t_1\dot{T})$

Energy equation
$\rho c(t_0 + t_2)\ddot{T} + \rho c\dot{T} - 2\tilde{c}_i\dot{T}_{,i} - (\kappa_{ij}T_{,j})_{,i} + t_0T_0\beta_{ij}\ddot{u}_{i,j} + T_0\beta_{ij}\dot{u}_{i,j} = R + t_0\dot{R}$

- ✓ $t_0 = t_1 = t_2 = \tilde{c}_i = 0 \rightarrow$ **classical** theory
- ✓ $t_1 = t_2 = \tilde{c}_i = 0 \rightarrow$ **LS** theory
- ✓ $t_0 = 0 \rightarrow$ **GL** theory.

Numerical approach - Development of method

FE formulation through Galerkin technique

- In 3D conventional FE method

$$u_i^{(e)}(x,y,z,t) = \phi_m(x,y,z)U_i^m(t)$$
$$T^{(e)}(x,y,z,t) = \phi_m(x,y,z)\Theta^m(t)$$

- $m = 1, \cdots, r$
- r = number of nodal points in a element

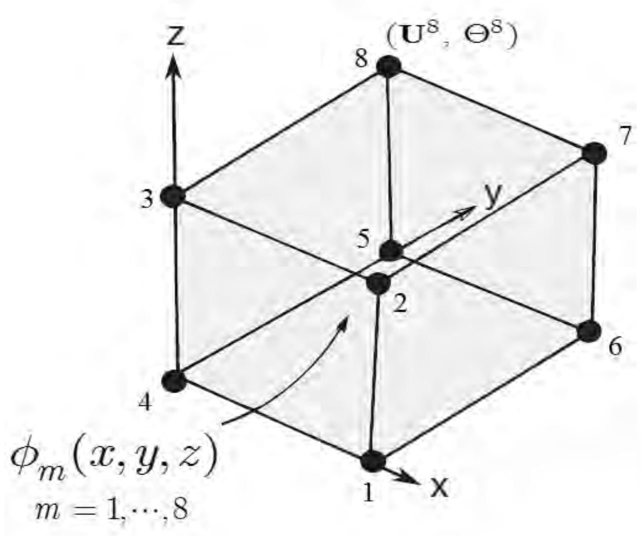

Numerical approach - Development of method

FE formulation through Galerkin technique

Weighting function

$$\phi_m(x, y, z)$$

Equation of motion

$$\int_{V^{(e)}} \left(\sigma_{ij,j} + X_i - \rho\ddot{u}_i - \zeta\dot{u}_i\right)\phi_m\, dV = 0$$

energy equation

$$\int_{V^{(e)}} \Big(\rho c(t_0 + t_2)\ddot{T} + \rho c\dot{T} - 2\tilde{c}_i\dot{T}_{,i} - \left(\kappa_{ij}T_{,j}\right)_{,i}$$

$$+t_0T_0\beta_{ij}\ddot{u}_{i,j} + T_0\beta_{ij}\dot{u}_{i,j} - R - t_0\dot{R}\Big)\phi_m dV = 0$$

Numerical approach - Development of method

FE formulation through Galerkin technique

Eq. of motion

$$\int_{V^{(e)}} (\rho\ddot{\mathbf{u}}\phi_m)dV + \int_{V^{(e)}} (\zeta\dot{\mathbf{u}}\phi_m)dV + \int_{V^{(e)}} (\mathbf{D}^{\mathrm{T}}\phi_m\boldsymbol{\sigma})dV$$
$$= \int_{V^{(e)}} (\mathbf{X}\phi_m)dV + \int_{S^{(e)}} (\mathbf{t}\phi_m)dS$$

---

energy Eq.

$$\int_{V^{(e)}} (t_0 T_0 \boldsymbol{\beta}^{\mathrm{T}}\mathbf{D}\ddot{\mathbf{u}}\phi_m)dV + \int_{V^{(e)}} (t_0\rho c\ddot{T}\phi_m)dV + \int_{V^{(e)}} (t_2\rho c\dddot{T}\phi_m)dV$$
$$+ \int_{V^{(e)}} (T_0\boldsymbol{\beta}^{\mathrm{T}}\mathbf{D}\dot{\mathbf{u}}\phi_m)dV + \int_{V^{(e)}} (\rho c\dot{T}\phi_m)dV - \int_{V^{(e)}} (2\tilde{\mathbf{c}}^{\mathrm{T}}\boldsymbol{\nabla}\dot{T}\phi_m)dV$$
$$+ \int_{V^{(e)}} (\boldsymbol{\nabla}^{\mathrm{T}}T\boldsymbol{\kappa}\boldsymbol{\nabla}\phi_m)dV = \int_{S^{(e)}} (\mathbf{q}^{\mathrm{T}}\mathbf{n}\phi_m)dS + \int_{V^{(e)}} (R\phi_m)dV + \int_{V^{(e)}} (t_0\dot{R}\phi_m)dV$$

Numerical approach - Development of method

Refined 1D FE model through Carrera unified formulation

3D beam-type structures

1D FE

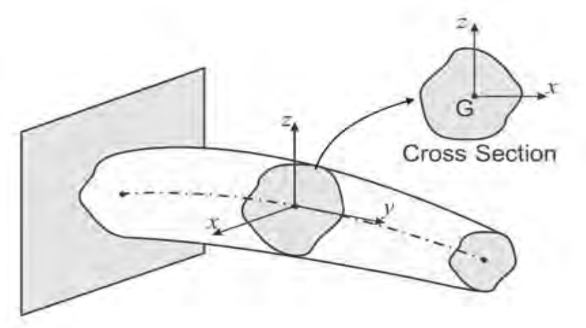

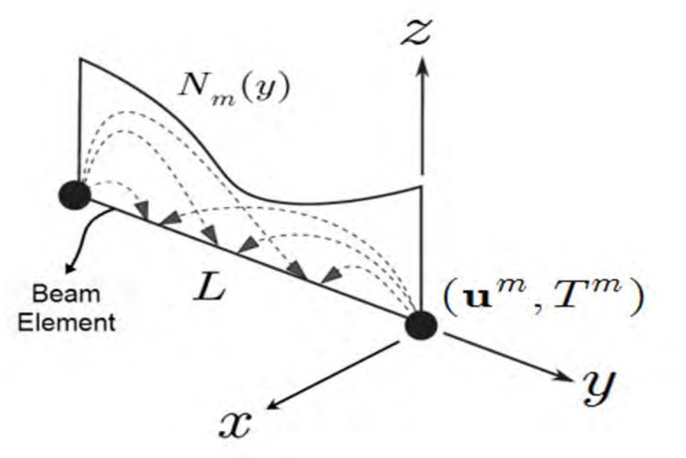

$$\mathbf{u} = N_m(y)\mathbf{u}^m$$
$$T = N_m(y)T^m$$

- $m = 1, \cdots, M$
- M = number of bar nodes

Numerical approach - Development of method

Refined 1D FE model through Carrera unified formulation

3D beam-type structures

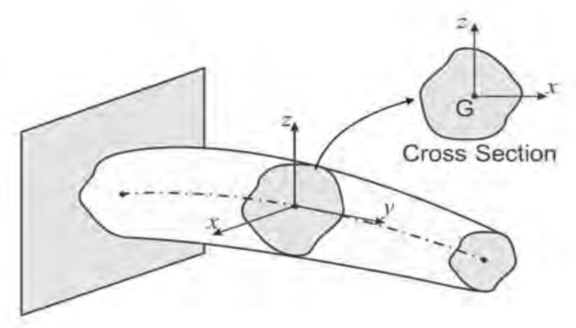

1D FE

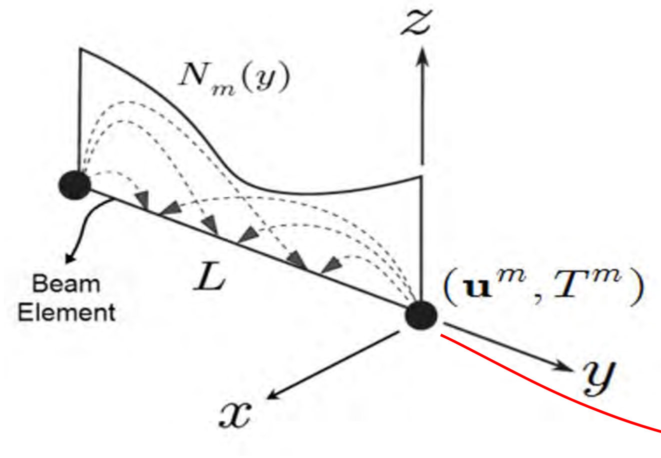

$$\mathbf{u} = N_m(y)\mathbf{u}^m$$
$$T = N_m(y)T^m$$

- $m = 1, \cdots, M$
- M = number of bar nodes

Carrera unified formulation (CUF)

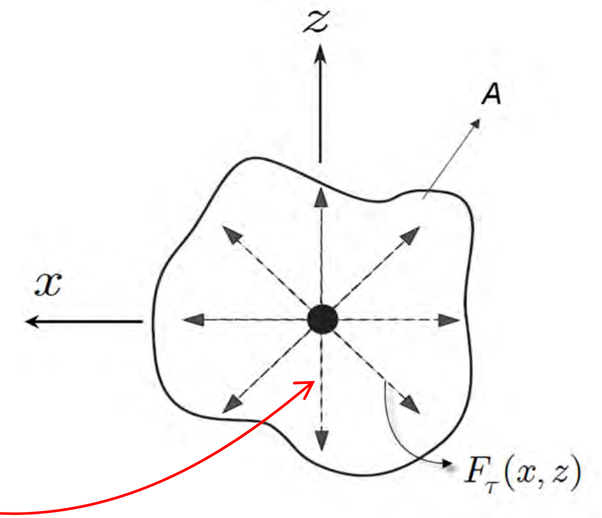

$$\mathbf{u}^m(x,z) = F_\tau(x,z)\mathbf{U}^{m\tau}(t)$$
$$T^m(x,z) = F_\tau(x,z)\Theta^{m\tau}(t)$$

- $\tau = 1, \cdots, N_{\mathrm{CUF}}$
- N_{CUF} = number of terms of the expansion.

Numerical approach - Development of method

Refined 1D FE model through CUF

1D FE

$$\mathbf{u} = N_m(y)\mathbf{u}^m$$
$$T = N_m(y)T^m$$

CUF

$$\mathbf{u}^m(x,z) = F_\tau(x,z)\mathbf{U}^{m\tau}(t)$$
$$T^m(x,z) = F_\tau(x,z)\Theta^{m\tau}(t)$$

1D FE-CUF

$$\mathbf{u}(x,y,z,t) = \phi_m(x,y,z)\,\mathbf{U}^{m\tau}(t)$$
$$T(x,y,z,t) = \phi_m(x,y,z)\,\Theta^{m\tau}(t)$$

weighting function in 1D FE-CUF → $\phi_m(x,y,z)=N_m(y)F_\tau(x,z)$

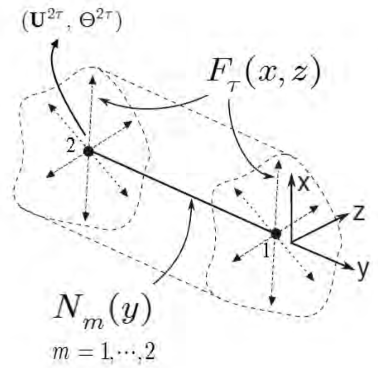

refined 1D 2-nodes element

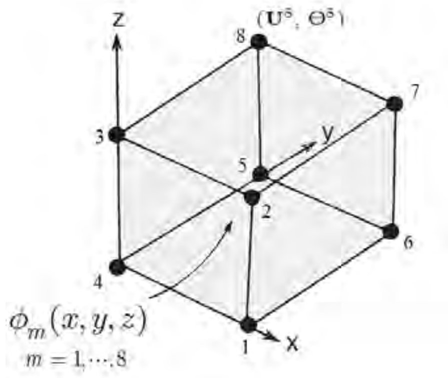

3D 8-nodes element

Numerical approach - Development of method

Refined 1D FE model through CUF

1D FE-CUF

$$\mathbf{u}(x,y,z,t) = N_m(y) F_\tau(x,z)\ \mathbf{U}^{m\tau}(t)$$
$$T(x,y,z,t) = N_m(y) F_\tau(x,z)\ \Theta^{m\tau}(t)$$

1D FE modeling

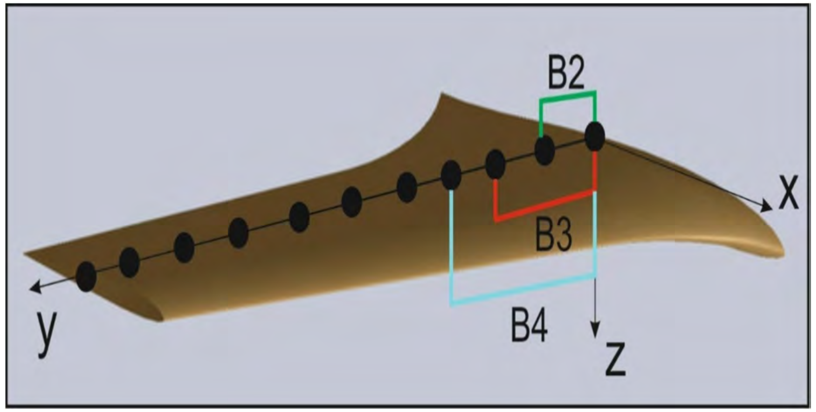

elements and shape functions in 1D FE modeling

element	$N_m(y)$
B2	linear
B2	quadratic
B4	cubic

Numerical approach - Development of method

Refined 1D FE model through CUF

1D FE-CUF

$$\mathbf{u}(x,y,z,t) = N_m(y)F_\tau(x,z)\,\mathbf{U}^{m\tau}(t)$$
$$T(x,y,z,t) = N_m(y)F_\tau(x,z)\,\Theta^{m\tau}(t)$$

- In **Carrera unified formulation**
  - ✓ selection of $F_\tau(x,z)$ and N_{CUF} $(\tau = 1,\cdots,N_{\mathrm{CUF}})$ is arbitrary.
  - ✓ various kinds of basic functions such as polynomials, harmonics and exponentials <u>of any-order</u>.
  - ✓ For instance, different classes of polynomials such as Taylor, Legendre and Lagrange polynomials.

Numerical approach - Development of method

Refined 1D FE model through CUF

1D FE-CUF

$$\mathbf{u}(x,y,z,t) = N_m(y)F_\tau(x,z)\ \mathbf{U}^{m\tau}(t)$$
$$T(x,y,z,t) = N_m(y)F_\tau(x,z)\ \Theta^{m\tau}(t)$$

$F_\tau(x,z)$ → bi-dimensional Lagrange functions

- cross-sections can be discretized using **Lagrange elements**
  - linear three-point (L3)
  - quadratic six-point (L6)
  - bilinear four-point (L4)
  - biquadratic nine-point (L9)
  - bi-cubic sixteen-point (L16)

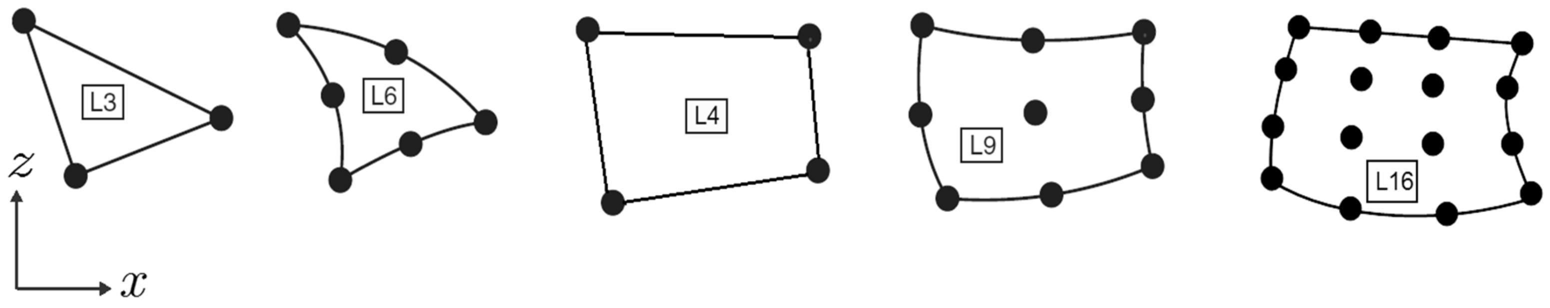

Numerical approach - Development of method

FE equations in CUF form

Substituting

1D FE-CUF
$\mathbf{u}(x,y,z,t) = N_m(y)F_\tau(x,z)\ \mathbf{U}^{m\tau}(t)$
$T(x,y,z,t) = N_m(y)F_\tau(x,z)\ \Theta^{m\tau}(t)$

weighting function
$\phi_m(x,y,z)=N_m(y)F_\tau(x,z)$

into the weak forms of equation of motion and energy equation gives

$$\boxed{\mathbf{M}^{lm\tau s}\ddot{\boldsymbol{\delta}}^{ls} + \mathbf{G}^{lm\tau s}\dot{\boldsymbol{\delta}}^{ls} + \mathbf{K}^{lm\tau s}\boldsymbol{\delta}^{ls} = \mathbf{p}^{m\tau}}$$

- $\mathbf{M}^{lm\tau s}$, $\mathbf{G}^{lm\tau s}$ and $\mathbf{K}^{lm\tau s}$ $\rightarrow$ 4×4 fundamental nuclei (FNs)of the mass, damping, and stiffness matrices
- $\mathbf{p}^{m\tau}$ $\rightarrow$ 4×1 FN of the load vector
- $\boldsymbol{\delta}^{ls}$ $\rightarrow$ 4×1 FN of the unknowns vector

Numerical approach - Development of method

FE equations in CUF form

$$\boxed{\mathbf{M}^{lm\tau s}\ddot{\boldsymbol{\delta}}^{ls}+\mathbf{G}^{lm\tau s}\dot{\boldsymbol{\delta}}^{ls}+\mathbf{K}^{lm\tau s}\boldsymbol{\delta}^{ls}=\mathbf{p}^{m\tau}}$$

or

$$\begin{bmatrix}\mathbf{M}_{UU}^{lm\tau s} & 0\\ \mathbf{M}_{\Theta U}^{lm\tau s} & \mathbf{M}_{\Theta\Theta}^{lm\tau s}\end{bmatrix}\begin{Bmatrix}\ddot{\mathbf{U}}^{ls}\\ \ddot{\Theta}^{ls}\end{Bmatrix}+\begin{bmatrix}\mathbf{G}_{UU}^{lm\tau s} & \mathbf{G}_{U\Theta}^{lm\tau s}\\ \mathbf{G}_{\Theta U}^{lm\tau s} & \mathbf{G}_{\Theta\Theta}^{lm\tau s}\end{bmatrix}\begin{Bmatrix}\dot{\mathbf{U}}^{ls}\\ \dot{\Theta}^{ls}\end{Bmatrix}+\begin{bmatrix}\mathbf{K}_{UU}^{lm\tau s} & \mathbf{K}_{U\Theta}^{lm\tau s}\\ 0 & \mathbf{K}_{\Theta\Theta}^{lm\tau s}\end{bmatrix}\begin{Bmatrix}\mathbf{U}^{ls}\\ \Theta^{ls}\end{Bmatrix}=\begin{Bmatrix}\mathbf{F}^{m\tau}\\ Q^{m\tau}\end{Bmatrix}$$

$\mathbf{G}_{UU}^{lm\tau s} \rightarrow$ structural damping effect

Rayleigh damping model

$$\mathbf{G}_{UU}^{lm\tau s}=\zeta_1\mathbf{M}_{UU}^{lm\tau s}+\zeta_2\mathbf{K}_{UU}^{lm\tau s}$$

Different theories of thermoelasticity through the 1D FE-CUF

	Conditions		Theory
Dynamic coupled	$t_0=0$		Generalized, GL
	$t_1=t_2=\tilde{\mathbf{c}}=0$		Generalized, LS
	$t_0=0$ $t_1=t_2=\tilde{\mathbf{c}}=0$		Classical
Uncoupled	$t_0=0$ $t_1=t_2=\tilde{\mathbf{c}}=0$	$\mathbf{G}_{\Theta U}^{lm\tau s}=0$	Dynamic
		$\mathbf{M}_{UU}^{lm\tau s}=0$ $\mathbf{G}_{\Theta U}^{lm\tau s}=0$	Quasi-static
		$\mathbf{M}_{UU}^{lm\tau s}=0$ $\mathbf{G}_{\Theta U}^{lm\tau s}=0$ $\mathbf{G}_{\Theta\Theta}^{lm\tau s}=0$	Static

Numerical approach - Development of method

Assembly procedure via Fundamental Nuclei

for each element
$\mathbf{M}^{lm\tau s}\ddot{\boldsymbol{\delta}}^{ls} + \mathbf{G}^{lm\tau s}\dot{\boldsymbol{\delta}}^{ls} + \mathbf{K}^{lm\tau s}\boldsymbol{\delta}^{ls} = \mathbf{p}^{m\tau}$

for whole structure
$\mathbf{M}\ddot{\boldsymbol{\Delta}} + \mathbf{G}\dot{\boldsymbol{\Delta}} + \mathbf{K}\boldsymbol{\Delta} = \mathbf{P}$

total degrees of freedom
$\mathrm{DOF} = \sum_{i=1}^{N_{BN}} (4 \times N_{LN}^{i})$

assembly procedure of FNs

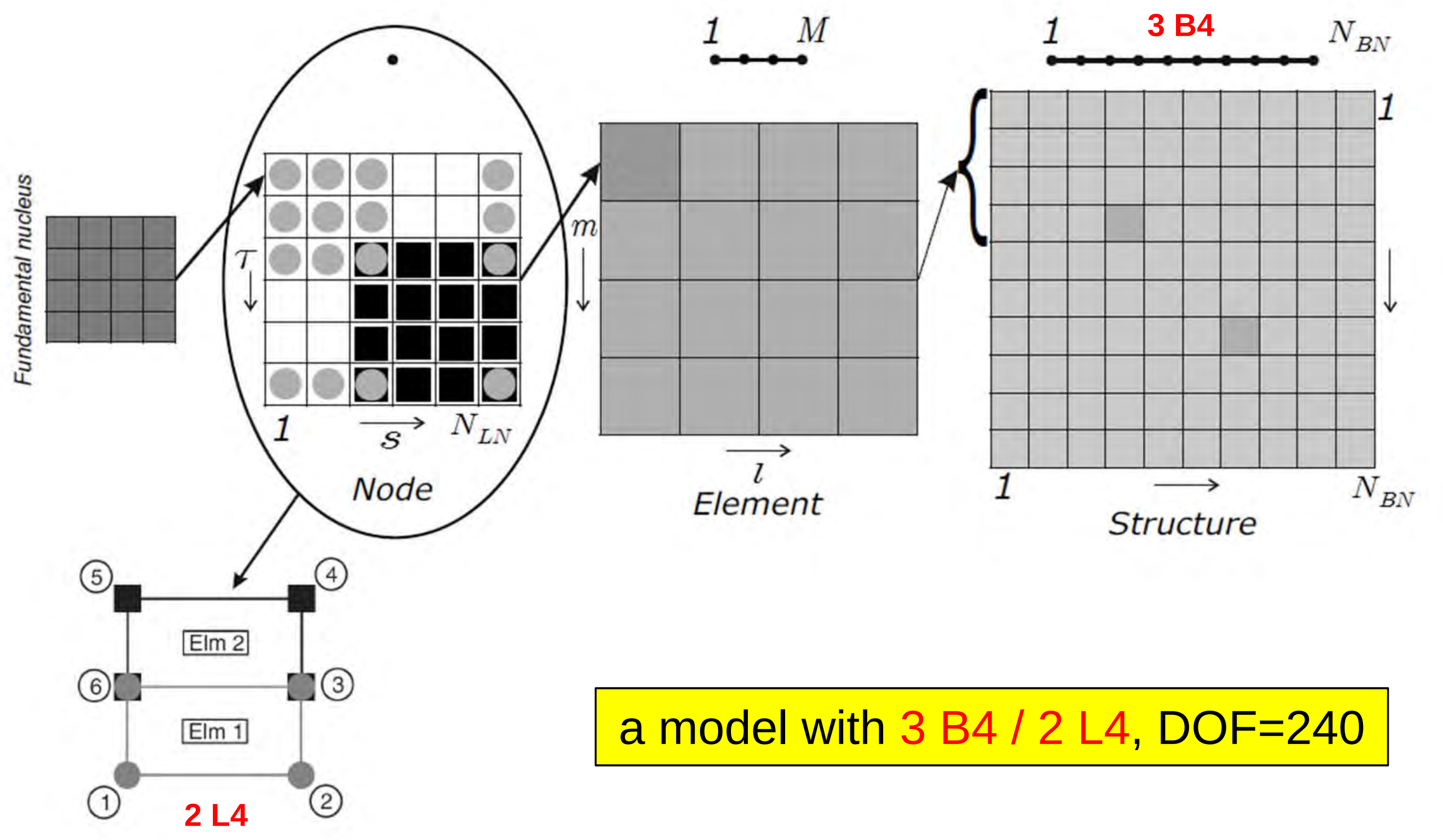

a model with 3 B4 / 2 L4, DOF=240

Numerical approach - Development of method

Time history analysis

Transfinite element technique

$$\mathbf{M}^{lm\tau s}\ddot{\boldsymbol{\delta}}^{ls} + \mathbf{G}^{lm\tau s}\dot{\boldsymbol{\delta}}^{ls} + \mathbf{K}^{lm\tau s}\boldsymbol{\delta}^{ls} = \mathbf{p}^{m\tau}$$

taking Laplace

$$\underbrace{\left[\mathbf{M}^{lm\tau s}\tilde{s}^2 + \mathbf{G}^{lm\tau s}\tilde{s} + \mathbf{K}^{lm\tau s}\right]}_{\mathbf{K}_{eq}^{lm\tau s}}\boldsymbol{\delta}^{ls^*} = \mathbf{p}^{m\tau^*}$$

Assembling $\mathbf{K}_{eq}^{lm\tau s}$ & $\mathbf{p}^{m\tau^*}$ for whole structure

$$\mathbf{K}_{\mathrm{eq}}\boldsymbol{\Delta}^* = \mathbf{P}^*$$

solve

solution in Laplace domain ($\boldsymbol{\Delta}^*$) → numerical inversion → solution in time domain ($\boldsymbol{\Delta}(t)$)

- $\tilde{s}$ → the Laplace variable
- $\mathbf{K}_{eq}^{lm\tau s}$ → FN of the equivalent stiffness matrix
- * denotes Laplace transform of the terms.

Numerical approach - Development of method

Non-dimensional Equation for isotropic FGMs

Non-dimensional parameters

$$\hat{x}_i = \frac{x_i}{l_m} \quad ; \quad \hat{t} = \frac{V_{e_m}}{l_m} t \quad ;$$

$$\hat{T} = \frac{T}{T_d} \quad ; \quad \hat{u}_i = \frac{(\lambda_m + 2\mu_m)}{l_m \beta_m T_d} u_i \quad ; \quad \hat{t}_0 = \frac{V_{e_m}}{l_m} t_0$$

$$\hat{q}_i = \frac{1}{c_m T_d \rho_m V_{e_m}} q_i \quad ; \quad \hat{\sigma}_{ij} = \frac{1}{\beta_m T_d} \sigma_{ij} \quad ; \quad \hat{t}_i^n = \frac{1}{T_d \beta_m} t_i^n$$

$$\hat{X}_i = \frac{l_m}{T_d \beta_m} X_i \quad ; \quad \hat{R} = \frac{D_m}{c_m T_d (\lambda_m + 2\mu_m)} R$$

---

velocity of elastic longitudinal wave

$$V_{e_m} = \sqrt{(\lambda_m + 2\mu_m)/\rho_m}$$

unit length

$$l_m = D_m / V_{e_m}$$

diffusivity

$$D_m = \kappa_m / c_m \rho_m$$

Numerical approach - Development of method

Non-dimensional FNs for isotropic FGMs based on LS theory

Transfinite element equation
$\mathbf{K}_{eq}^{lm\tau s}\boldsymbol{\delta}^{ls^*} = \mathbf{p}^{m\tau^*}$
or
$\begin{bmatrix} K_{11}^{\tau slm} & K_{12}^{\tau slm} & K_{13}^{\tau slm} & K_{14}^{\tau slm} \\ K_{21}^{\tau slm} & K_{22}^{\tau slm} & K_{23}^{\tau slm} & K_{24}^{\tau slm} \\ K_{31}^{\tau slm} & K_{32}^{\tau slm} & K_{33}^{\tau slm} & K_{34}^{\tau slm} \\ K_{41}^{\tau slm} & K_{42}^{\tau slm} & K_{43}^{\tau slm} & K_{44}^{\tau slm} \end{bmatrix} \begin{Bmatrix} U_x^{ls^*} \\ U_y^{ls^*} \\ U_z^{ls^*} \\ \Theta^{ls^*} \end{Bmatrix} = \begin{Bmatrix} p_1^{m\tau^*} \\ p_2^{m\tau^*} \\ p_3^{m\tau^*} \\ p_4^{m\tau^*} \end{Bmatrix}$

$$
\begin{aligned}
K_{11}^{\tau slm} &= \tilde{s}^2 \lhd \hat{C}_\rho F_\tau F_s \rhd I_L^{ml} + \lhd \hat{C}_{22} F_{\tau,x} F_{s,x} \rhd I_L^{ml} \\
&\quad + \lhd \hat{C}_{66} F_\tau F_s \rhd I_L^{m,_y l,_y} + \lhd \hat{C}_{44} F_{\tau,z} F_{s,z} \rhd I_L^{ml} \\
K_{12}^{\tau slm} &= \lhd \hat{C}_{66} F_\tau F_{s,x} \rhd I_L^{m,_y l} + \lhd \hat{C}_{23} F_{\tau,x} F_s \rhd I_L^{ml,_y} \\
K_{13}^{\tau slm} &= \lhd \hat{C}_{44} F_{\tau,z} F_{s,x} \rhd I_L^{ml} + \lhd \hat{C}_{21} F_{\tau,x} F_{s,z} \rhd I_L^{ml} \\
K_{14}^{\tau slm} &= - \lhd \hat{C}_\beta F_{\tau,x} F_s \rhd I_L^{ml}
\end{aligned}
$$

$$
\begin{aligned}
K_{41}^{\tau slm} &= C(\tilde{s}^2 \hat{t}_0 + \tilde{s}) \lhd \hat{C}_\beta F_\tau F_{s,x} \rhd I_L^{ml} \\
K_{42}^{\tau slm} &= C(\tilde{s}^2 \hat{t}_0 + \tilde{s}) \lhd \hat{C}_\beta F_\tau F_s \rhd I_L^{ml,_y} \\
K_{43}^{\tau slm} &= C(\tilde{s}^2 \hat{t}_0 + \tilde{s}) \lhd \hat{C}_\beta F_\tau F_{s,z} \rhd I_L^{ml} \\
K_{44}^{\tau slm} &= (\tilde{s}^2 \hat{t}_0 + \tilde{s}) \lhd \hat{C}_\rho \hat{C}_c F_\tau F_s \rhd I_L^{ml} + \\
&\quad + \lhd \hat{C}_\kappa F_{\tau,x} F_{s,x} \rhd I_L^{ml} + \lhd \hat{C}_\kappa F_\tau F_s \rhd I_L^{m,_y l,_y} \\
&\quad + \lhd \hat{C}_\kappa F_{\tau,z} F_{s,z} \rhd I_L^{ml}
\end{aligned}
$$

$$
\begin{aligned}
p_1^{m\tau^*} &= \int_{S^{(e)}} \hat{t}_x^{n^*} F_\tau N_m \, dS + \int_{V^{(e)}} \hat{X}_x^* F_\tau N_m \, dV \\
p_2^{m\tau^*} &= \int_{S^{(e)}} \hat{t}_y^{n^*} F_\tau N_m \, dS + \int_{V^{(e)}} \hat{X}_y^* F_\tau N_m \, dV \\
p_3^{m\tau^*} &= \int_{S^{(e)}} \hat{t}_z^{n^*} F_\tau N_m \, dS + \int_{V^{(e)}} \hat{X}_z^* F_\tau N_m \, dV \\
p_4^{m\tau^*} &= \int_{V^{(e)}} [(\hat{t}_0 s + 1)\hat{R}^*] F_\tau N_m \, dV + \int_{S^{(e)}} (\hat{q}_i^* n_i) F_\tau N_m \, dS
\end{aligned}
$$

Numerical approach - Development of method

Non-dimensional FNs for isotropic FGMs based on LS theory

$$\triangleleft \cdots \triangleright = \int_{A^{(e)}} (\cdots)\, dA$$

$$I_L^{ml} \; \Big| I_L^{m_{,y}l} \; \Big| I_L^{ml_{,y}} \; \Big| I_L^{m_{,y}l_{,y}} = \int_{L^{(e)}} \Big(N_m N_l \; \Big| N_{m_{,y}} N_l \; \Big| N_m N_{l_{,y}} \; \Big| N_{m_{,y}} N_{l_{,y}} \Big) dy$$

$$\hat{C}_\rho = \frac{\rho}{\rho_{\mathrm{m}}},\quad \hat{C}_\beta = \frac{\beta}{\beta_{\mathrm{m}}},\quad \hat{C}_\kappa = \frac{\kappa}{\kappa_{\mathrm{m}}},\quad \hat{C}_c = \frac{c}{c_{\mathrm{m}}}$$

$$\hat{C}_{11} = \hat{C}_{22} = \hat{C}_{33} = \frac{(2\mu + \lambda)}{(\lambda_{\mathrm{m}} + 2\mu_{\mathrm{m}})}$$

$$\hat{C}_{44} = \hat{C}_{55} = \hat{C}_{66} = \frac{\mu}{(\lambda_{\mathrm{m}} + 2\mu_{\mathrm{m}})}$$

$$\hat{C}_{12} = \hat{C}_{13} = \hat{C}_{23} = \frac{\lambda}{(\lambda_{\mathrm{m}} + 2\mu_{\mathrm{m}})}$$

thermoelastic coupling parameter $\rightarrow$ $C = \dfrac{T_0 \beta_{\mathrm{m}}^2}{c_{\mathrm{m}} \rho_{\mathrm{m}} (\lambda_{\mathrm{m}} + \mu_{\mathrm{m}})}$

$$K_{11}^{\tau slm} = \tilde{s}^2 \triangleleft \hat{C}_\rho F_\tau F_s \triangleright I_L^{ml} + \triangleleft \hat{C}_{22} F_{\tau,x} F_{s,x} \triangleright I_L^{ml} + \triangleleft \hat{C}_{66} F_\tau F_s \triangleright I_L^{m_{,y}l_{,y}} + \triangleleft \hat{C}_{44} F_{\tau,z} F_{s,z} \triangleright I_L^{ml}$$

$$K_{12}^{\tau slm} = \triangleleft \hat{C}_{66} F_\tau F_{s,x} \triangleright I_L^{m_{,y}l} + \triangleleft \hat{C}_{23} F_{\tau,x} F_s \triangleright I_L^{ml_{,y}}$$

$$K_{13}^{\tau slm} = \triangleleft \hat{C}_{44} F_{\tau,z} F_{s,x} \triangleright I_L^{ml} + \triangleleft \hat{C}_{21} F_{\tau,x} F_{s,z} \triangleright I_L^{ml}$$

$$K_{14}^{\tau slm} = - \triangleleft \hat{C}_\beta F_{\tau,x} F_s \triangleright I_L^{ml}$$

$$K_{41}^{\tau slm} = C(\tilde{s}^2 \hat{t}_0 + \tilde{s}) \triangleleft \hat{C}_\beta F_\tau F_{s,x} \triangleright I_L^{ml}$$

$$K_{42}^{\tau slm} = C(\tilde{s}^2 \hat{t}_0 + \tilde{s}) \triangleleft \hat{C}_\beta F_\tau F_s \triangleright I_L^{ml_{,y}}$$

$$K_{43}^{\tau slm} = C(\tilde{s}^2 \hat{t}_0 + \tilde{s}) \triangleleft \hat{C}_\beta F_\tau F_{s,z} \triangleright I_L^{ml}$$

$$K_{44}^{\tau slm} = (\tilde{s}^2 \hat{t}_0 + \tilde{s}) \triangleleft \hat{C}_\rho \hat{C}_c F_\tau F_s \triangleright I_L^{ml} + \triangleleft \hat{C}_\kappa F_{\tau,x} F_{s,x} \triangleright I_L^{ml} + \triangleleft \hat{C}_\kappa F_\tau F_s \triangleright I_L^{m_{,y}l_{,y}} + \triangleleft \hat{C}_\kappa F_{\tau,z} F_{s,z} \triangleright I_L^{ml}$$

Outlines

1. Introduction to rotating disk
2. Fundamentals of Linear Thermoelasticity
3. Literature review & present work
4. Analytical approach
5. **Numerical approach**
   - Motivation
   - Development of method
   - **Evaluations and results**
6. Conclusion

Outlines

Outlines

1. Introduction to rotating disk
2. Fundamentals of Linear Thermoelasticity
3. Literature review & present work
4. Analytical approach
5. **Numerical approach**
   - Motivation
   - Development of method
   - **Evaluations and results**
     - **Static structural analysis**
       - ✓ **Example 1. Rotating variable thickness disk**
       - ✓ Example 2. Rotating variable thickness disk subjected thermal load
       - ✓ Example 3. Complex rotor
     - Static structural-thermal analysis – Example 4. simple beam
     - Quasi-static structural-thermal analysis – Example 5. simple beam
     - Dynamic coupled structural-thermal analysis
       - ✓ Example 6. Constant thickness disk made of isotropic homogeneous materials
       - ✓ Example 7. Constant thickness disk made of isotropic FGMs
       - ✓ Example 8. variable thickness disk made of isotropic FGMs
6. Conclusion

Numerical approach - Evaluations and results

Static structural analysis

Example 1. Rotating variable thickness disk

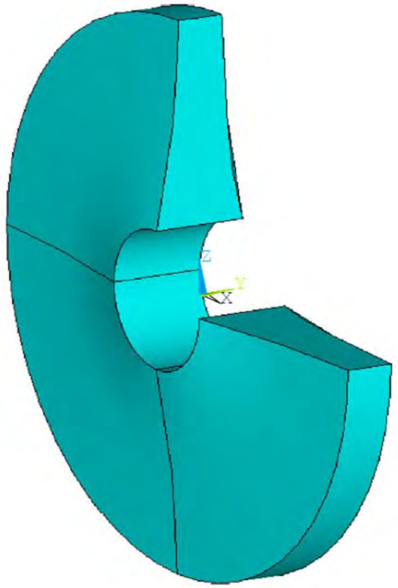

Material properties	
Young's modulus E	$207\ \mathrm{GPa}$
Poisson's ratio ν	0.28
density (ρ)	$7860\ \mathrm{kg/m^3}$

annular disk with hyperbolic profile

$r_{\mathrm{in}} = 0.05\ \mathrm{m}$ $\quad h_{\mathrm{in}} = 0.06\ \mathrm{m}$

$r_{\mathrm{o}} = 0.2\ \mathrm{m}$ $\quad h_{\mathrm{o}} = 0.03\ \mathrm{m}$

$$h(r) = 0.0134\, r^{-0.5}$$

- $\omega = 2000\ \ \mathrm{rad/s}$
- hub is assumed to be fully fixed

Numerical approach - Evaluations and results

Static structural analysis

Example 1. Rotating variable thickness disk

1D FE-CUF modeling

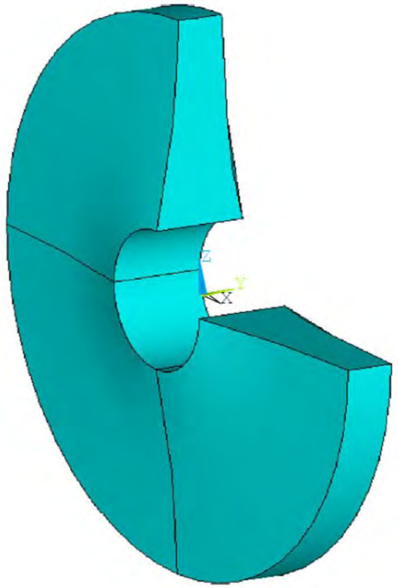

Different 1D FE-CUF models of the disk			
Model	Discretizing		DOF
	Along the axis	Over the corss sections	
(1)	8 B2, 3 CS*	$(2/6/8) \times 32$ L4	6240
(2)	8 B2, 4 CS	$(2/4/6/8) \times 32$ L4	5472
(3)	10 B2, 4 CS	$(2/4/6/8) \times 32$ L4	7200
(4)	12 B2, 5 CS	$(1/2/4/6/8) \times 32$ L4	7584
(5)	14 B2, 6 CS	$(1/2/3/4/6/8) \times 32$ L4	8352
(6)	16 B2, 7 CS	$(1/2/3/4/5/6/8) \times 32$ L4	9504
(7)	18 B2, 8 CS	$(1/2/3/4/5/6/7/8) \times 32$ L4	11040
(8)	22 B2, 8 CS	$(1/2/3/4/5/6/7/8) \times 32$ L4	14496

* 3 types of cross section (CS) with different radii

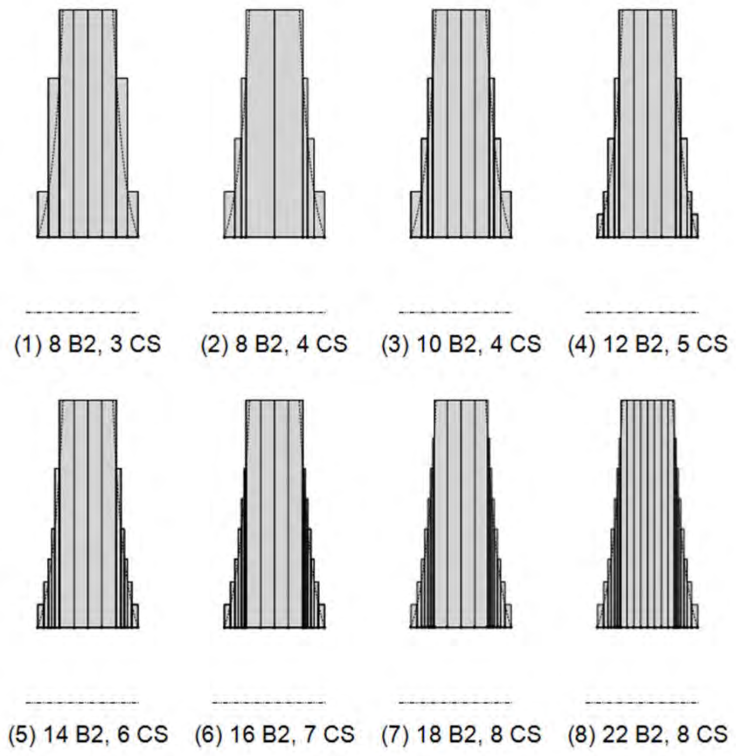

discretization along the axis

Numerical approach - Evaluations and results

Static structural analysis

Example 1. Rotating variable thickness disk

verification of results

Radial displacement

Model	DOF	Radial displacement u_r (μm)	
		At mid-radius	At outer radius
Analytical	1	119.01	157.57
1D CUF- FE			
(1)	6240	120.32 (1.10)	156.00 (1.00)
(2)	5472	118.36 (0.54)	157.00 (0.36)
(3)	7200	118.36 (0.54)	156.42 (0.73)
(4)	7584	118.75 (0.22)	157.15 (0.27)
(5)	8352	119.50 (0.41)	158.08 (0.32)
(6)	9504	118.50 (0.43)	157.93 (0.23)
(7)	11040	117.26 (1.47)	154.92 (1.68)
(8)	14496	117.06 (1.64)	155.00 (1.63)
3D ANSYS	14400	119.00 (0.01)	157.10 (0.30)

( ): % difference with respect to the analytical solution.

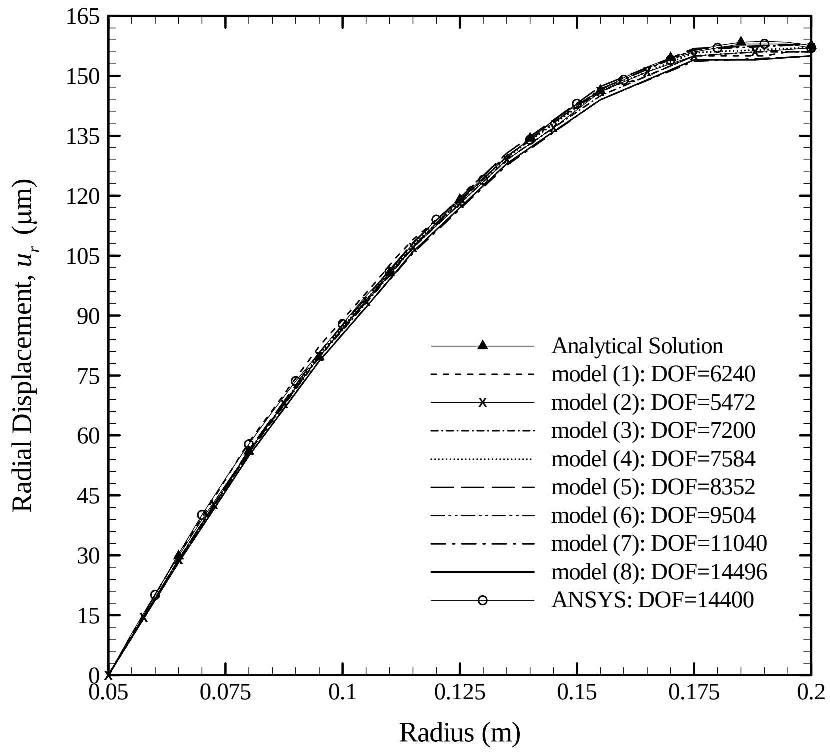

Numerical approach - Evaluations and results

Static structural analysis

Example 1. Rotating variable thickness disk

verification of results

Radial displacement

Model	DOF	Radial displacement $u_r\,(\mu\text{m})$ At mid-radius		Radial displacement $u_r\,(\mu\text{m})$ At outer radius	
Analytical	1	119.01		157.57	
1D CUF- FE					
(1)	6240	120.32	(1.10)	156.00	(1.00)
(2)	5472	118.36	(0.54)	157.00	(0.36)
(3)	7200	118.36	(0.54)	156.42	(0.73)
(4)	7584	118.75	(0.22)	157.15	(0.27)
(5)	8352	119.50	(0.41)	158.08	(0.32)
(6)	9504	118.50	(0.43)	157.93	(0.23)
(7)	11040	117.26	(1.47)	154.92	(1.68)
(8)	14496	117.06	(1.64)	155.00	(1.63)
3D ANSYS	14400	119.00	(0.01)	157.10	(0.30)

( ): % difference with respect to the analytical solution.

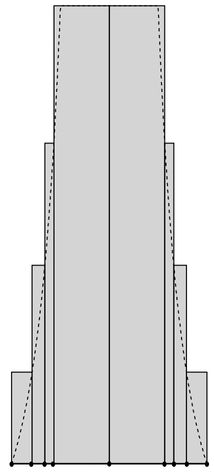

Model (2)

- ✓ Error < 0.6%
- ✓ 2.6 times less DOFs of the 3D ANSYS model !!

Static structural analysis

Example 1. Rotating variable thickness disk

1D FE-CUF modeling

Mesh refinement over the cross-sections

model	1D FE-CUF Model	DOF
1	8 B2, (1/2/3/4) × 32 L4	3168
2	8 B2, (2/4/6/8) × 32 L4	5472
3	8 B2, (5/7/9/14) × 32 L4	8928
4	8 B2, (4/8/12/16) × 32 L4	10080
5	8 B2, (10/12/14/20) × 32 L4	13536

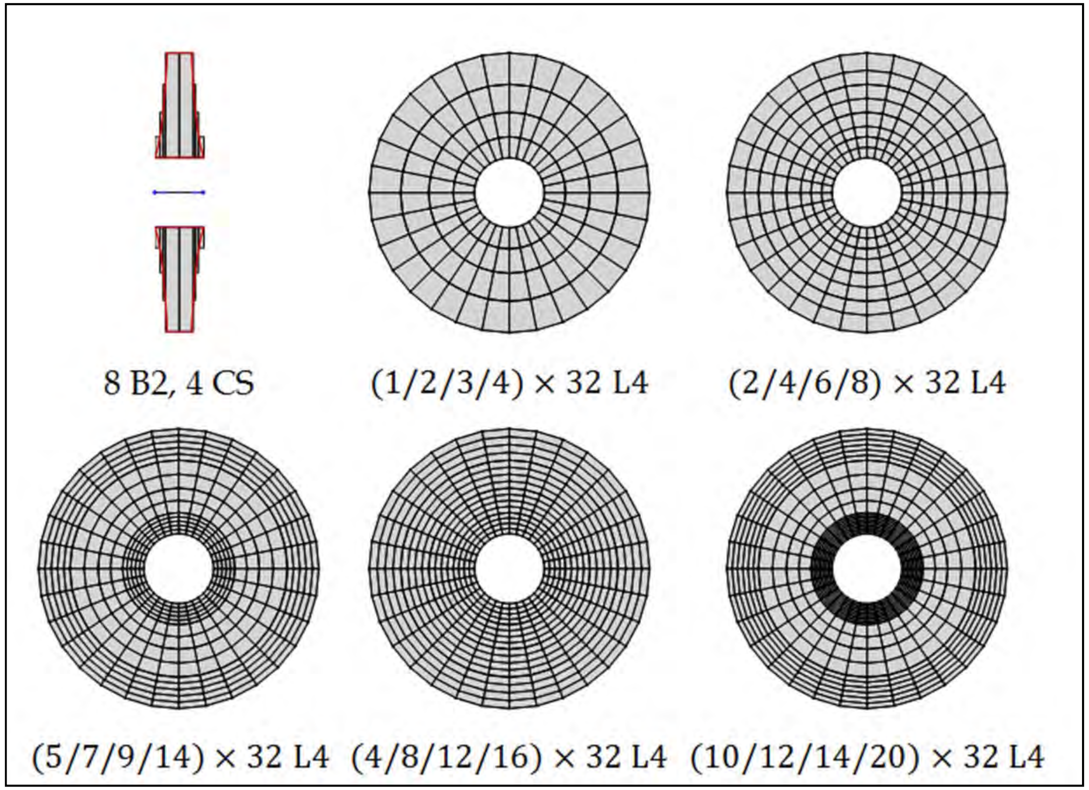

Numerical approach - Evaluations and results

Static structural analysis

Example 1. Rotating variable thickness disk

verification of results

Radial displacement

effect of enriching the radial discretization

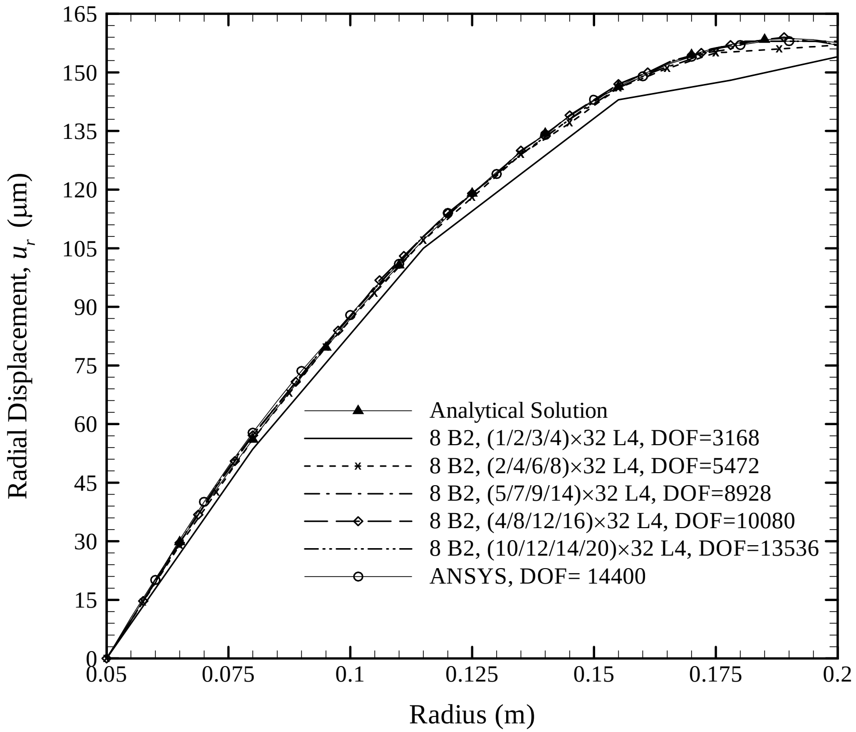

Model	DOF	Radial displacement u_r (μm)			
		At mid-radius		At outer radius	
Analytical	1	119.01		157.57	
1D CUF FE					
8 B2, $(1/2/3/4) \times 32$ L4	3168	114.50	(3.79)	154.00	(2.27)
8 B2, $(2/4/6/8) \times 32$ L4	5472	118.36	(0.54)	157.00	(0.36)
8 B2, $(5/7/9/14) \times 32$ L4	8928	119.00	(0.01)	157.00	(0.36)
8 B2, $(4/8/12/16) \times 32$ L4	10080	119.00	(0.01)	158.00	(0.27)
8 B2, $(10/12/14/20) \times 32$ L4	13536	119.00	(0.01)	157.00	(0.36)
3D FE (ANSYS)	**14400**	119.00	(0.01)	157.10	(0.30)

( ) Absolute percentage difference with respect to the analytical solution.

✓ Converged solution

with 1.6 times less DOFs of the 3D ANSYS model !!

Outlines

1. Introduction to rotating disk
2. Fundamentals of Linear Thermoelasticity
3. Literature review & present work
4. Analytical approach
5. **Numerical approach**
   - Motivation
   - Development of method
   - **Evaluations and results**
     - **Static structural analysis**
       - ✓ Example 1. Rotating variable thickness disk
       - ✓ **Example 2. Rotating variable thickness disk subjected thermal load**
       - ✓ Example 3. Complex rotor
     - Static structural-thermal analysis – Example 4. simple beam
     - Quasi-static structural-thermal analysis – Example 5. simple beam
     - Dynamic coupled structural-thermal analysis
       - ✓ Example 6. Constant thickness disk made of isotropic homogeneous materials
       - ✓ Example 7. Constant thickness disk made of isotropic FGMs
       - ✓ Example 8. variable thickness disk made of isotropic FGMs
6. Conclusion

Static structural analysis

Example 2. Rotating variable thickness disk subjected thermal load

- The disk is subjected to radial temperature gradient.
- hub is assumed to be axially fixed.

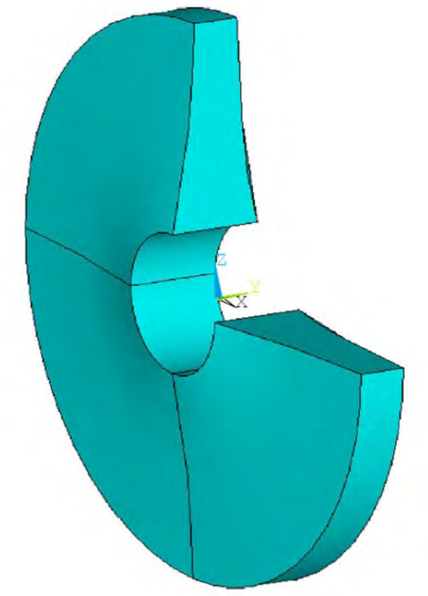

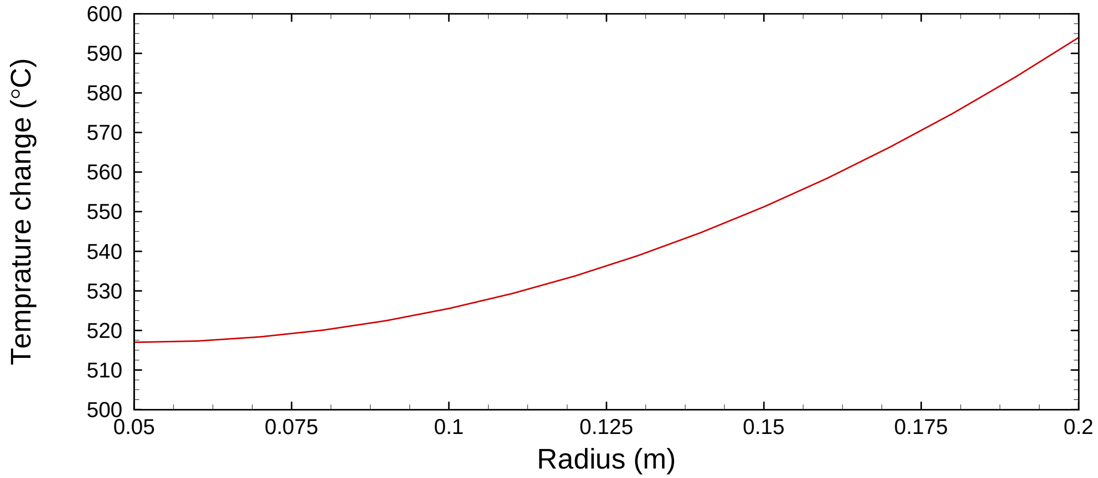

radial steady-state temperature distribution

Numerical approach - Evaluations and results

Static structural analysis

Example 2. Rotating variable thickness disk subjected thermal load

radial displacement

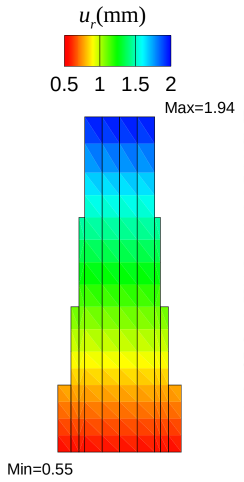

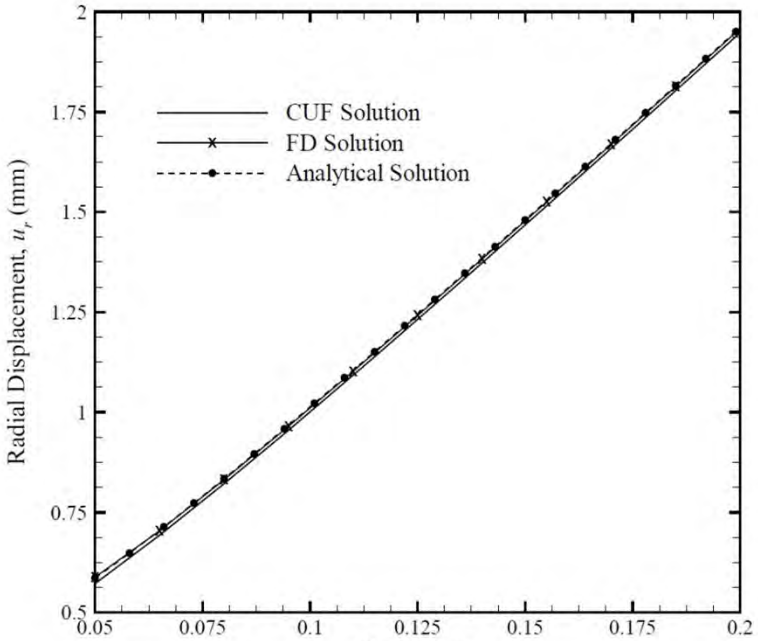

radius

Radial and circumferential stresses

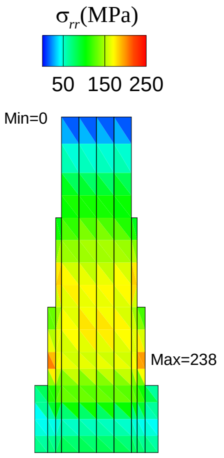

radial stress

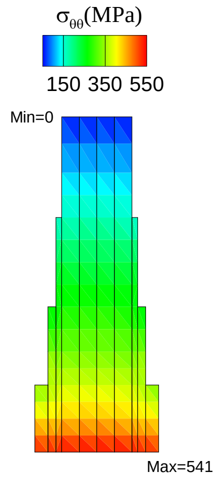

circumferential stress

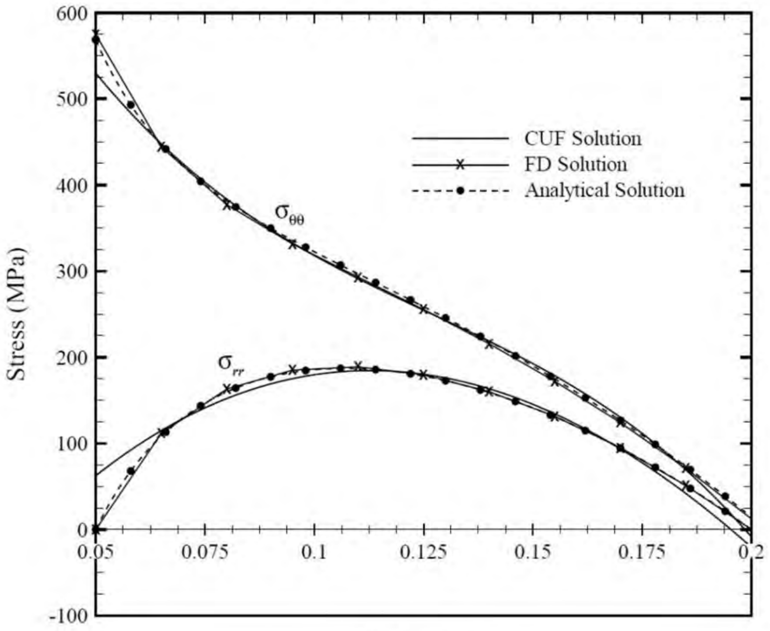

radius

Outlines

1. Introduction to rotating disk
2. Fundamentals of Linear Thermoelasticity
3. Literature review & present work
4. Analytical approach
5. **Numerical approach**
   - Motivation
   - Development of method
   - **Evaluations and results**
     - **Static structural analysis**
       - ✓ Example 1. Rotating variable thickness disk
       - ✓ Example 2. Rotating variable thickness disk subjected thermal load
       - ✓ **Example 3. Complex rotor**
     - Static structural-thermal analysis – Example 4. simple beam
     - Quasi-static structural-thermal analysis – Example 5. simple beam
     - Dynamic coupled structural-thermal analysis
       - ✓ Example 6. Constant thickness disk made of isotropic homogeneous materials
       - ✓ Example 7. Constant thickness disk made of isotropic FGMs
       - ✓ Example 8. variable thickness disk made of isotropic FGMs
6. Conclusion

Static structural analysis

Example 3. Complex rotor

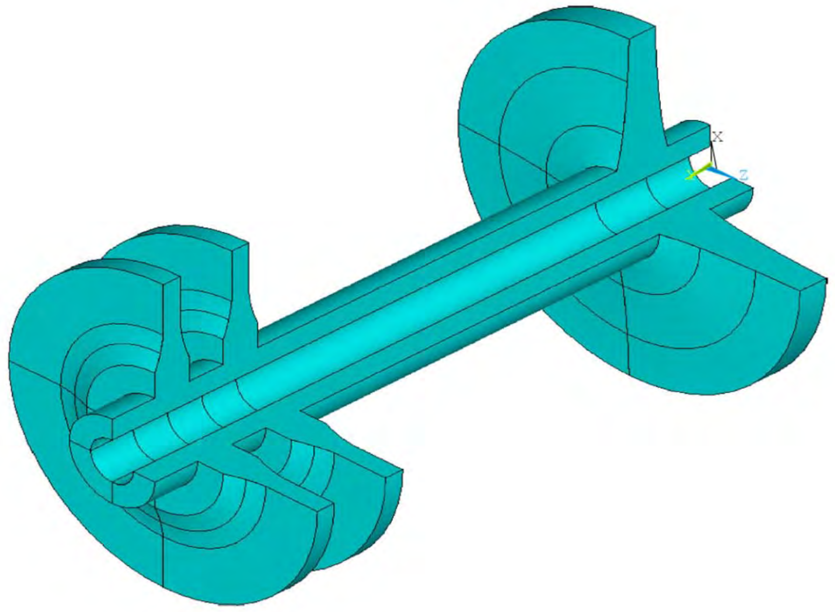

3D model of a complex rotor

- The profile hyperbolic for the turbine disk
- web-type profile for the compressor disks
- Both ends of the shaft are fully fixed.

Static structural analysis

Example 3. Complex rotor

1D FE-CUF modeling

discretizing along the axis

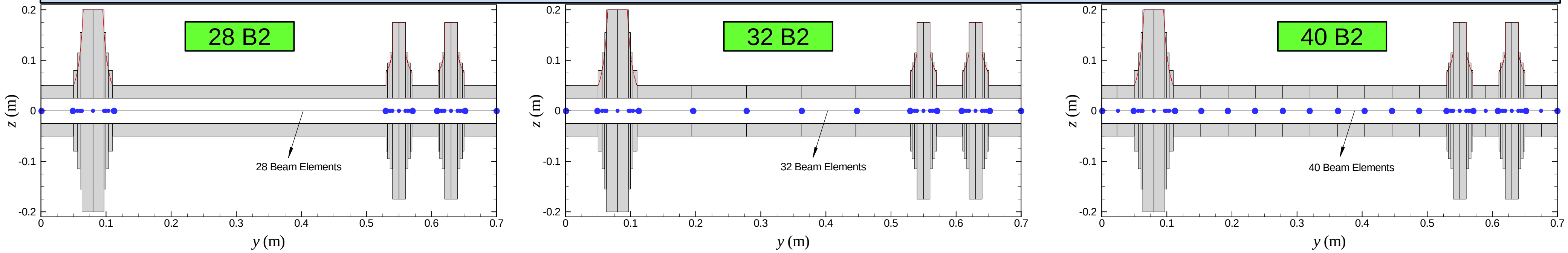

Lagrange mesh over the cross-section with the largest radius

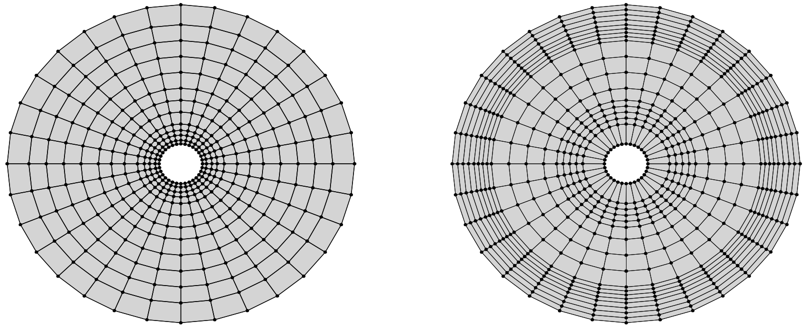

uniform 12 × 32 L4

refined 17 × 32 L4

Numerical approach - Evaluations and results

Static structural analysis

Example 3. Complex rotor

1D FE-CUF modeling

Converged model

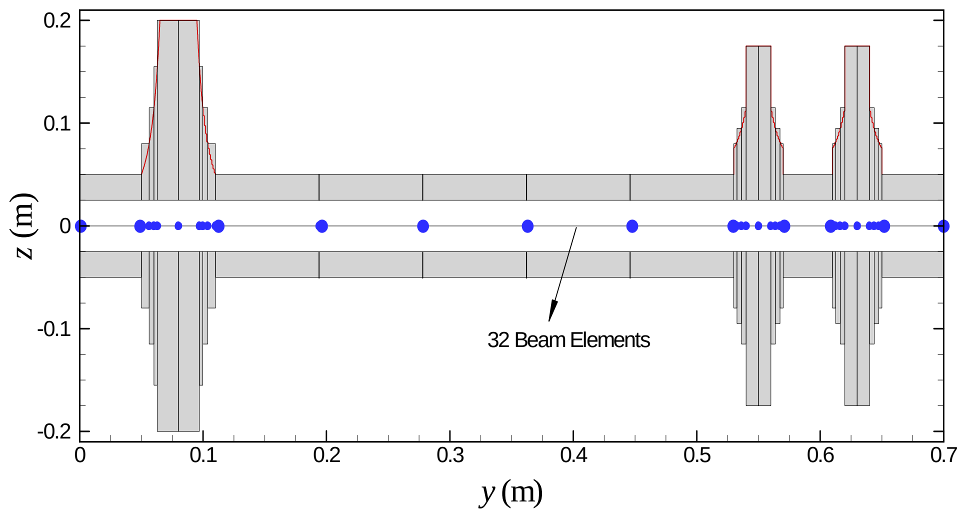

32 B2 along the axis

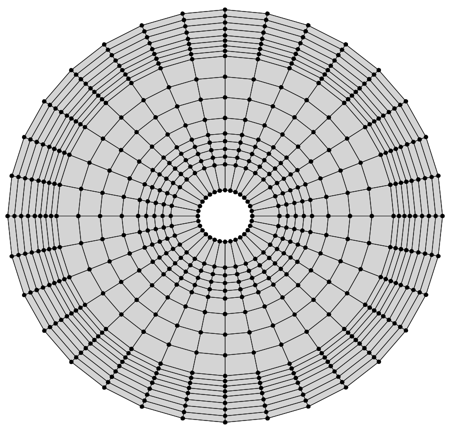

refined 17 × 32 L4

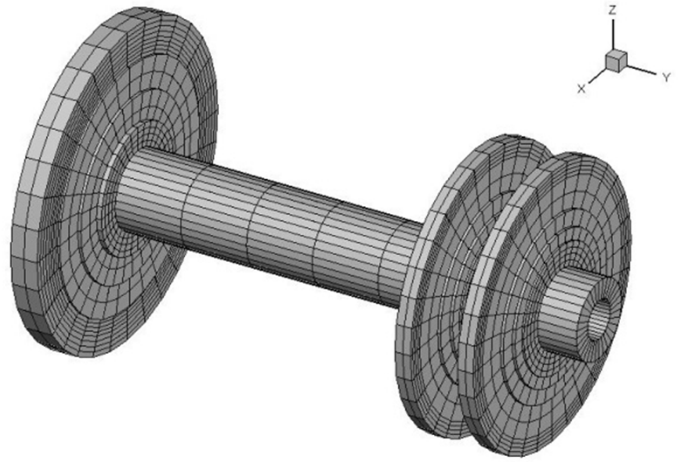

computational model, DOF=27072

Numerical approach - Evaluations and results

Static structural analysis

Example 3. Complex rotor

verification of results

Radial displacement

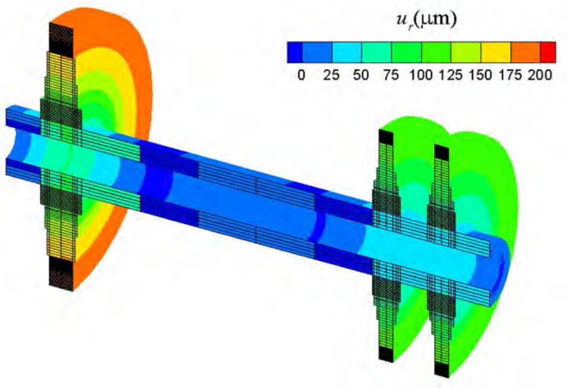

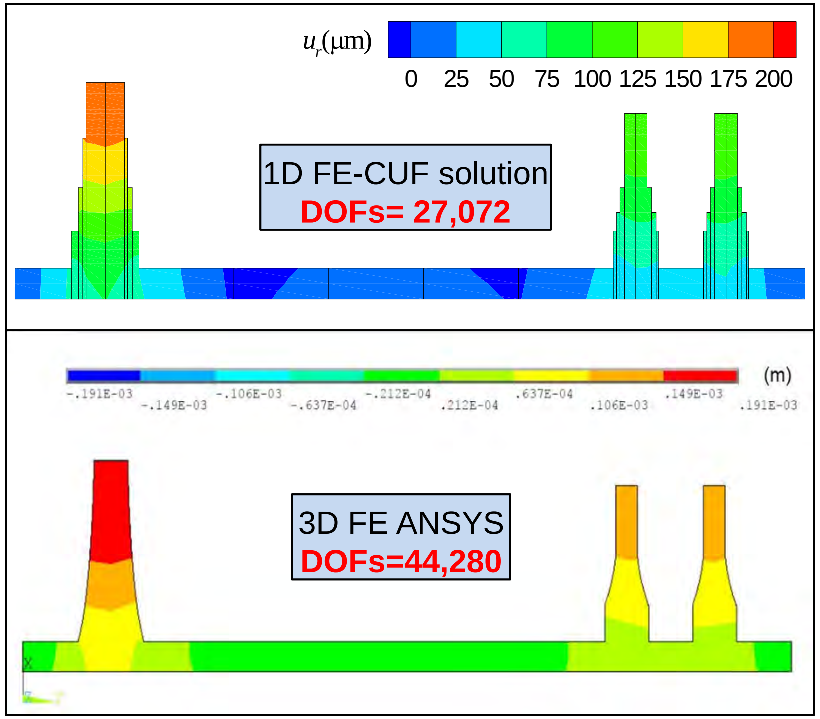

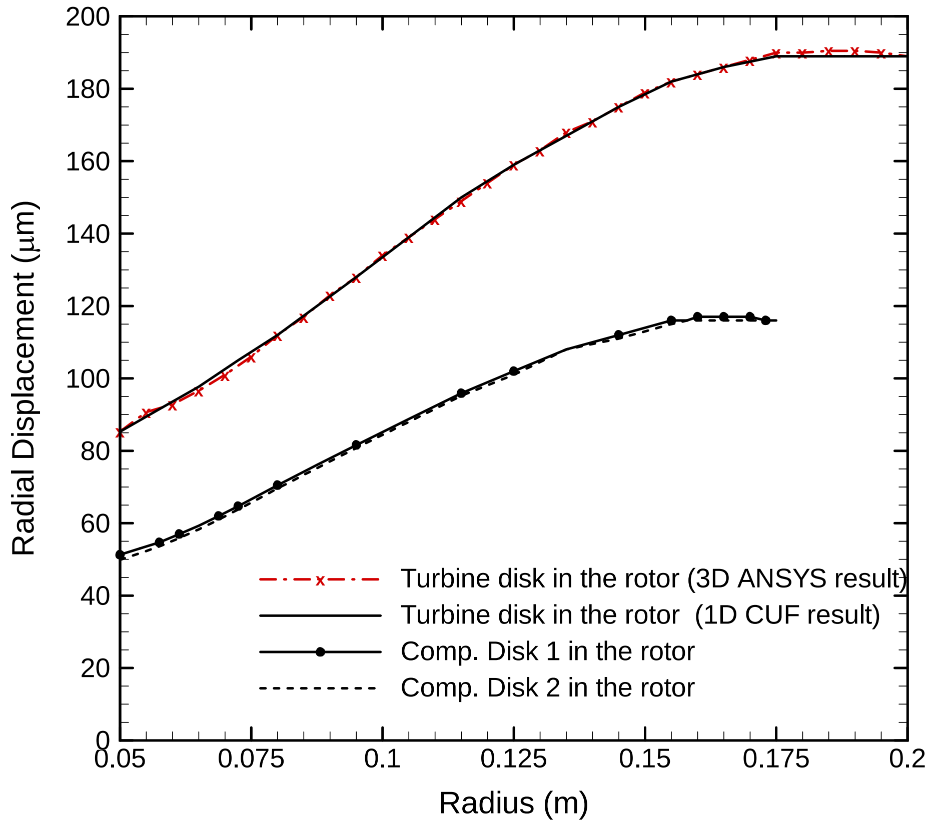

1D FE-CUF solution

✓ with 1.6 times less DOFs of the 3D ANSYS model !!

Numerical approach - Evaluations and results

Static structural analysis

Example 3. Complex rotor

verification of results

Radial and circumferential stresses

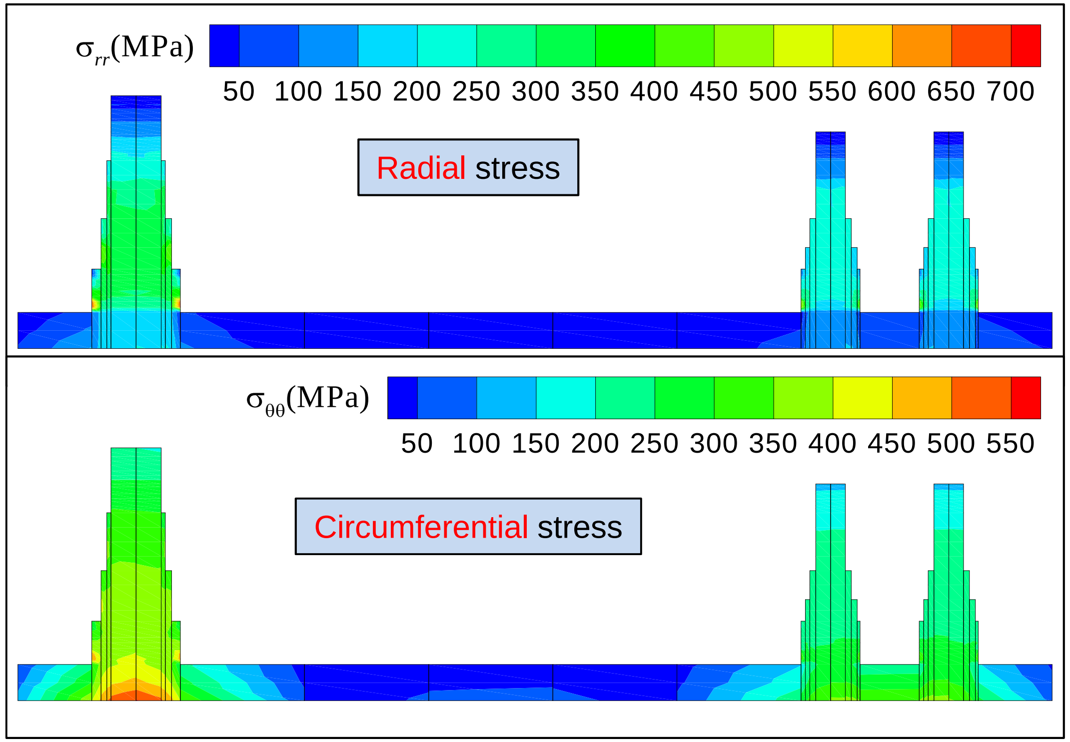

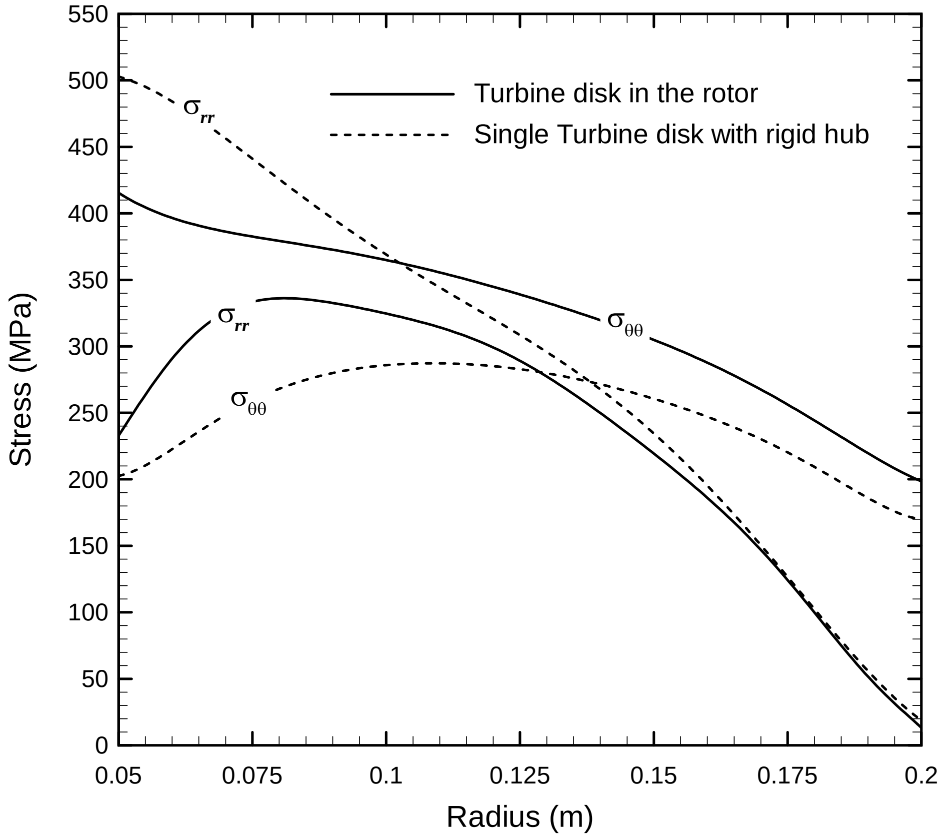

Outlines

1. Introduction to rotating disk
2. Fundamentals of Linear Thermoelasticity
3. Literature review & present work
4. Analytical approach
5. **Numerical approach**
   - Motivation
   - Development of method
   - **Evaluations and results**
     - Static structural analysis
       - ✓ Example 1. Rotating variable thickness disk
       - ✓ Example 2. Rotating variable thickness disk subjected thermal load
       - ✓ Example 3. Complex rotor
     - **Static structural-thermal analysis** – **Example 4. simple beam**
     - Quasi-static structural-thermal analysis – Example 5. simple beam
     - Dynamic coupled structural-thermal analysis
       - ✓ Example 6. Constant thickness disk made of isotropic homogeneous materials
       - ✓ Example 7. Constant thickness disk made of isotropic FGMs
       - ✓ Example 8. variable thickness disk made of isotropic FGMs
6. Conclusion

Static structural-thermal analysis

Example 4. simple beam

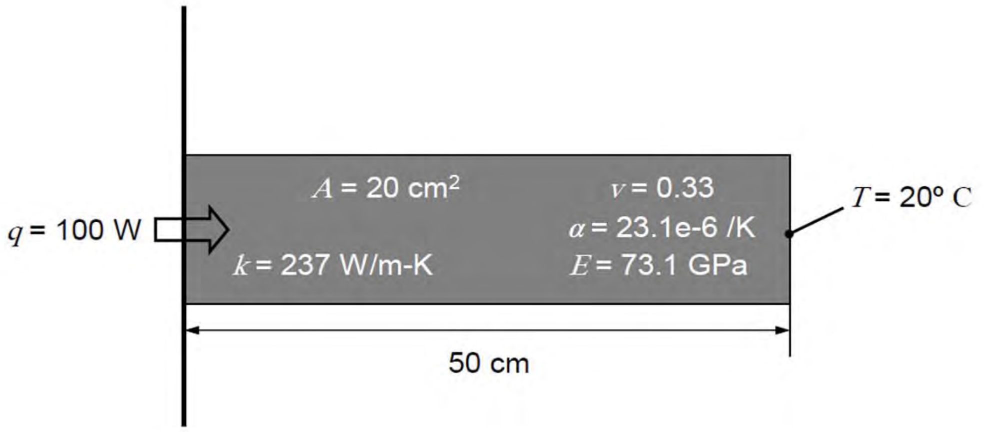

- Aluminum cantilever beam.
- Conduction from wall and constant temperature at end of beam.

1D FE-CUF modeling

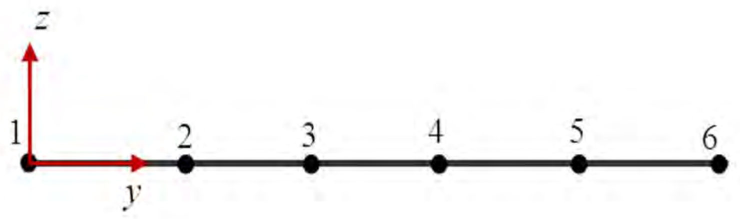

discretizing along the axis

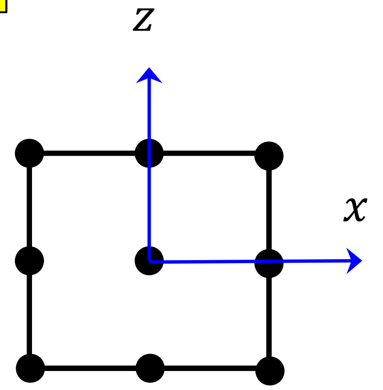

Lagrange elements over the cross-section

Numerical approach - Evaluations and results

Static structural-thermal analysis

Example 4. simple beam

results

Temperature change

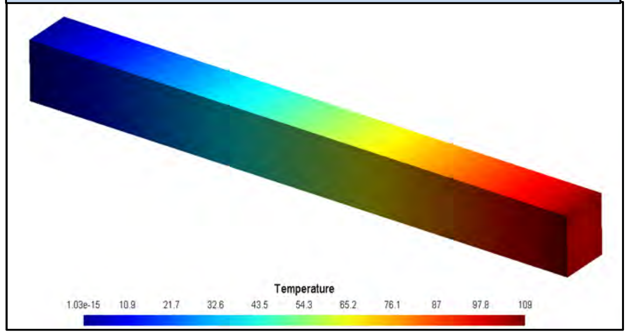

Axial displacement

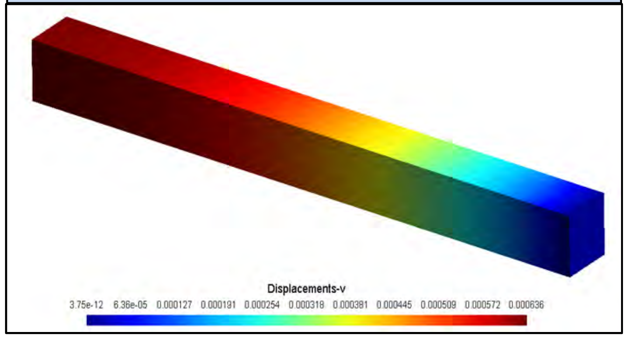

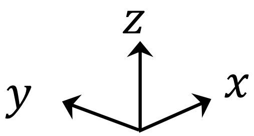

		Location along the y-axis in mm (y_i)					
Nr. elements		0.0	0.1	0.2	0.3	0.4	0.5
5-B2	u_y	0.0	0.319	0.473	0.597	0.670	0.696
	T	105.5	84.38	63.28	42.19	21.09	0.0
10-B2	u_y	0.0	0.263	0.435	0.556	0.629	0.654
	T	105.5	84.38	63.28	42.19	21.09	0.0
20-B2	u_y	0.0	0.245	0.416	0.537	0.611	0.635
	T	105.5	84.38	63.28	42.19	21.09	0.0
30-B2	u_y	0.0	0.240	0.410	0.532	0.605	0.630
	T	105.5	84.38	63.28	42.19	21.09	0.0
50-B2	u_y	0.0	0.236	0.407	0.529	0.602	0.626
	T	105.5	84.38	63.28	42.19	21.09	0.0
100-B2	u_y	0.0	0.235	0.406	0.527	0.601	0.625
	T	105.5	84.38	63.28	42.19	21.09	0.0

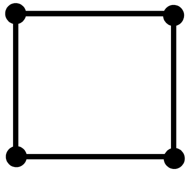

1 L4 over the cross-section

Numerical approach - Evaluations and results

Static structural-thermal analysis

Example 4. simple beam

results

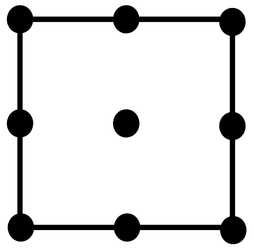

1 **L9** over the cross-section

Nr. elements		Location along the y-axis in mm (y_i)					
		0.0	0.1	0.2	0.3	0.4	0.5
5-B4	u_y	0.0	0.242	0.409	0.531	0.604	0.629
	T	105.5	84.38	63.28	42.19	21.09	0.0
10-B4	u_y	0.0	0.233	0.404	0.526	0.601	0.623
	T	105.5	84.38	63.28	42.19	21.09	0.0
20-B4	u_y	0.0	0.232	0.403	0.525	0.599	0.622
	T	105.5	84.38	63.28	42.19	21.09	0.0
30-B4	u_y	0.0	0.232	0.403	0.525	0.598	0.622
	T	105.5	84.38	63.28	42.19	21.09	0.0
50-B4	u_y	0.0	0.232	0.403	0.525	0.598	0.622
	T	105.5	84.38	63.28	42.19	21.09	0.0
100-B4	u_y	0.0	0.232	0.403	0.525	0.598	0.622
	T	105.5	84.38	63.28	42.19	21.09	0.0

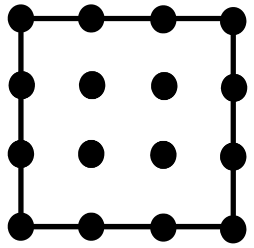

1 **L16** over the cross-section

Nr. elements		Location along the y-axis in mm (y_i)					
		0.0	0.1	0.2	0.3	0.4	0.5
5-B4	u_y	0.0	0.242	0.409	0.531	0.604	0.629
	T	105.5	84.38	63.28	42.19	21.09	0.0
10-B4	u_y	0.0	0.233	0.404	0.526	0.598	0.623
	T	105.5	84.38	63.28	42.19	21.09	0.0
20-B4	u_y	0.0	0.231	0.402	0.524	0.597	0.621
	T	105.5	84.38	63.28	42.19	21.09	0.0
100-B4	u_y	0.0	0.231	0.402	0.524	0.597	0.621
	T	105.5	84.38	63.28	42.19	21.09	0.0

Static structural-thermal analysis

Example 4. simple beam

verification of results

Does heat conduction equation satisfy?

$$q_{cond} = k\,A\frac{\Delta T}{l}$$

$$q_{cond} = \left(237\frac{\mathrm{W}}{\mathrm{m\,K}}\right)\left(0.002\,\mathrm{m}^2\right)\left(\frac{(398.49-293)\,\mathrm{K}}{0.5\,\mathrm{m}}\right) = 100\,\mathrm{W}$$

Yes!!

Numerical approach - Evaluations and results

Static structural-thermal analysis

Example 4. simple beam

verification of results

Check free thermal expansion !

$$\text{Elongation} = L\alpha T_{average}$$

$$\text{At } y = 0.1 \rightarrow u_y = (0.1)(23.1 \times 10^{-6})\frac{(84.38+105.5)}{2} = 0.219\ \text{mm}$$

$$\text{At } y = 0.5 \rightarrow u_y = (0.5)(23.1 \times 10^{-6})\frac{(0+105.5)}{2} = 0.6092\ \text{mm}$$

Outlines

1. Introduction to rotating disk
2. Fundamentals of Linear Thermoelasticity
3. Literature review & present work
4. Analytical approach
5. **Numerical approach**
    - Motivation
    - Development of method
    - **Evaluations and results**
        - Static structural analysis
            - ✓ Example 1. Rotating variable thickness disk
            - ✓ Example 2. Rotating variable thickness disk subjected thermal load
            - ✓ Example 3. Complex rotor
        - Static structural-thermal analysis – Example 4. simple beam
        - **Quasi-static structural-thermal analysis** – **Example 5. simple beam**
        - Dynamic coupled structural-thermal analysis
            - ✓ Example 6. Constant thickness disk made of isotropic homogeneous materials
            - ✓ Example 7. Constant thickness disk made of isotropic FGMs
            - ✓ Example 8. variable thickness disk made of isotropic FGMs
6. Conclusion

Quasi-static structural-thermal analysis

Example 5. simple beam

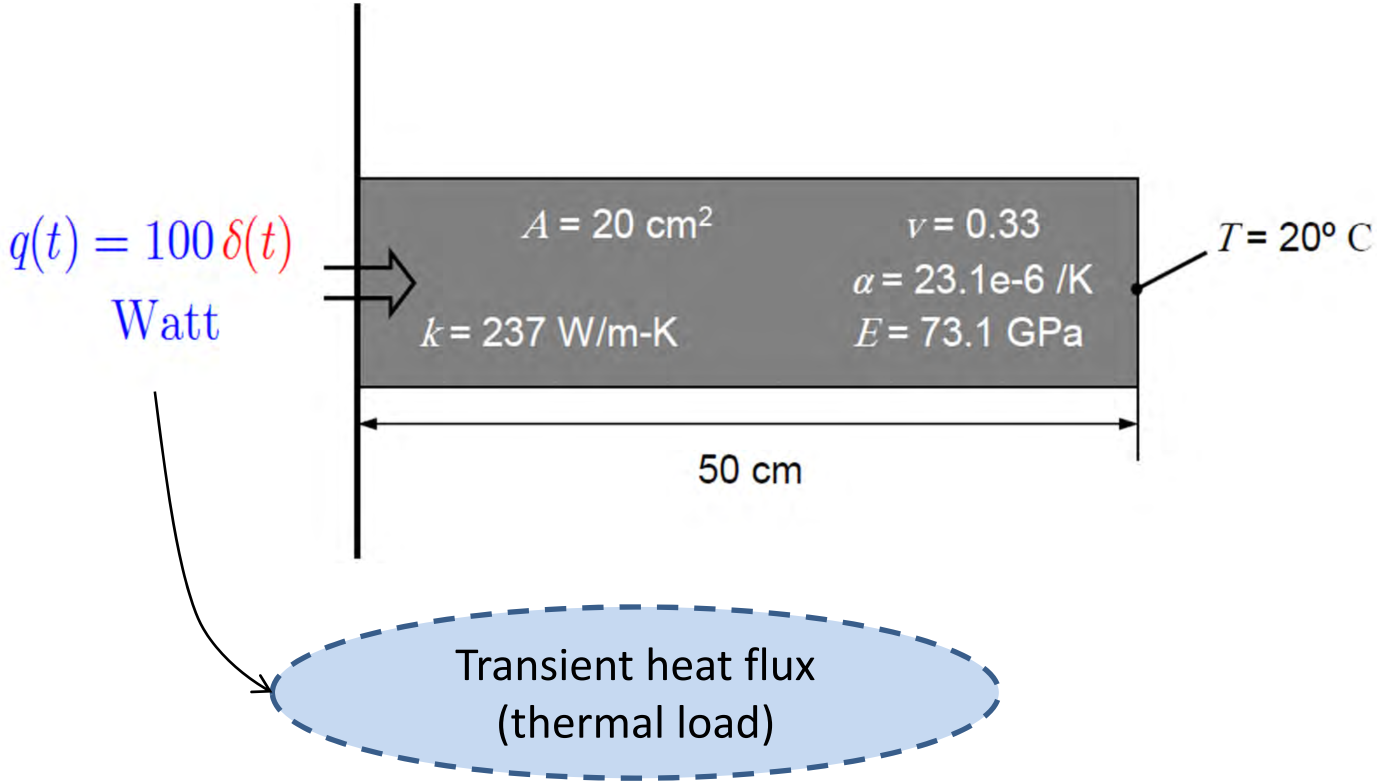

Numerical approach - Evaluations and results

Quasi-static structural-thermal analysis

Example 5. simple beam | results | 10B4/1L4 model

Axial displacement

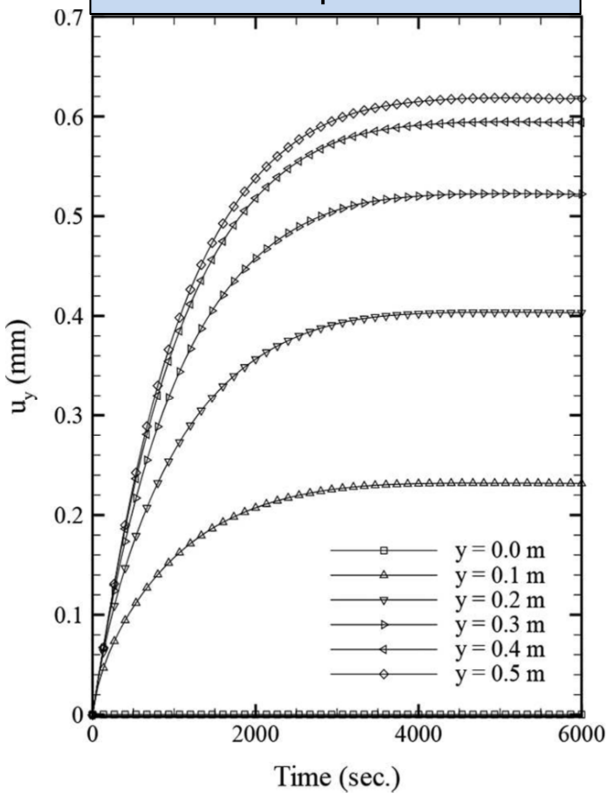

Temperature change

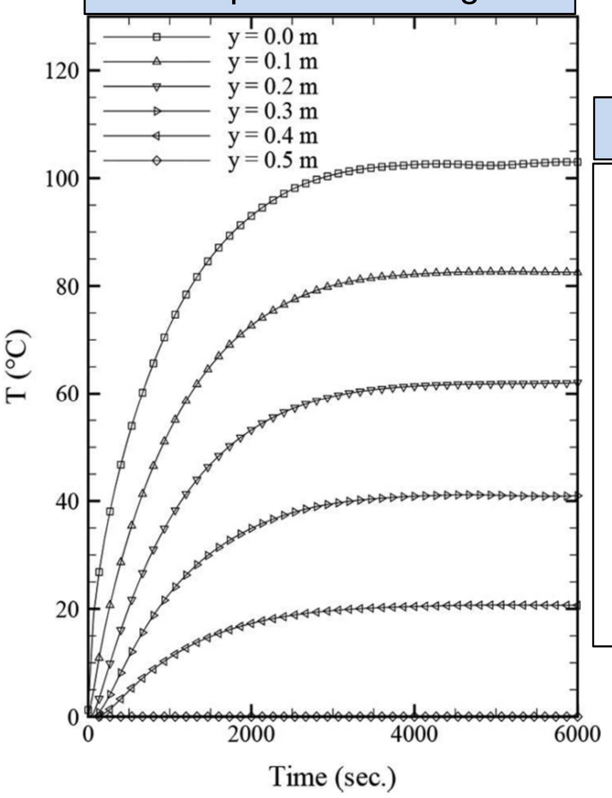

Axial displacement

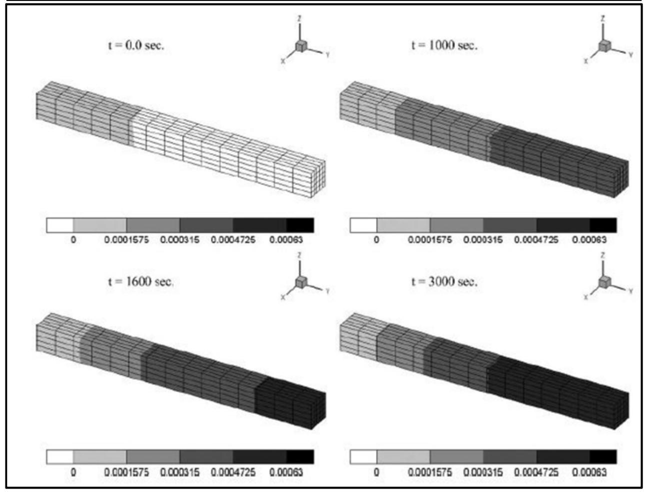

Temperature change

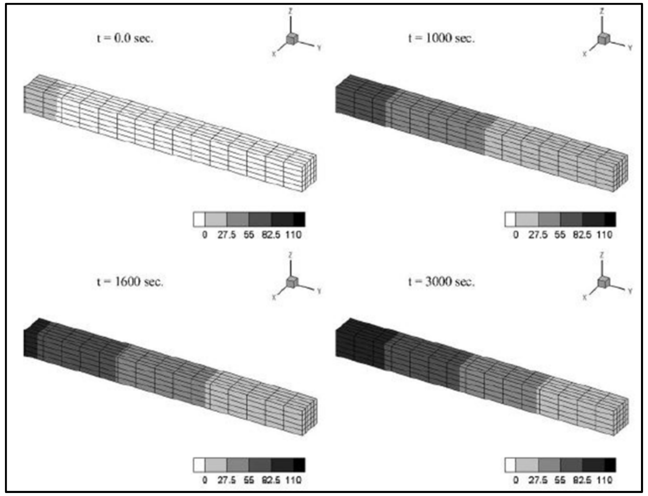

Outlines

1. Introduction to rotating disk
2. Fundamentals of Linear Thermoelasticity
3. Literature review & present work
4. Analytical approach
5. **Numerical approach**
   - Motivation
   - Development of method
   - **Evaluations and results**
     - Static structural analysis
       - ✓ Example 1. Rotating variable thickness disk
       - ✓ Example 2. Rotating variable thickness disk subjected thermal load
       - ✓ Example 3. Complex rotor
     - Static structural-thermal analysis – Example 4. simple beam
     - Quasi-static structural-thermal analysis – Example 5. simple beam
     - **Dynamic coupled structural-thermal analysis**
       - ✓ **Example 6. Constant thickness disk made of isotropic homogeneous materials**
       - ✓ Example 7. Constant thickness disk made of isotropic FGMs
       - ✓ Example 8. variable thickness disk made of isotropic FGMs
6. Conclusion

Numerical approach - Evaluations and results

Dynamic coupled structural-thermal analysis

Example 6. Constant thickness disk made of isotropic homogeneous materials

Material properties	
Lame'constant λ	$40.4\ \mathrm{GPa}$
Lame' constant μ	$27\ \mathrm{GPa}$
coefficient of linear thermal expansion (α)	$23 \times 10^{-6}\ \mathrm{K}^{-1}$
density (ρ)	$2707\ \mathrm{kg/m^3}$
thermal conductivity (κ)	$204\ \mathrm{W/m \cdot K}$
specific heat (c)	$903\ \mathrm{J/kg \cdot K}$

Boundary conditions

$$\hat{r} = a \rightarrow \begin{cases} -\dfrac{\partial \hat{T}}{\partial \hat{r}} = \hat{q}_{in}(t) \\ \hat{u} = 0 \end{cases}$$

$$\hat{r} = b \rightarrow \begin{cases} \hat{T} = 0 \\ \hat{\sigma}_{rr} = 0 \end{cases}$$

where

$$\hat{q}_{in}(t) = \begin{cases} 0 & \hat{t} \leq 0 \\ 1 & \hat{t} > 0 \end{cases}$$

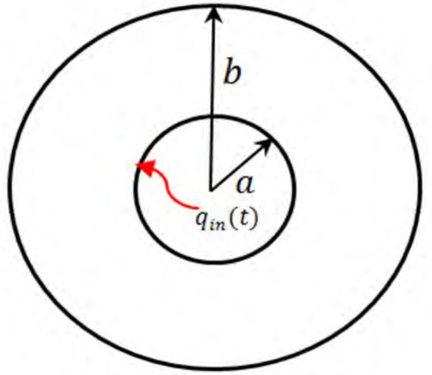

geometry

$a = 1$
$b = 2$
Thickness = 0.1

Numerical approach - Evaluations and results

Dynamic coupled structural-thermal analysis

Example 6. Constant thickness disk made of isotropic homogeneous materials

1D FE-CUF modeling

discretizing along the axis

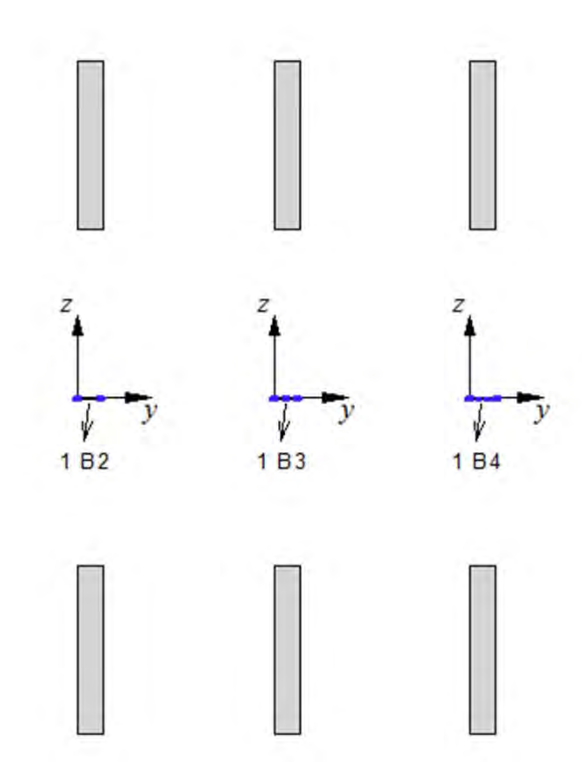

Different 1D FE-CUF models for the constant thickness disk

Model	Discretizing: Along the axis	Discretizing: corss sections	DOF
(1)	1 B2		1680
(2)	1 B3	(6×30) L4	2520
(3)	1 B4		3360
(4)		(3×15) L9	1680
(5)	1 B2	(2×10) L16	
(6)		(6×18) L9	3744

Lagrange mesh over the cross-section with the largest radius

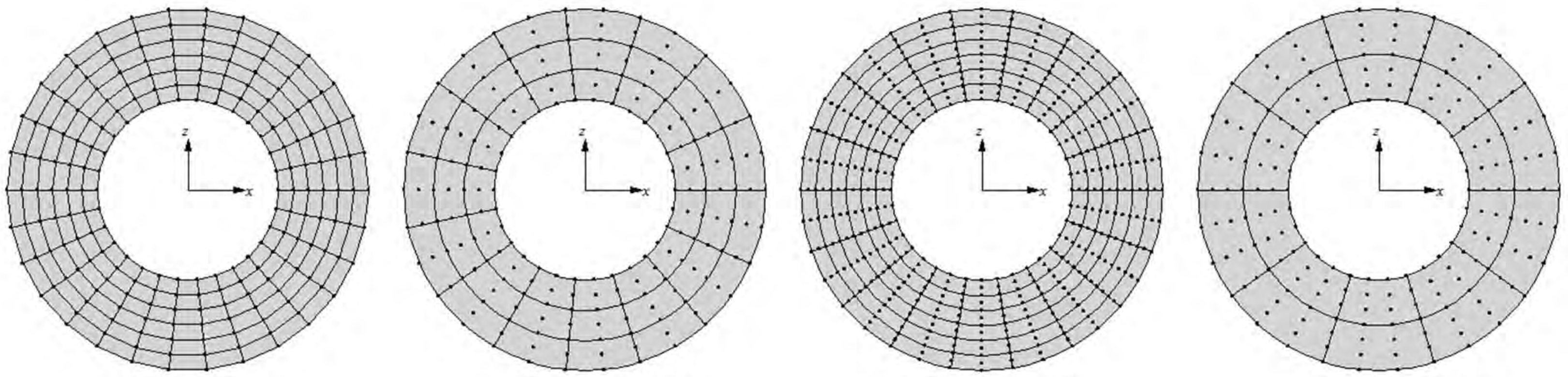

(6×30) L4 (3×15) L9 (6×18) L9 (2×10) L16

Numerical approach - Evaluations and results

Dynamic coupled structural-thermal analysis

Example 6. Constant thickness disk made of isotropic homogeneous materials

verification of results

Based on the LS theory of thermoelasticity

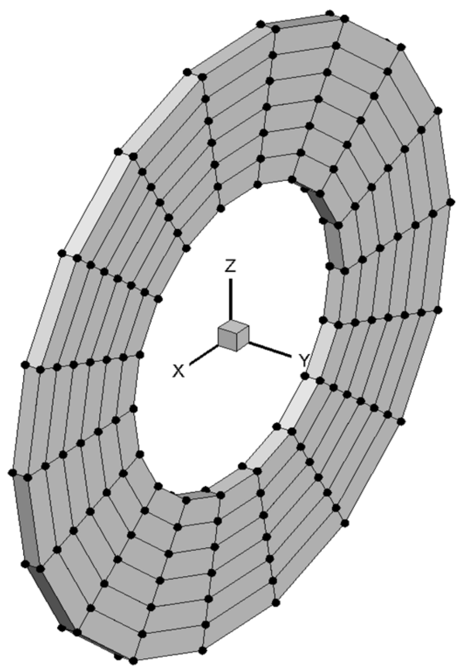

1B2 / (6 × 18) L9

Temperature change

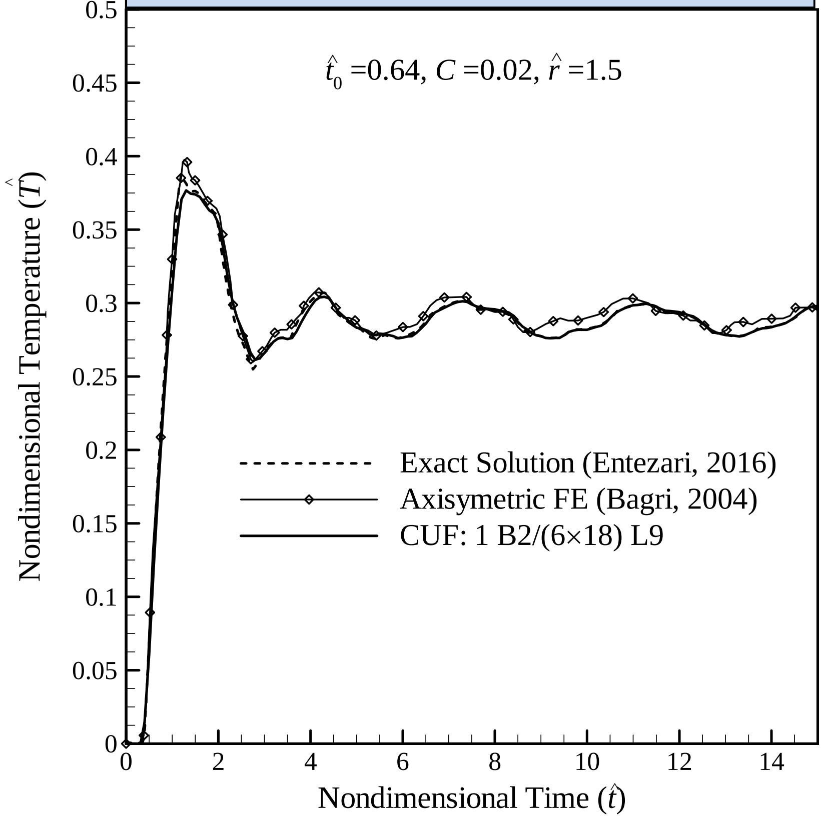

Radial displacement

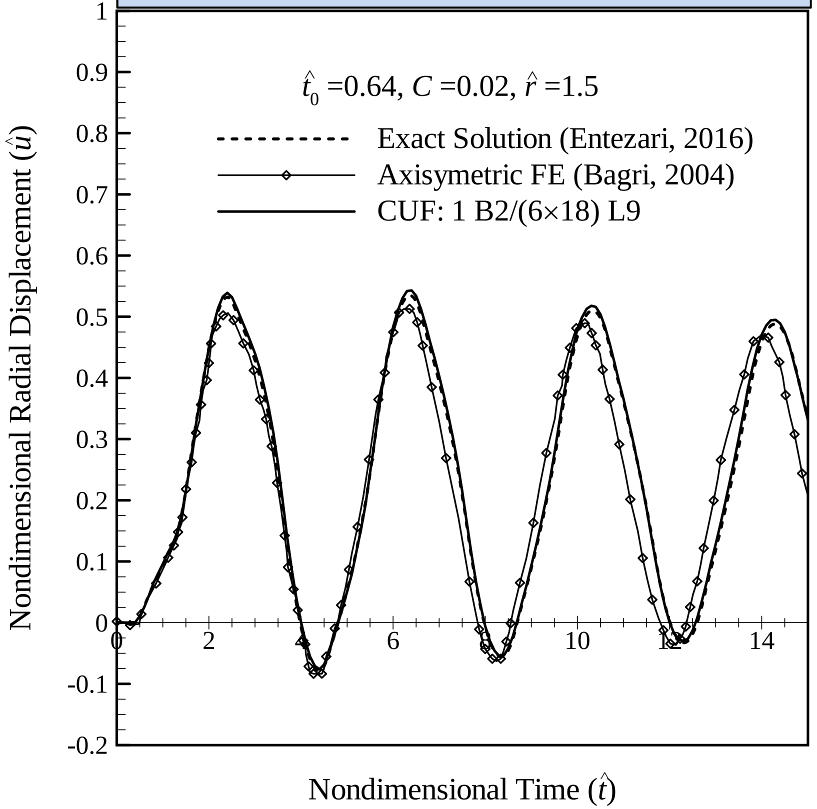

Time history of solution at mid-radius of the disk.

Numerical approach - Evaluations and results

Dynamic coupled structural-thermal analysis

Example 6. Constant thickness disk made of isotropic homogeneous materials

verification of results

Based on the LS theory of thermoelasticity

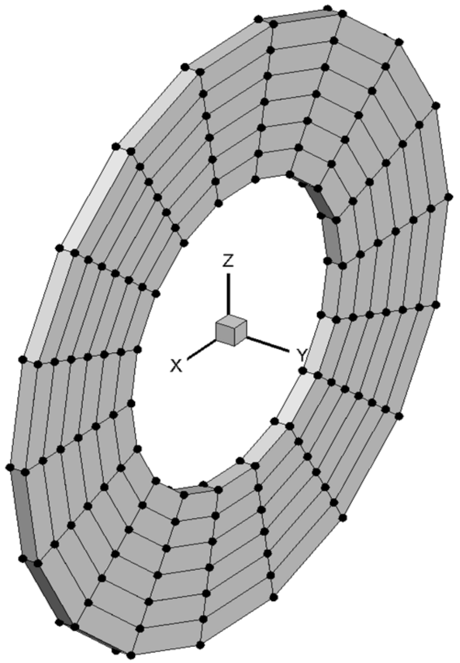

1B2 / (6 × 18) L9

Radial stress

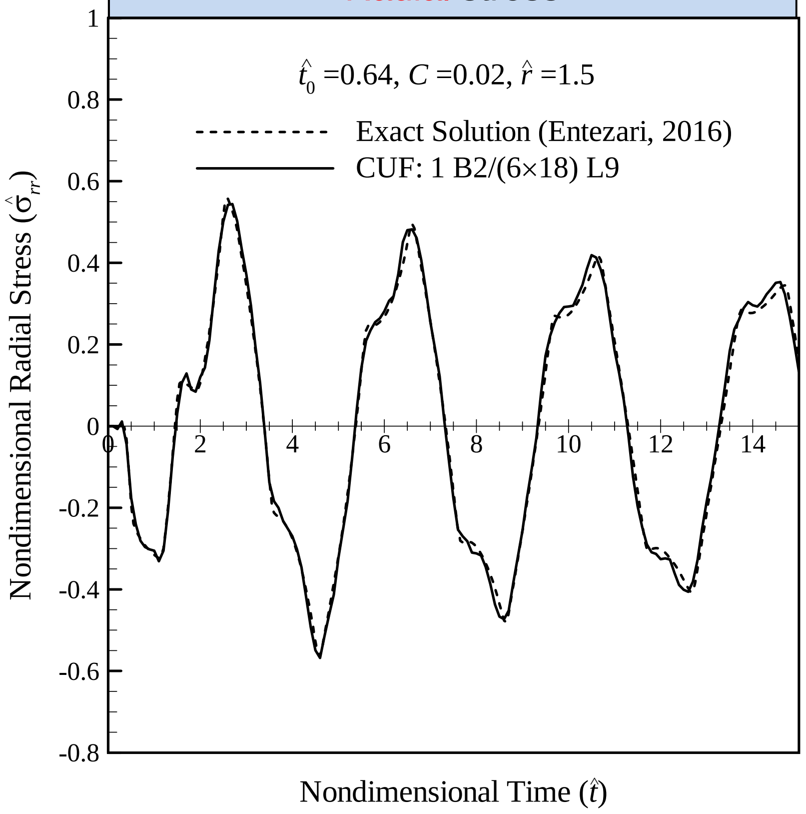

Circumferential stress

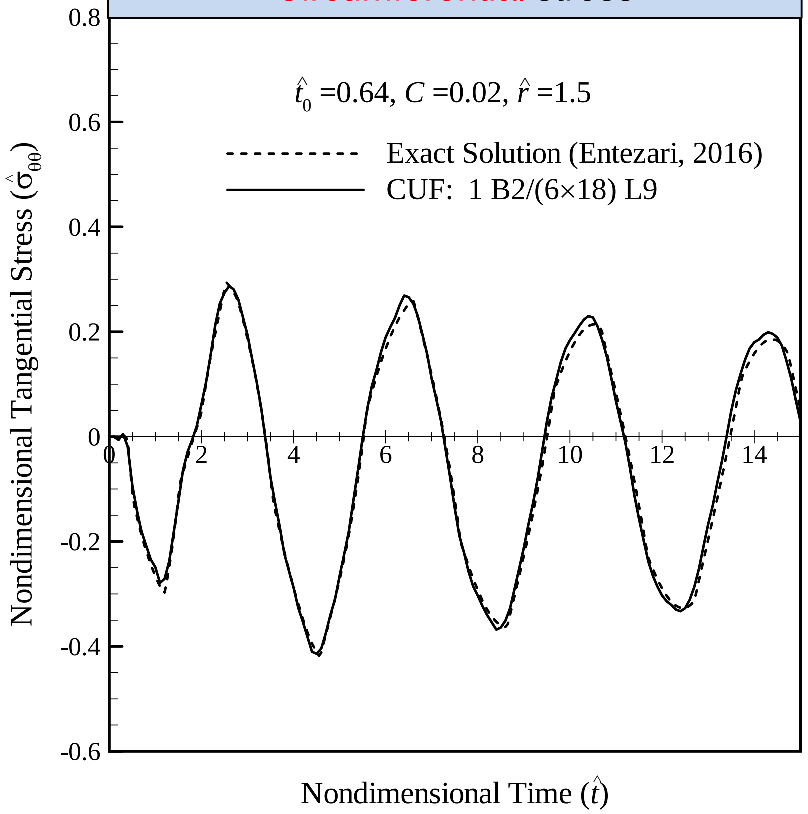

Time history of solution at mid-radius of the disk.

Outlines

1. Introduction to rotating disk
2. Fundamentals of Linear Thermoelasticity
3. Literature review & present work
4. Analytical approach
5. **Numerical approach**
   - Motivation
   - Development of method
   - **Evaluations and results**
     - Static structural analysis
       - ✓ Example 1. Rotating variable thickness disk
       - ✓ Example 2. Rotating variable thickness disk subjected thermal load
       - ✓ Example 3. Complex rotor
     - Static structural-thermal analysis – Example 4. simple beam
     - Quasi-static structural-thermal analysis – Example 5. simple beam
     - **Dynamic coupled structural-thermal analysis**
       - ✓ Example 6. Constant thickness disk made of isotropic homogeneous materials
       - ✓ **Example 7. Constant thickness disk made of isotropic FGM**
       - ✓ Example 8. variable thickness disk made of isotropic FGMs
6. Conclusion

Numerical approach - Evaluations and results

Dynamic coupled structural-thermal analysis

Example 7. Constant thickness disk made of isotropic FGM

Geometry and material

Material properties Metal-Ceramic FGM		
	Metal: Aluminum	**Ceramic: Alumina**
Lame'constant λ	40.4 GPa	219.2 GPa
shear modulus μ	27.0 GPa	146.2 GPa
density (ρ)	2707 kg/m^3	3800 kg/m^3
coefficient of linear thermal expansion (α)	23.0×10^{-6} K^{-1}	7.4×10^{-6} K^{-1}
thermal conductivity (κ)	204 W/m·K	28.0 W/m·K
specific heat (c)	903 J/kg·K	760 J/kg·K
dimensionless relaxation time ($\hat{t}_0$)	0.64	1.5625

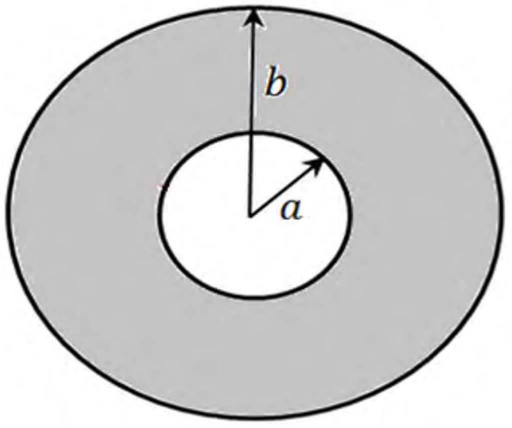

effective properties

$$P = V_m P_m + V_c P_c = V_m (P_m - P_c) + P_c$$

metal volume fraction

$$V_m = \left(\frac{b-\hat{r}}{b-a}\right)^n$$

geometry

$a = 1$

$b = 2$

Thickness = 0.1

Numerical approach - Evaluations and results

Dynamic coupled structural-thermal analysis

Example 7. Constant thickness disk made of isotropic FGM

$$T_0 = 293\ \text{K},\ \hat{\omega}=0.01$$

$$\text{at } t = 0 \rightarrow T = \dot{\mathbf{u}} = \dot{T} = \mathbf{u} = 0$$

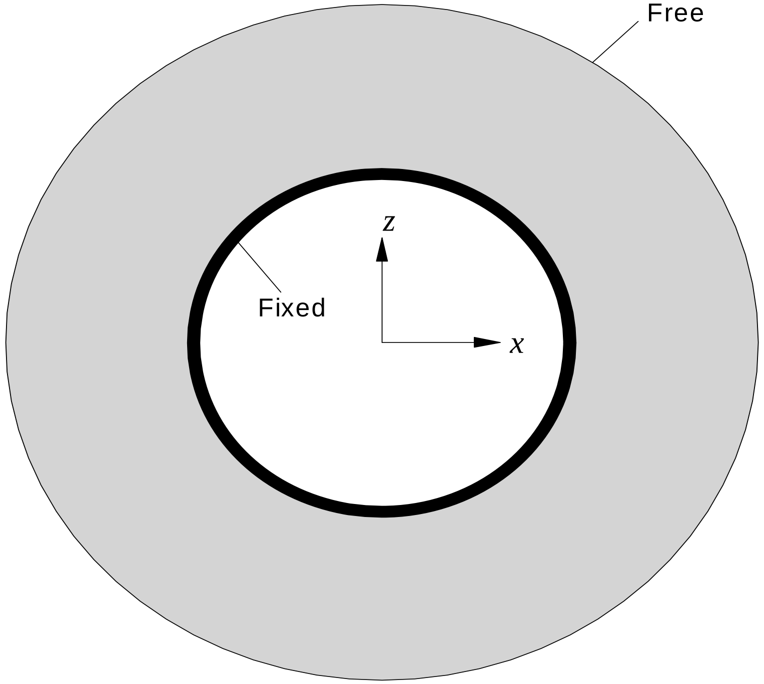

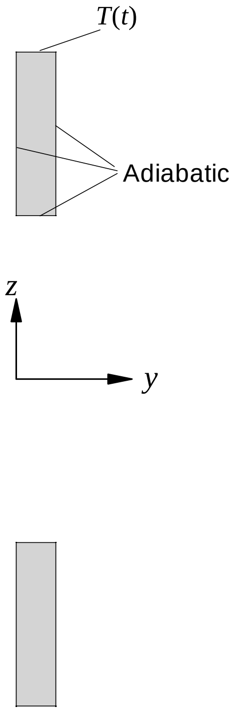

Operational, boundary & initial conditions

$$T(t) = T_d\left(1 - \left[1 + 100\frac{tV_{em}^2}{D_m}\right]e^{-100tV_{em}^2/D_m}\right)$$

Non-dimensional form

$$\hat{T}(\hat{t}) = 1 - (1 + 100\hat{t})e^{-100\hat{t}}$$

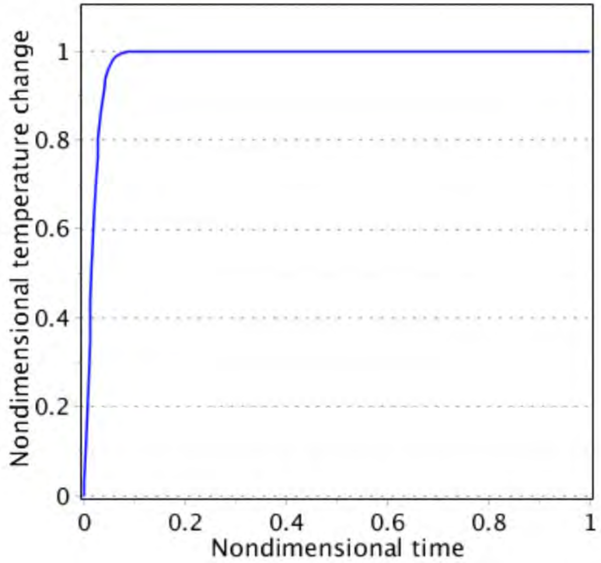

Numerical approach - Evaluations and results

Dynamic coupled structural-thermal analysis

Example 7. Constant thickness disk made of isotropic FGM | results | Time history

- ✓ the material properties linearly change through the radius ($n = 1$)
- ✓ Based on the LS theory of thermoelasticity

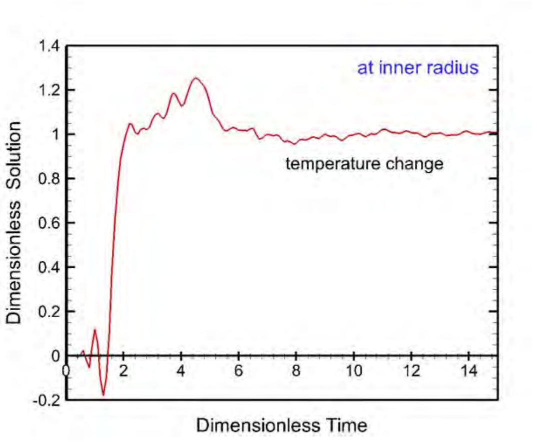

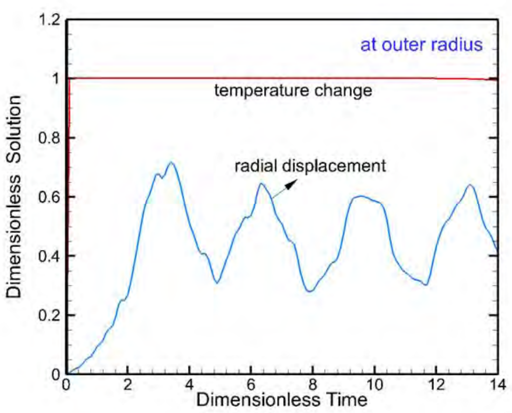

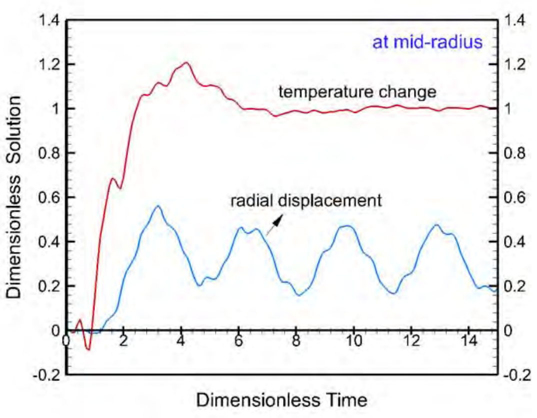

Temperature change

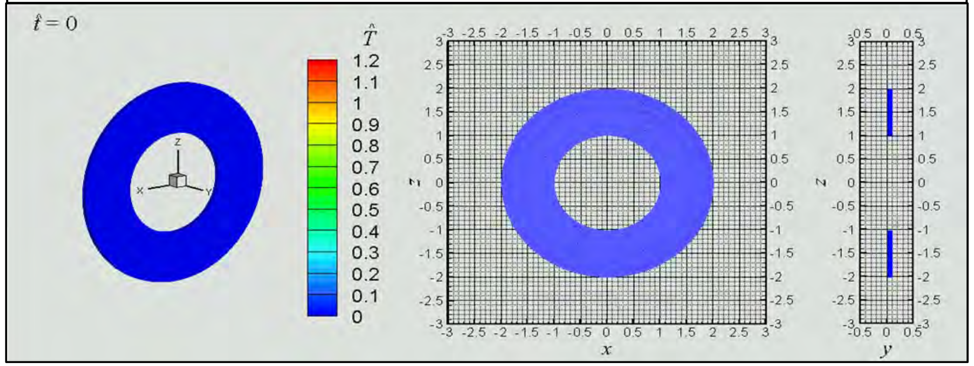

Radial displacement

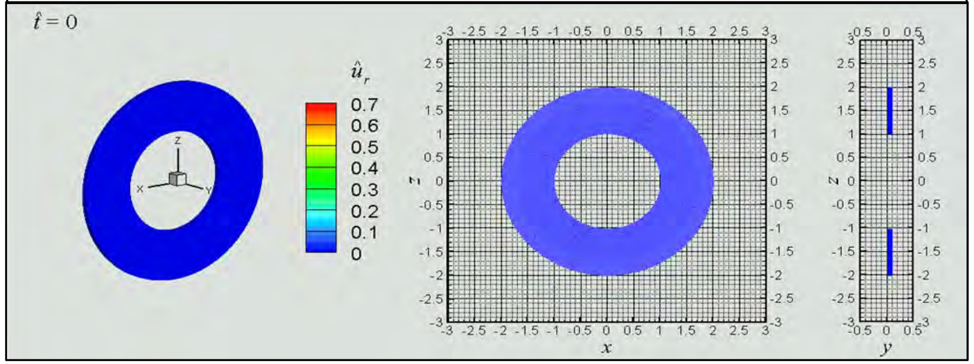

Numerical approach - Evaluations and results

Dynamic coupled structural-thermal analysis

Example 7. Constant thickness disk made of isotropic FGM | results | Time history

- ✓ the material properties linearly change through the radius ($n = 1$)
- ✓ Based on the LS theory of thermoelasticity

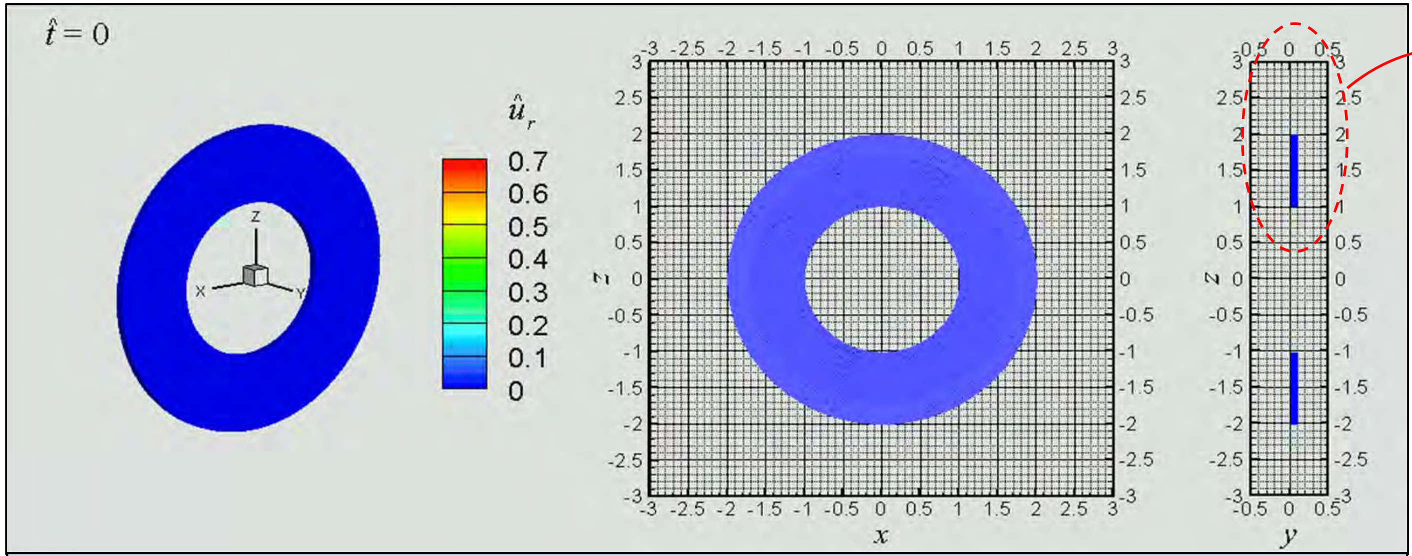

Radial displacement

Deformations of disk profile

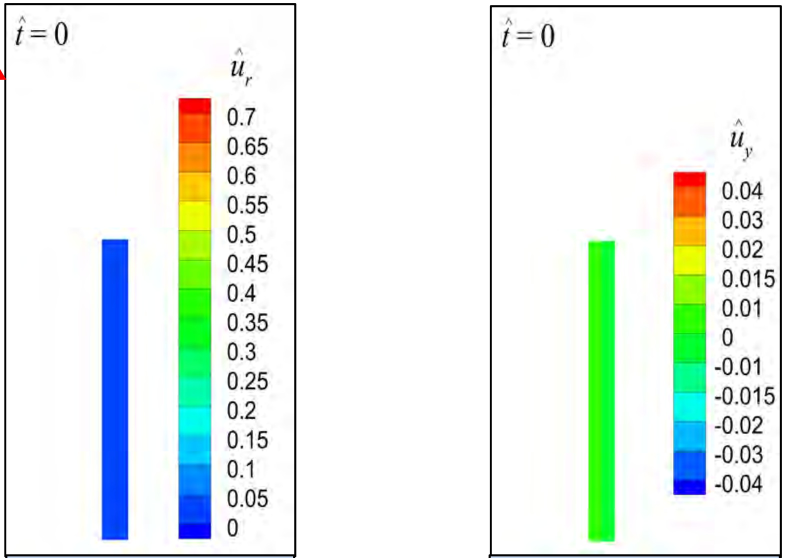

radial deformation

Axial deformation

Numerical approach - Evaluations and results

Dynamic coupled structural-thermal analysis

Example 7. Constant thickness disk made of isotropic FGM

results

Speed range of the thermal wave

- ✓ the material properties linearly change through the radius ($n = 1$)
- ✓ Based on the LS theory of thermoelasticity

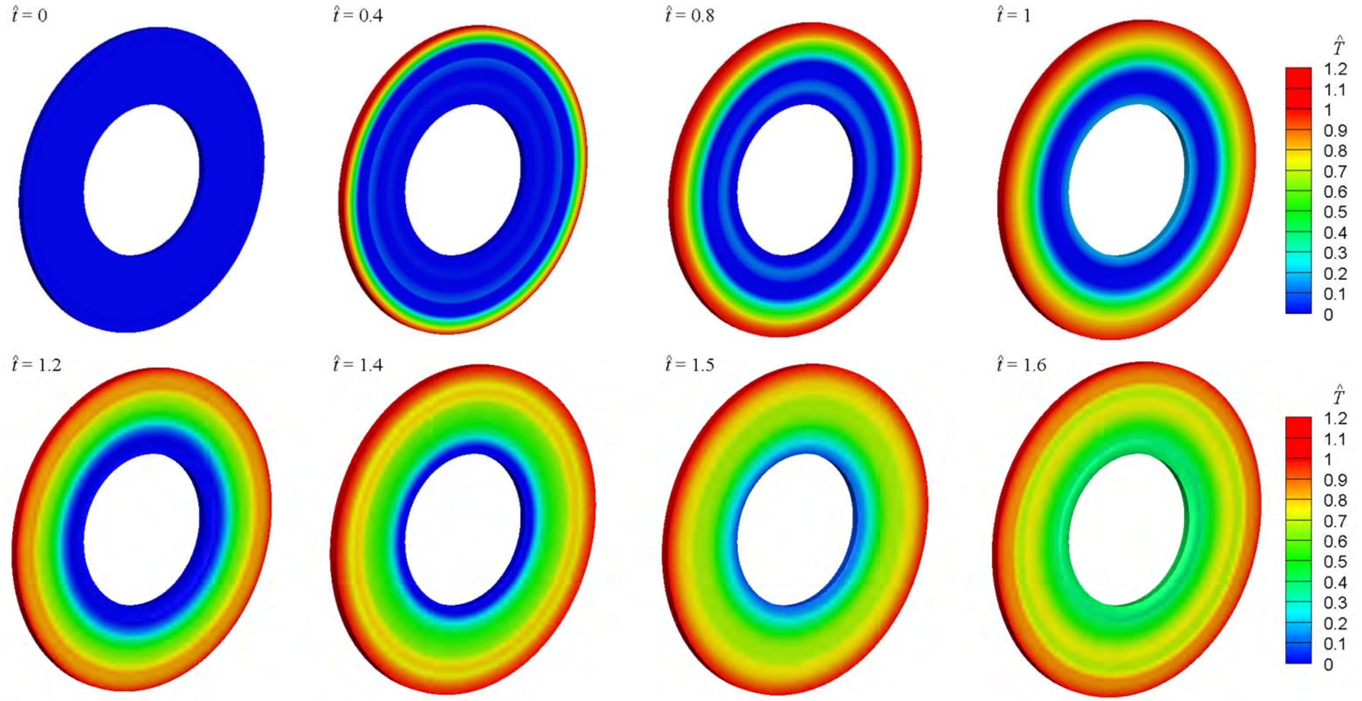

Dynamic coupled structural-thermal analysis

Example 7. Constant thickness disk made of isotropic FGM | results | Speed range of the thermal wave

- ✓ the material properties linearly change through the radius ($n = 1$)
- ✓ Based on the LS theory of thermoelasticity

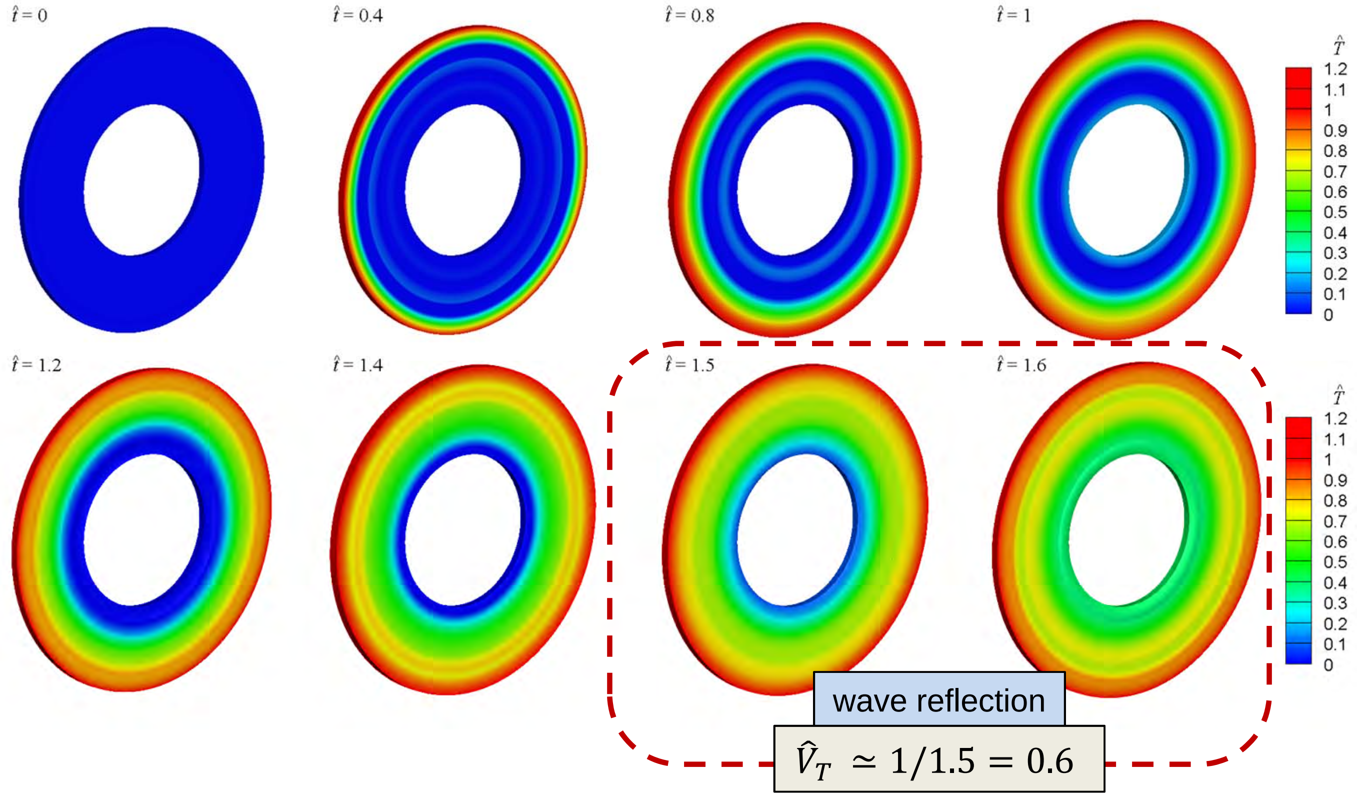

Numerical approach - Evaluations and results

Dynamic coupled structural-thermal analysis

Example 7. Constant thickness disk made of isotropic FGM | results | Thermal wave propagation

- ✓ the material properties linearly change through the radius ($n = 1$)
- ✓ Based on the LS theory of thermoelasticity

Non-dimensional form of energy equation

$$\left(\frac{\kappa}{\kappa_{\mathrm{m}}}\hat{T}_{,i}\right)_{,i} - \frac{\rho c}{c_{\mathrm{m}}\rho_{\mathrm{m}}}\left(\hat{t}_0\hat{\ddot{T}} + \hat{\dot{T}}\right) - C\,\frac{\beta}{\beta_{\mathrm{m}}}\left(\hat{t}_0\hat{\ddot{u}}_{i,i} + \hat{\dot{u}}_{i,i}\right) + \left(\hat{t}_0\hat{\dot{R}} + \hat{R}\right) = 0$$

$$\left.\begin{aligned} \hat{V}_{T\mathrm{c}} &= \sqrt{D_{\mathrm{c}}/D_{\mathrm{m}}}\sqrt{1/\hat{t}_{0\mathrm{c}}} = 0.27 \\ \hat{V}_{T\mathrm{m}} &= \sqrt{1/\hat{t}_{0\mathrm{m}}} = 1.25 \end{aligned}\right\}$$

Speed range of the thermal wave

$$0.27 \le \hat{V}_{T,\mathrm{FGM}} \le 1.25$$

$$1/1.25 \le \hat{t}_{reff} \le 1/0.27$$

$$0.8 \le \hat{t}_{reff} \le 3.7$$

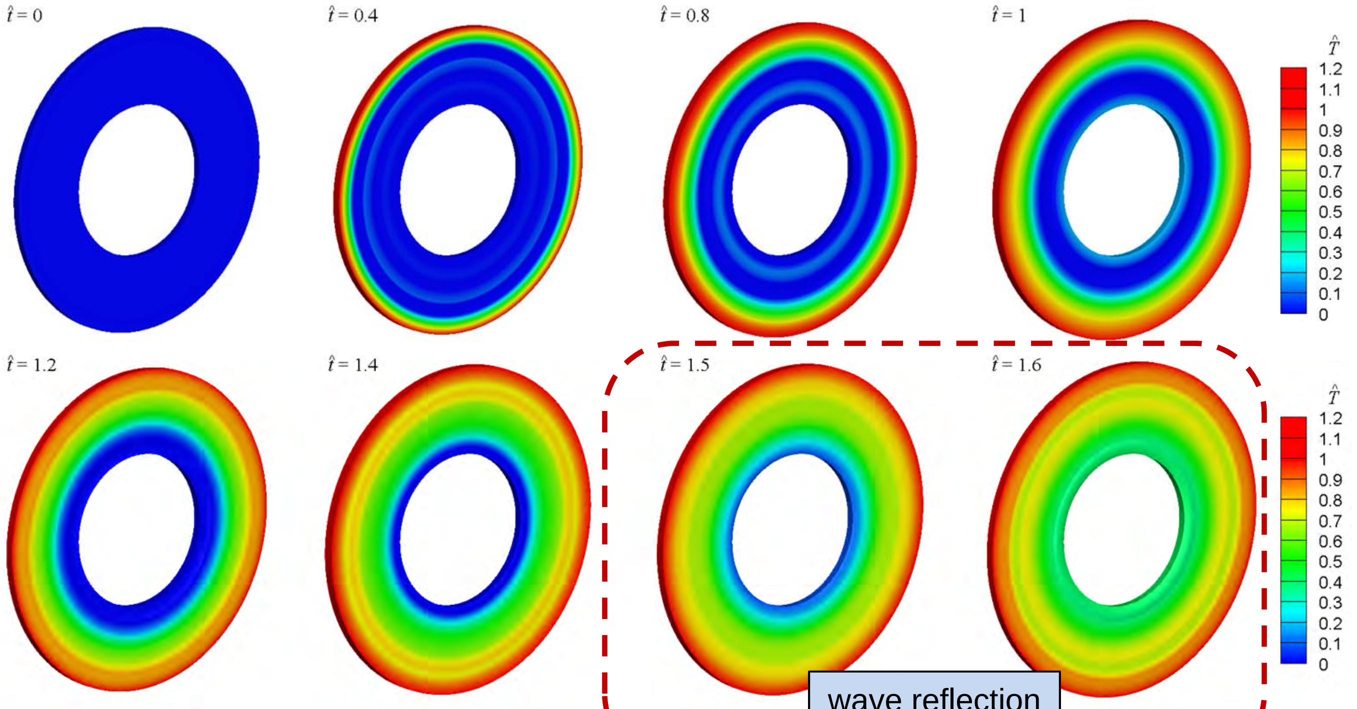

wave reflection

$\hat{V}_T \simeq 1/1.5 = 0.6$

Numerical approach - Evaluations and results

Dynamic coupled structural-thermal analysis

Example 7. Constant thickness disk made of isotropic FGM | results | Elastic wave propagation

- ✓ the material properties linearly change through the radius ($n = 1$)
- ✓ Based on the LS theory of thermoelasticity

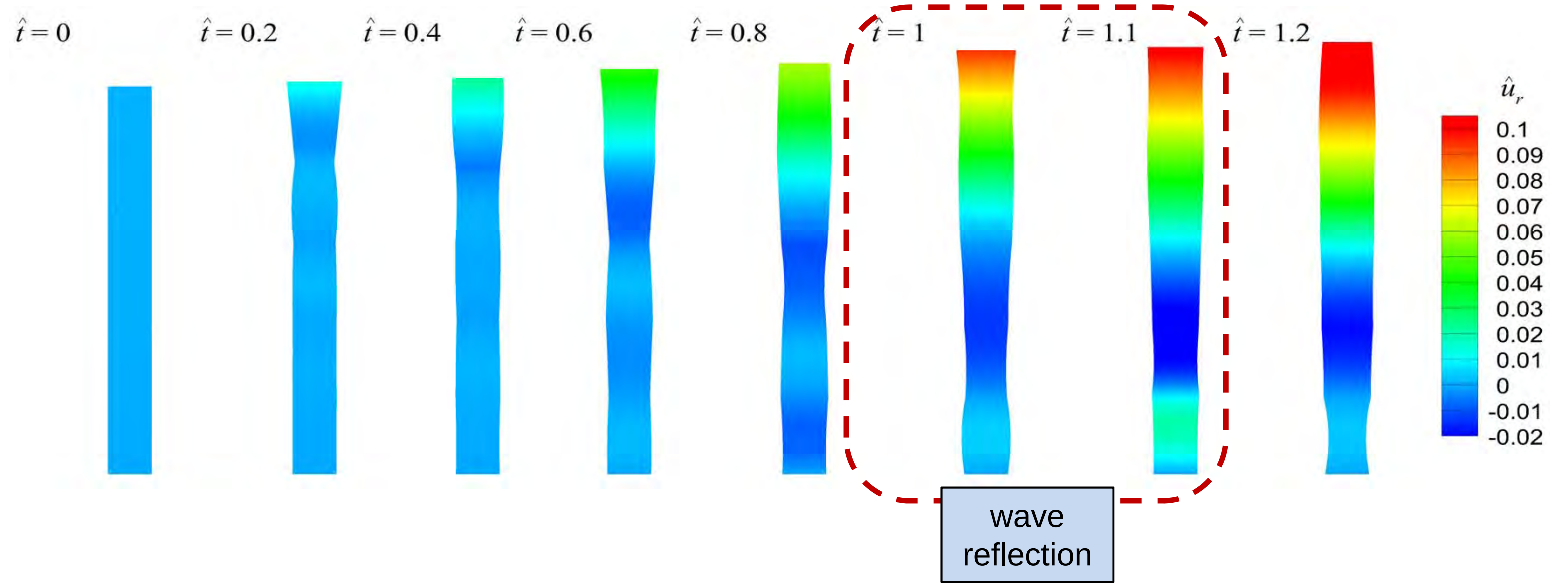

Numerical approach - Evaluations and results

Dynamic coupled structural-thermal analysis

Example 7. Constant thickness disk made of isotropic FGM | results | Elastic wave propagation

- ✓ the material properties linearly change through the radius ($n = 1$)
- ✓ Based on the LS theory of thermoelasticity

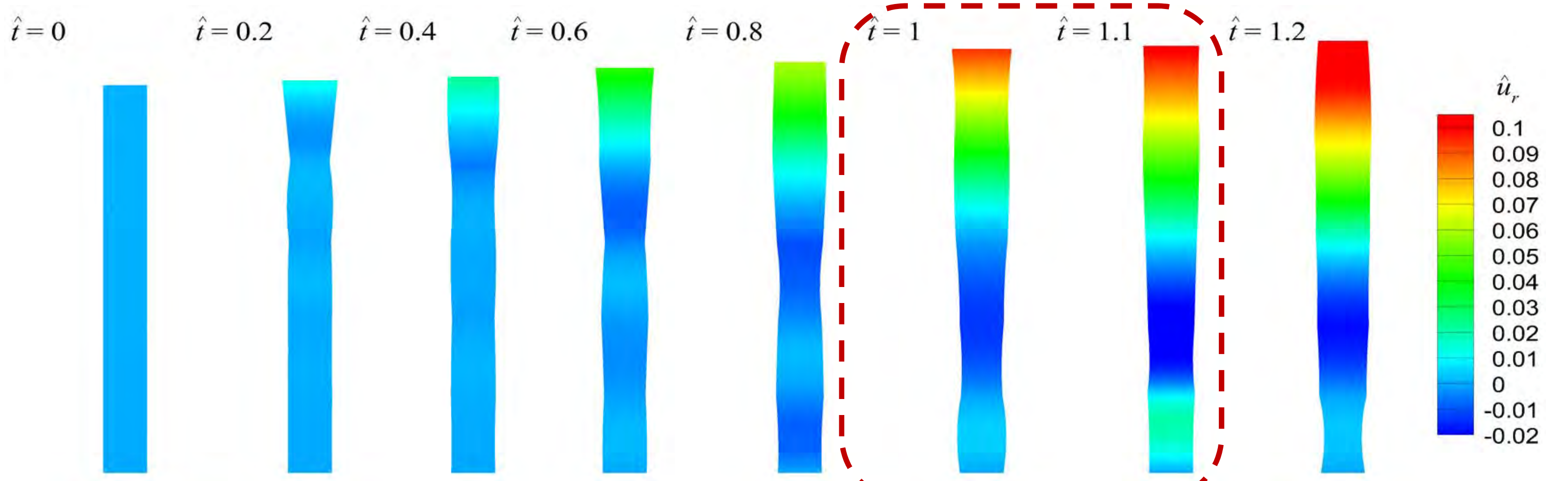

wave reflection

Non-dimensional form of equation of motion

$$\frac{\mu}{(\lambda_m + 2\mu_m)}\hat{u}_{i,jj} + \frac{(\lambda+\mu)}{(\lambda_m + 2\mu_m)}\hat{u}_{j,ji} + \frac{1}{(\lambda_m + 2\mu_m)}\lambda_{,i}\hat{u}_{j,j} + \frac{1}{(\lambda_m + 2\mu_m)}\mu_{,j}(u_{i,j} + u_{j,i}) - \frac{\rho}{\rho m}\hat{\ddot{u}}_i - \frac{1}{\beta m}\left(\beta_{,i}\hat{T} + \beta\hat{T}_{,i}\right) + \hat{X}_i = 0$$

Speed range of elastic wave

$$\left.\begin{aligned}\hat{V}_{ec} &= 1.96\\ \hat{V}_{em} &= 1\end{aligned}\right\} \rightarrow 1 \le \hat{V}_{e\mathrm{FGM}} \le 1.96$$

$$0.51 \le \hat{t}_{reff} \le 1$$

Numerical approach - Evaluations and results

Dynamic coupled structural-thermal analysis

Example 7. Constant thickness disk made of isotropic FGM | results | effects of power law index (n)

Temperature change

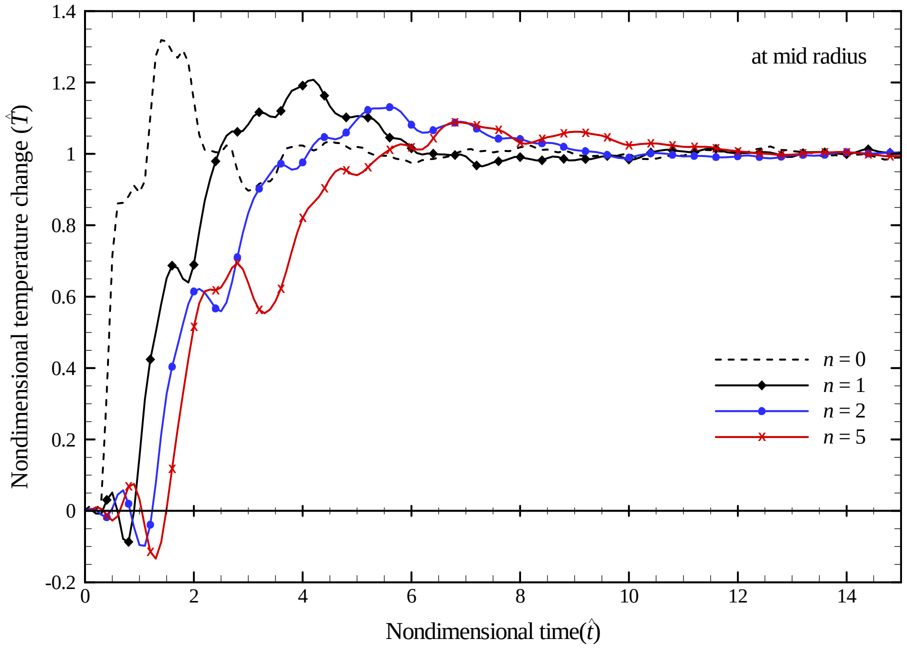

Radial displacement

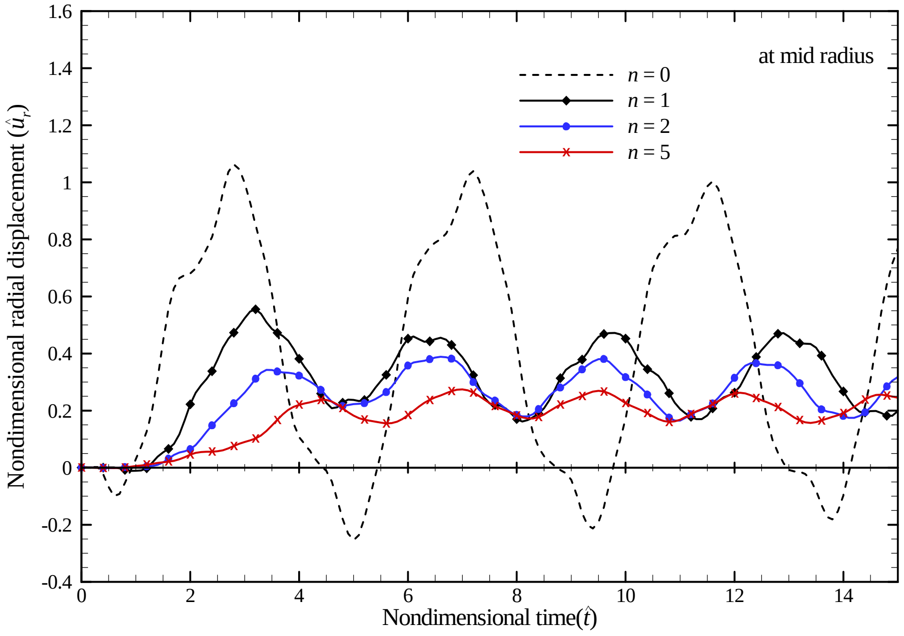

metal volume fraction

$$V_m = \left(\frac{b - \hat{r}}{b - a}\right)^n$$

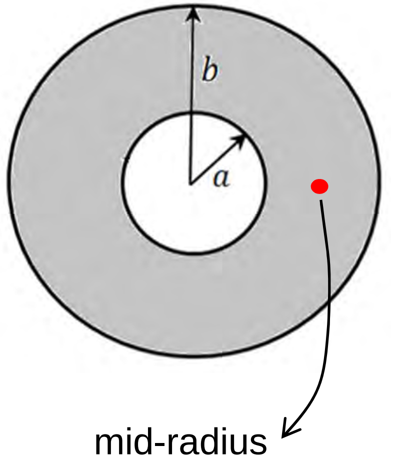

Time history based on the LS theory at mid-radius of the disk

Numerical approach - Evaluations and results

Dynamic coupled structural-thermal analysis

Example 7. Constant thickness disk made of isotropic FGM | results | effects of power law index (n)

Radial stress

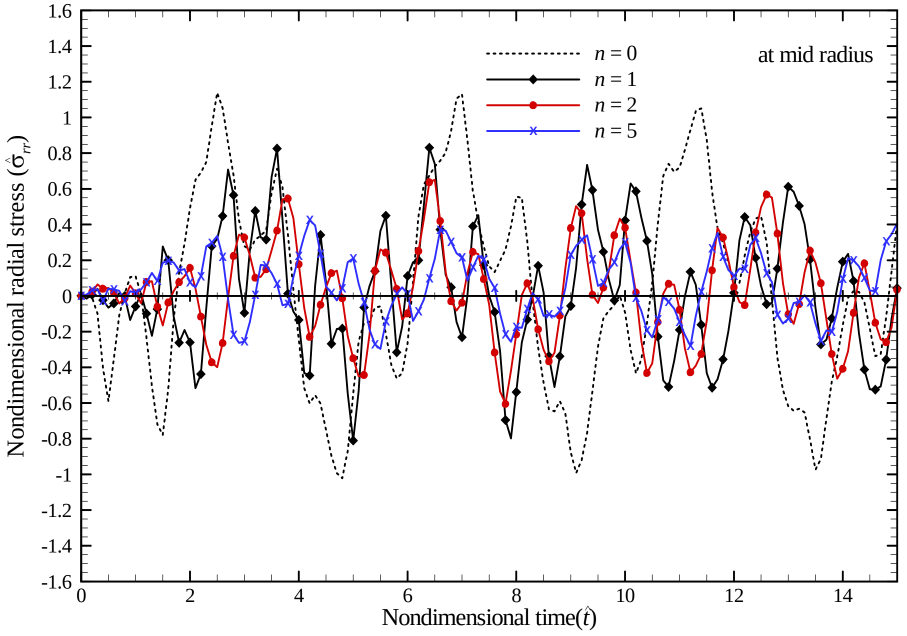

Circumferential stress

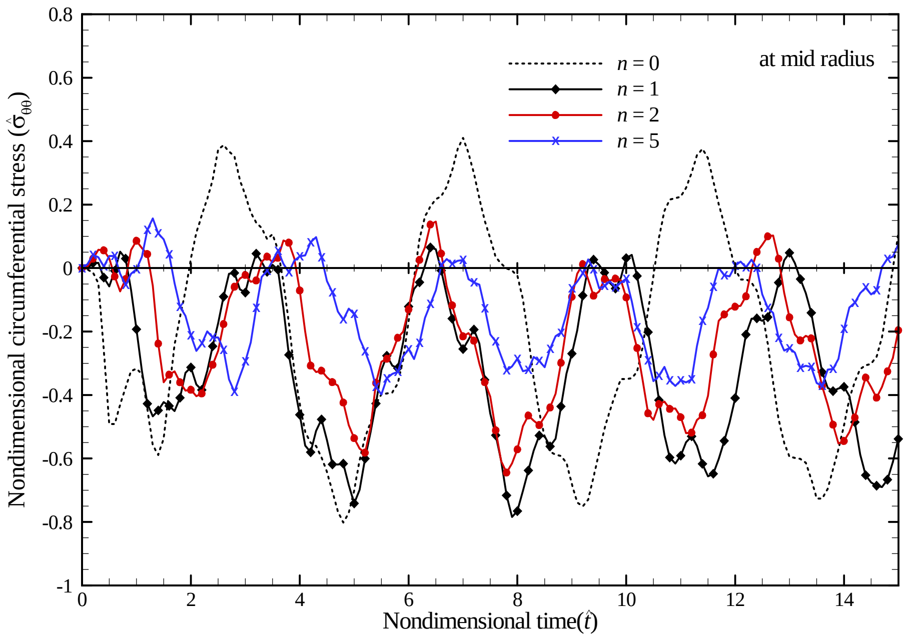

metal volume fraction

$$V_m = \left(\frac{b-\hat{r}}{b-a}\right)^n$$

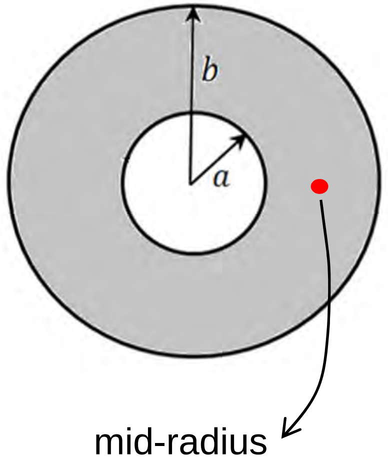

mid-radius

Time history based on the LS theory at mid-radius of the disk

Numerical approach - Evaluations and results

Dynamic coupled structural-thermal analysis

Example 7. Constant thickness disk made of isotropic FGM | results | effects of reference temperature (T_0)

Temperature change

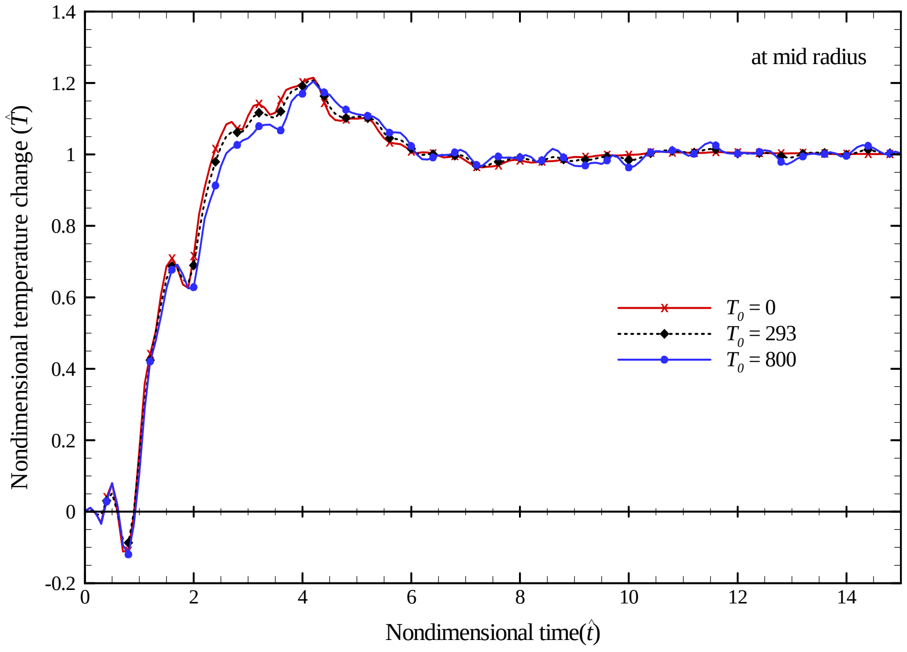

Radial displacement

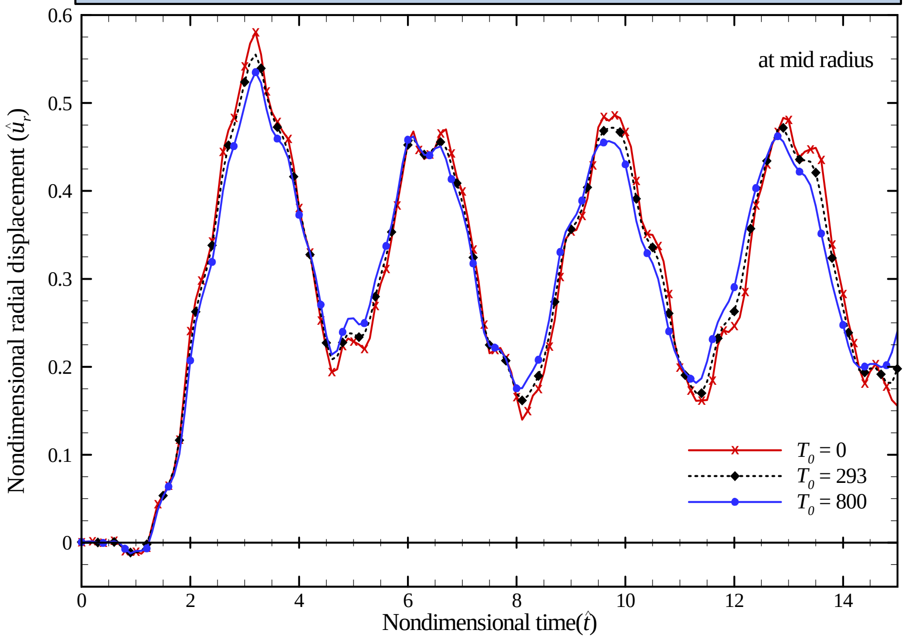

coupling parameter

$$C = \frac{T_0 \beta_{\mathrm{m}}^2}{c_{\mathrm{m}} \rho_{\mathrm{m}} (\lambda_{\mathrm{m}} + \mu_{\mathrm{m}})}$$

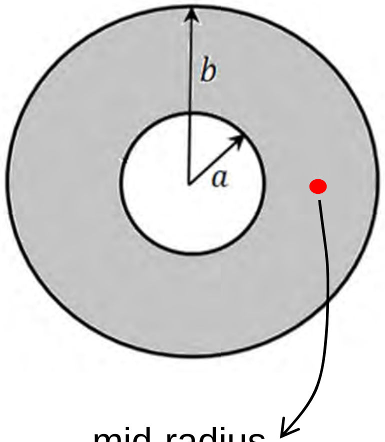

mid-radius

Time history based on the LS theory at mid-radius of the disk ($n = 1$)

Numerical approach - Evaluations and results

Dynamic coupled structural-thermal analysis

Example 7. Constant thickness disk made of isotropic FGM | results | effects of reference temperature (T_0)

Radial stress

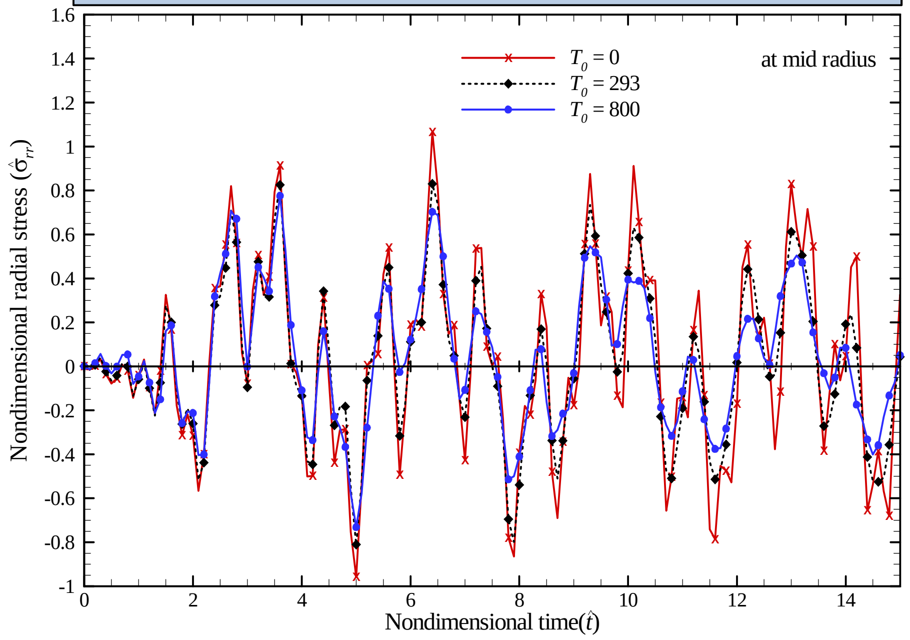

Circumferential stress

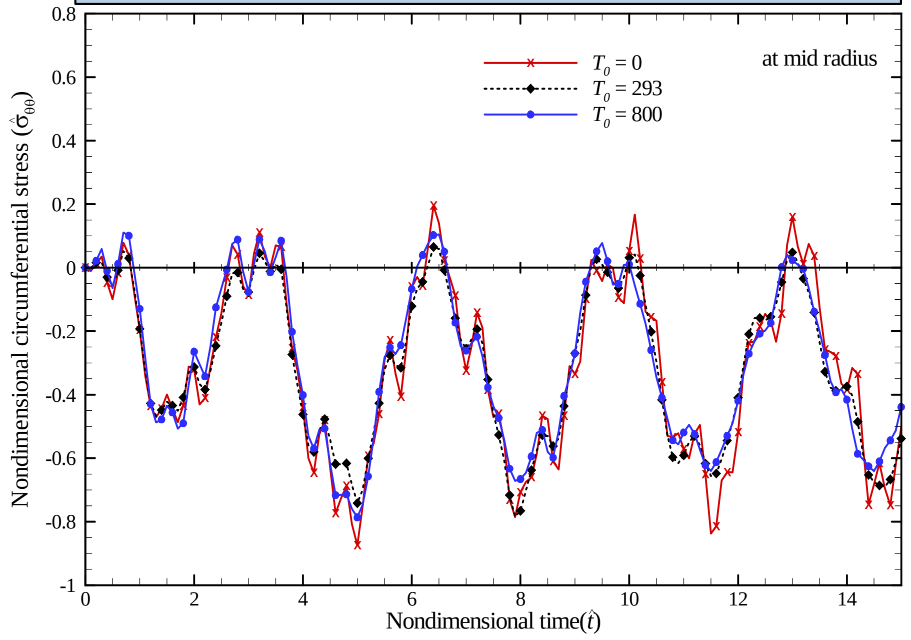

coupling parameter

$$C = \frac{T_0 \beta_{\mathrm{m}}^2}{c_{\mathrm{m}} \rho_{\mathrm{m}} (\lambda_{\mathrm{m}} + \mu_{\mathrm{m}})}$$

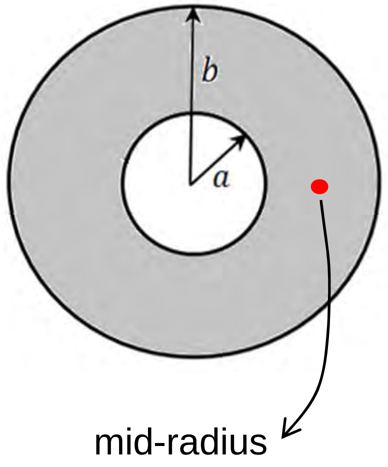

Time history based on the LS theory at mid-radius of the disk (n =1)

Outlines

1. Introduction to rotating disk
2. Fundamentals of Linear Thermoelasticity
3. Literature review & present work
4. Analytical approach
5. **Numerical approach**
   - Motivation
   - Development of method
   - **Evaluations and results**
     - Static structural analysis
       - ✓ Example 1. Rotating variable thickness disk
       - ✓ Example 2. Rotating variable thickness disk subjected thermal load
       - ✓ Example 3. Complex rotor
     - Static structural-thermal analysis – Example 4. simple beam
     - Quasi-static structural-thermal analysis – Example 5. simple beam
     - **Dynamic coupled structural-thermal analysis**
       - ✓ Example 6. Constant thickness disk made of isotropic homogeneous materials
       - ✓ Example 7. Constant thickness disk made of isotropic FGM
       - ✓ **Example 8. variable thickness disk made of isotropic FGM**
6. Conclusion

Numerical approach - Evaluations and results

Dynamic coupled structural-thermal analysis

Example 8. variable thickness disk made of isotropic FGM

Geometry and material

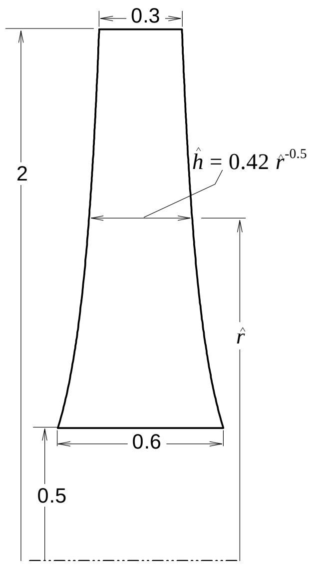

Material properties Metal-Ceramic FGM

	Metal: Aluminum	**Ceramic: Alumina**
Lame'constant λ	40.4 GPa	219.2 GPa
shear modulus μ	27.0 GPa	146.2 GPa
density (ρ)	2707 kg/m^3	3800 kg/m^3
coefficient of linear thermal expansion (α)	23.0×10^{-6} K^{-1}	7.4×10^{-6} K^{-1}
thermal conductivity (κ)	204 W/m·K	28.0 W/m·K
specific heat (c)	903 J/kg·K	760 J/kg·K
dimensionless relaxation time ($\hat{t}_0$)	0.64	1.5625

geometry

$$\hat{r}_{\text{inner}} = a = 0.5$$
$$\hat{r}_{\text{outer}} = b = 2$$
$$\hat{h}_{\text{inner}} = 0.6$$
$$\hat{h}_{\text{outer}} = 0.3$$

effective properties

$$P = V_m P_m + V_c P_c = V_m (P_m - P_c) + P_c$$

metal volume fraction

$$V_m = \left(\frac{b-\hat{r}}{b-a}\right)^n$$

Numerical approach - Evaluations and results

Dynamic coupled structural-thermal analysis

Example 8. variable thickness disk made of isotropic FGM

$T_0 = 293\ \mathrm{K}$, $\widehat{\omega}$=0.05

at $t = 0 \rightarrow T = \dot{\mathbf{u}} = \dot{T} = \mathbf{u} = 0$

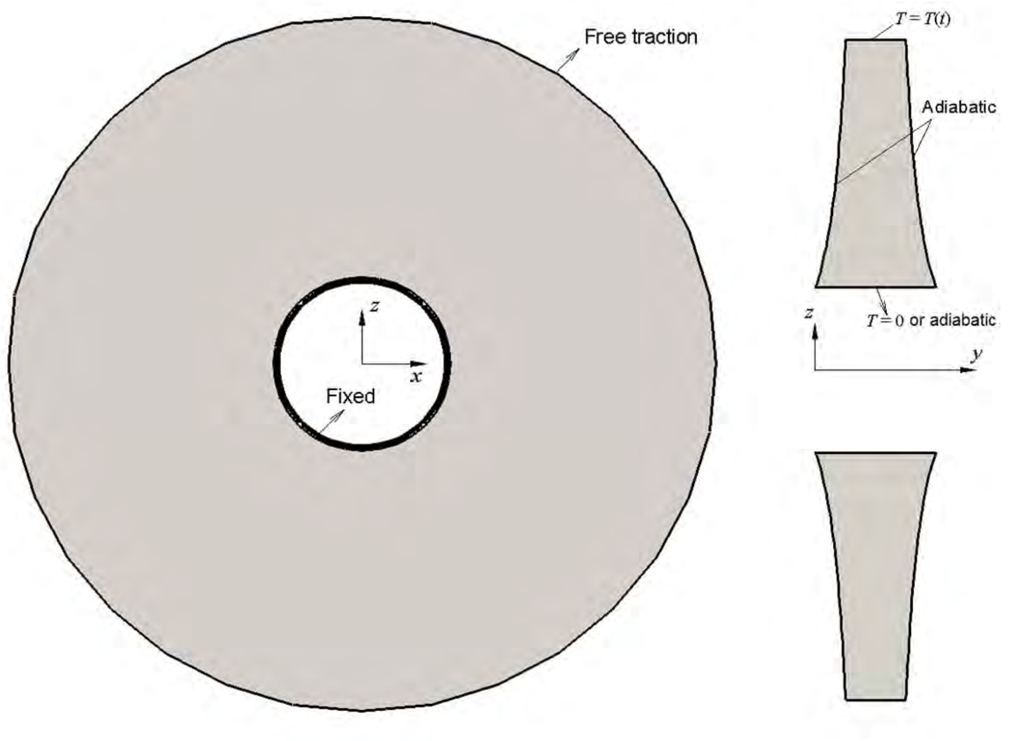

Operational, boundary & initial conditions

$$T(t) = T_d(1 - e^{-100tV_{em}^2/D\mathrm{m}})$$

Non-dimensional form

$$\hat{T}(\hat{t}) = 1 - e^{-100\hat{t}}$$

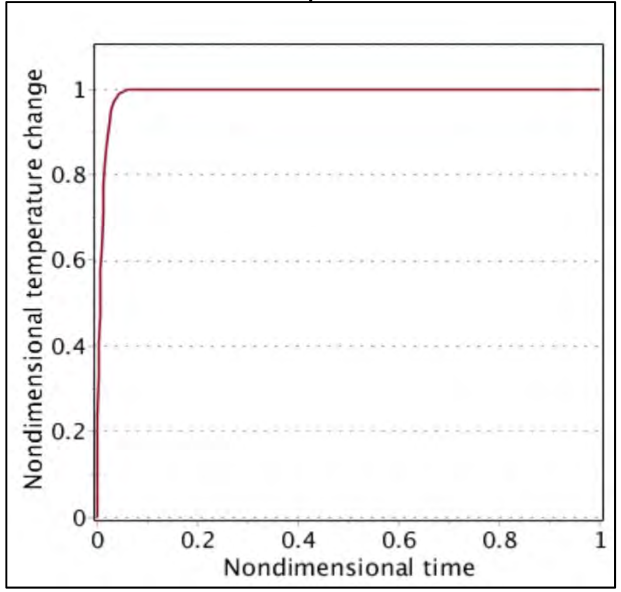

Numerical approach - Evaluations and results

Dynamic coupled structural-thermal analysis

Example 8. variable thickness disk made of isotropic FGM

Results for $n = 0$

Temperature change

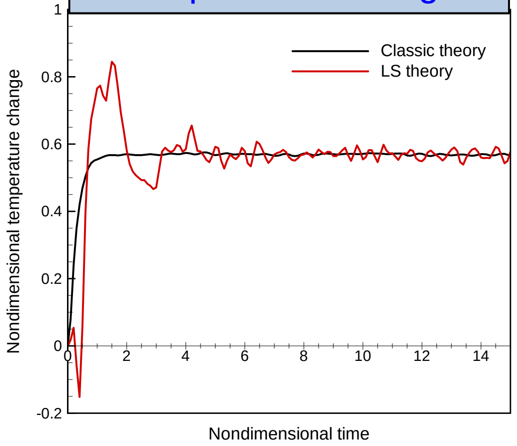

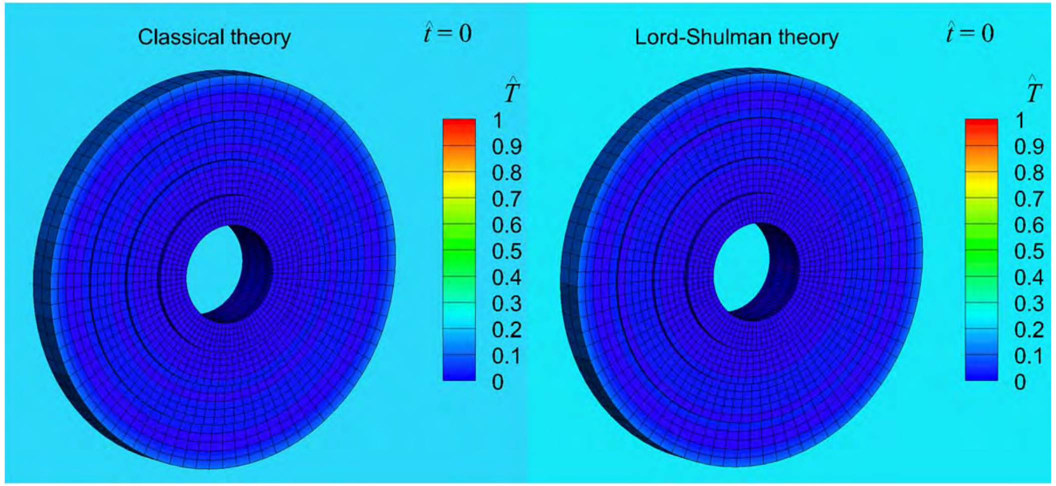

Radial displacement

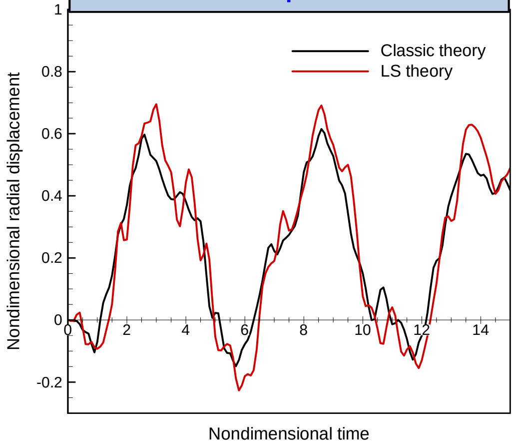

Radial stress

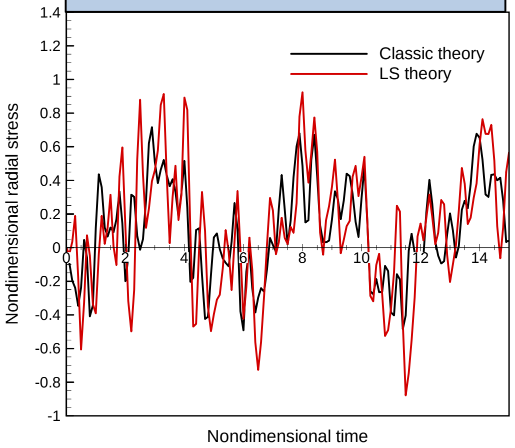

Circumferential stress

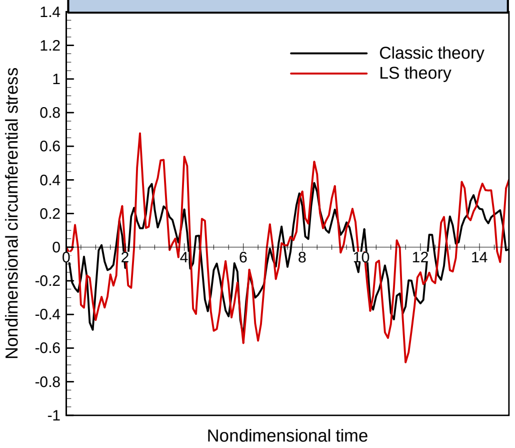

Von mises stress

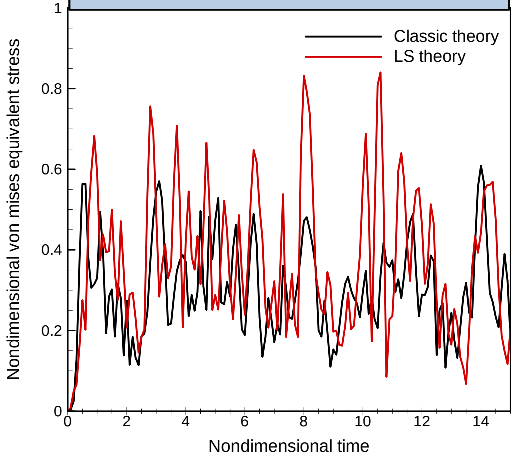

Numerical approach - Evaluations and results

Dynamic coupled structural-thermal analysis

Example 8. variable thickness disk made of isotropic FGM

Results for $n = 0$ based LS theory

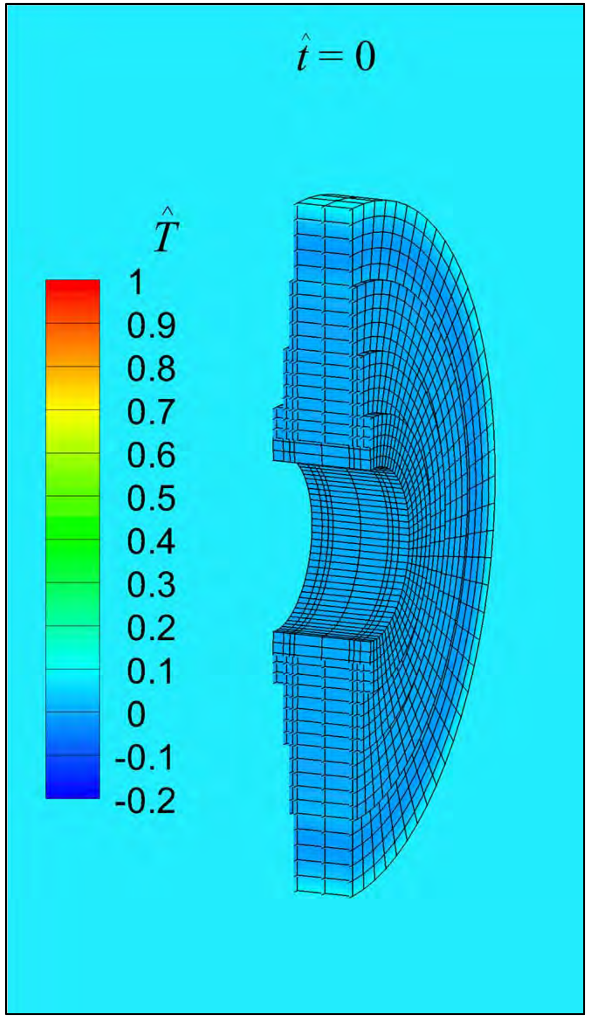

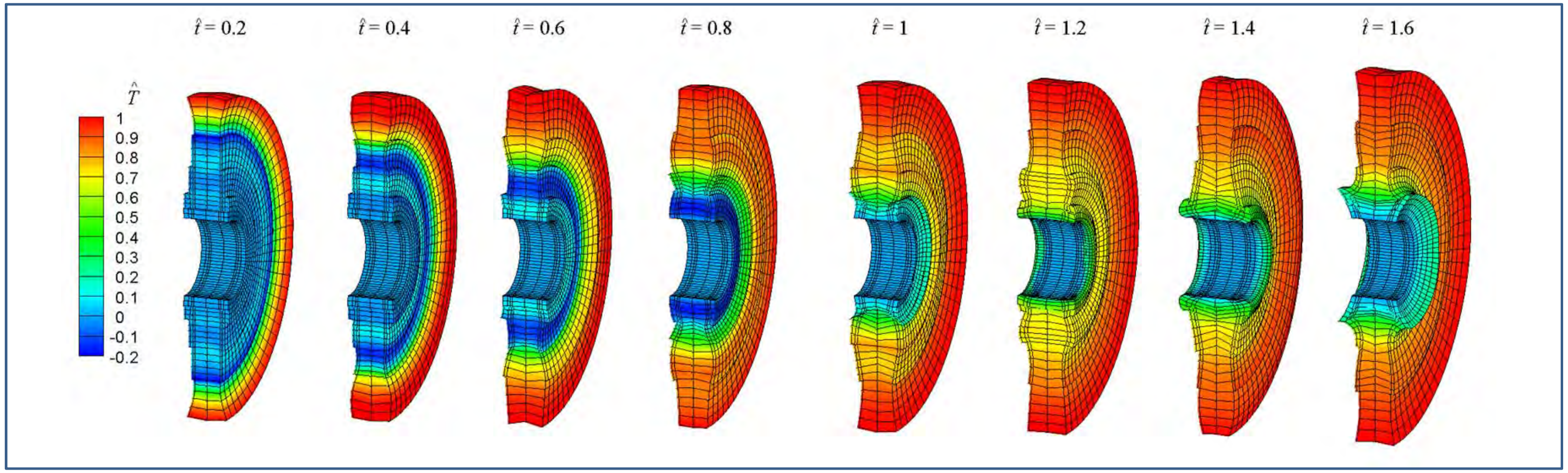

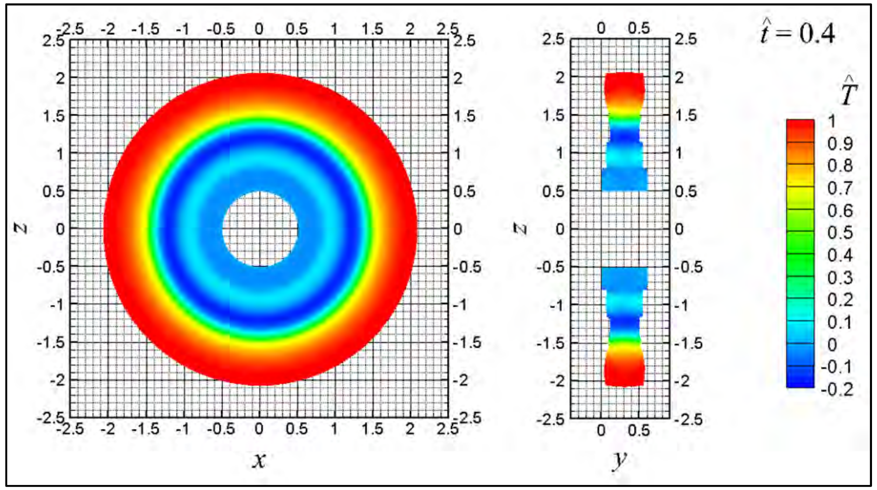

Numerical approach - Evaluations and results

Dynamic coupled structural-thermal analysis

Example 8. variable thickness disk made of isotropic FGM

Results for $n = 0$ based LS theory

Radial displacement

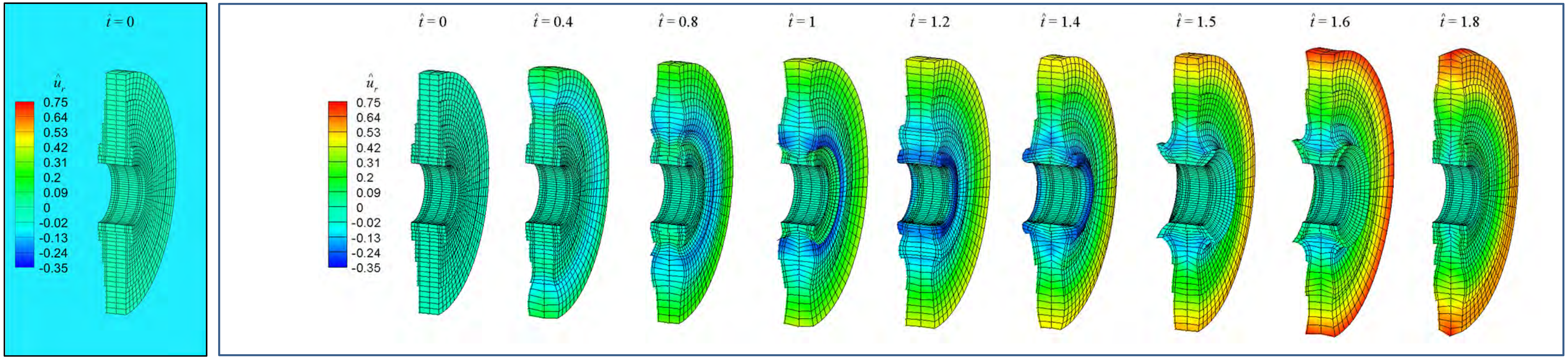

Axial displacement

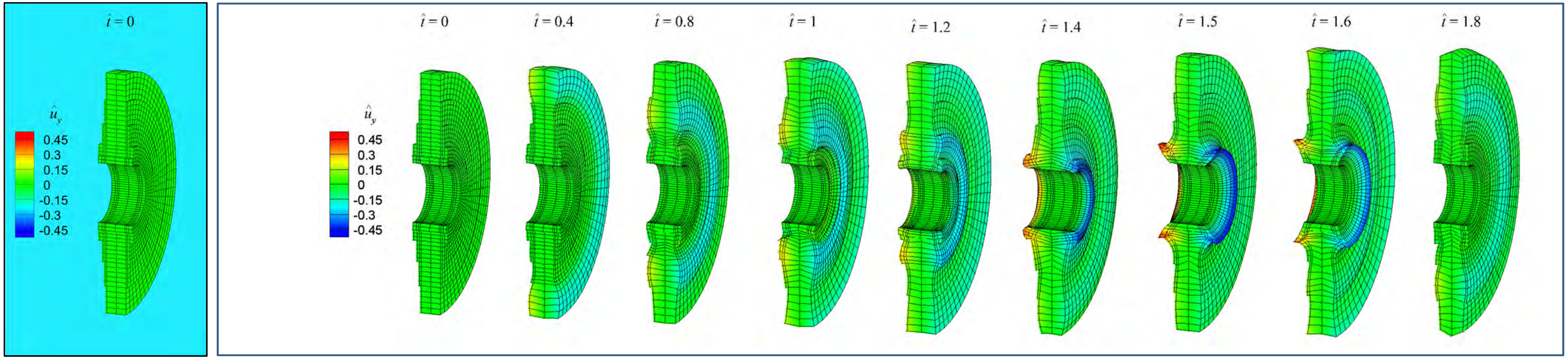

Outlines

1. Introduction to rotating disks

2. Fundamentals of Linear Thermoelasticity

3. Literature review & present work

4. Analytical approach

5. Numerical approach

6. **Conclusion**

Conclusion - Summary of results

Some results obtained from coupled thermoelasticity solution

- ✓ Transient deformations and stresses may be higher than those of a steady-state condition.
- ✓ Time history of temperature is damped faster than time history of displacements.
- ✓ Deformations and stresses oscillate along the time in a harmonic form.
- ✓ Under the propagating longitudinal elastic waves along the radius, thickness of the disk also expands and contracts, due to the Poisson effect.
- ✓ When the coupling parameter takes a greater value, the amplitudes of oscillations of temperature increase.
- ✓ Lord–Shulman generalized coupled thermoelasticity predicts larger temperature and stresses compared to the classical theories.
- ✓ A functionally graded disk may be used as thermal barrier to reduce the thermal shock effects.

Conclusion - Summary of results

Some general points on the 1D FE-CUF modeling of disks

- ✓ The 1D FE method refined by the CUF can be effectively employed to analyze disks reduce the computational cost of 3D FE analysis without affecting the accuracy.

- ✓ the models provides a unified formulation that can easily consider different higher-order theories where large bending loads are involved in the problem.

- ✓ Increasing 1D elements along the axis of disks may not have significant effect on accuracy of results and only leads to more DOFs.

- ✓ A proper distribution of the Lagrange elements and type of element used over the cross sections may lead to a reduction in computational costs and the convergence of results.

- ✓ Making use of higher-order Lagrange elements (like L9 and L16) can reduce DOFs, while preserving the accuracy.

- ✓ increase of number of elements along the radial direction, compared to circumferential direction, is more effective in improving the results.

Conclusion - Future works

It is of interests to extend the study to

- ✓ Nonlinear thermoelasticity problems
- ✓ Dynamic analysis of rotors subjected to transient thermal pre-stresses.
- ✓ Study of thermoelastic damping effect on dynamic behaviors of rotors.

Publications in international Journals

1. Entezari A, Filippi M, Carrera E., Kouchakzadeh M A, ***3D Dynamic Coupled Thermoelastic Solution For Constant Thickness Disks Using Refined 1D Finite Element Models***. European Journal of Mechanics - A/Solids. (Under review).
2. Entezari A, Filippi M, Carrera E. ***Unified finite element approach for generalized coupled thermoelastic analysis of 3D beam-type structures, part 1: Equations and formulation***. Journal of Thermal Stresses. 2017:1-16.
3. Filippi M, Entezari A, Carrera E. ***Unified finite element approach for generalized coupled thermoelastic analysis of 3D beam-type structures, part 2: Numerical evaluations***. Journal of Thermal Stresses. 2017:1-15.
4. Entezari A, Filippi M, Carrera E. ***On dynamic analysis of variable thickness disks and complex rotors subjected to thermal and mechanical prestresses***. *Journal of Sound and Vibration*. 2017;405:68-85.
5. Kouchakzadeh MA, Entezari A, Carrera E. ***Exact Solutions for Dynamic and Quasi-Static Thermoelasticity Problems in Rotating Disks***. Aerotecnica Missili & Spazio. 2016;95:3-12.
6. Entezari A, Kouchakzadeh MA, Carrera E, Filippi M. ***A refined finite element method for stress analysis of rotors and rotating disks with variable thickness***. Acta Mechanica. 2016:1-20.
7. Entezari A, Kouchakzadeh MA. ***Analytical solution of generalized coupled thermoelasticity problem in a rotating disk subjected to thermal and mechanical shock loads***. Journal of Thermal Stresses. 2016:1-22.
8. Carrera E, Entezari A, Filippi M, Kouchakzadeh MA. ***3D thermoelastic analysis of rotating disks having arbitrary profile based on a variable kinematic 1D finite element method***. Journal of Thermal Stresses. 2016:1-16.
9. Kouchakzadeh MA, Entezari A. ***Analytical Solution of Classic Coupled Thermoelasticity Problem in a Rotating Disk***. Journal of Thermal Stresses. 2015;38:1269-91.

Acknowledgements

- ✓ Professor **M. A. Kouchakzadeh** and **Erasmo Carrera**, my supervisors
- ✓ Dr. **Matteo Filippi**, my advisor and colleague in Italy.
- ✓ Professors **Hassan Haddadpour** and **Ali Hosseini Kordkheili**, my Iranian committee members
- ✓ Professors **Maria Cinefra** and **Elvio Bonisoli**, my Italian committee members

Cotutelle Doctoral Program

Doctoral Dissertation on

Solution of Coupled Thermoelasticity Problem In Rotating Disks

by
Ayoob Entezari

Thank you for your attention!

[1]Sharif University of Technology
Department of Aerospace Engineering, Tehran, Iran

[2]MUL2 research group,
Polytechnic University of Turin, Italy

[2]Polytechnic University of Turin,
Department of Mechanical and Aerospace Engineering, Italy

26 September, 2017